

VISIBILITY REDUCTION AS RELATED TO AEROSOL CONSTITUENTS

Interagency Agreement No. ARB A1-081-32

Final Report

October 1983

Prepared by

B. R. Appel, Y. Tokiwa, J. Hsu, E. L. Kothny,  
E. Hahn and J. J. Wesolowski

Air and Industrial Hygiene Laboratory  
California State Department of Health Services  
2151 Berkeley Way  
Berkeley Way  
Berkeley, California 94704

Prepared for: Research Division  
California Air Resources Board  
P.O. Box 2815  
Sacramento, CA 95812

The statements and conclusions in this report are those of the Contractor and not necessarily those of the State Air Resources Board. The mention of commercial products, their source or their use in connection with material reported herein is not to be construed as either an actual or implied endorsement of such products.

## ABSTRACT

A laboratory and field study was performed to assess the contribution to visibility reduction of both light-scattering and absorption by air pollutant particles and gases. Gaseous precursors to important visibility-reducing aerosol species were measured. Emphasis was placed on minimizing sampling artifacts for nitrate and sulfate since previous visibility studies were generally subject to substantial errors from these sources. Optical techniques for measuring the particle absorption coefficient and elemental carbon were evaluated. The aerosol species measured were fine and coarse particulate mass, sulfate, nitrate, and elemental carbon, plus organic carbon and ammonium ion. The gases measured were nitric acid,  $\text{NH}_3$ ,  $\text{SO}_2$ ,  $\text{NO}_2$ , and  $\text{O}_3$ . Sampling was done at San Jose, Riverside and downtown Los Angeles.

At all sites light scattering by sulfate, nitrate and elemental carbon particles contributed more than half of the light extinction. Light absorption by particles, due almost exclusively to elemental carbon, contributed 10 to 20% of the extinction. The light-scattering efficiency of fine particulate nitrate appeared to be higher than that of sulfate, in contrast to the findings of most prior studies.

## ACKNOWLEDGEMENT

We wish to acknowledge the assistance of Vincent Ling who performed many of the carbon determinations and aided in data analysis. Meyer Haik also performed carbon determinations. SuzAnne Twiss supervised the multiple regression analysis of the data. Dr. Allen Waggoner, University of Washington, provided the modified integrating nephelometers together with detailed instructions and advice on their calibration and use. Dr. Ray Weiss, University of Washington, provided valuable comments and aid in setting up and comparing results for the integrating plate method. Dr. Stephen Cadle, General Motors Research Laboratory, provided analyses permitting interlaboratory comparison of our procedures for elemental carbon measurement. Drs. T. Novakov, H. Rosen, A. Hansen and L. Gundel, University of California, Lawrence Berkeley Laboratory, provided information on the design of their laser transmission method, samples for interlaboratory comparison, and useful discussions. Dr. John Trijonis provided many valuable comments on the final report.

Sampling sites were furnished by Professor Kenneth MacKay, San Jose State University, Dr. Arthur Winer, University of California, Riverside, and Mr. Frank Baumann, Southern California Branch Laboratory Section, Laboratory Services Branch, California Department of Health Services.

Finally, we acknowledge Dr. Douglas Lawson and Dr. John Holmes, Air Resources Board Research Division, for their helpfulness and support throughout this program.

This report was submitted in fulfillment of Interagency Agreement No. A1-081-32, Visibility Reduction as Related to Aerosol Constituents by the California Department of Health Services under the sponsorship of the California Air Resources Board. Work was completed as of November 10, 1983.

## TABLE OF CONTENTS

Abstract Acknowledgements List of Figures List of Tables	<u>Page</u>
I. Summary and Conclusions	12
II. Introduction	
A. Visibility and its Relation to Aerosol Constituents.....	17
B. Limitations of Prior Studies.....	20
C. Objectives of the Present Study.....	24
D. Strategy.....	24
III. Measurement of the Particle Absorption Coefficient ( $b_{ap}$ )	
A. The Integrating Plate Method (IPM).....	26
B. A Laser Transmission Method (LTM).....	29
C. Comparison of $B_{ap}$ Determinations by the IPM and LTM.....	30
IV. Determination of Elemental Carbon ( $C_e$ )	
A. Introduction .....	32
B. The Laser Transmission Method for $C_e$ .....	32
C. Intermethod and Interlaboratory Comparisons.....	33
D. Comparison of $C_e$ by Optical Methods with Particle Absorption Coefficient Results.....	35
V. Measurement of the Scattering Coefficient for Liquid Water	
A. Introduction .....	37
B. Method Evaluation and Correlation with Aerosol Constituents.....	37
VI. Assessment of Sampling Artifacts	
A. Artifact Particulate Sulfate on Glass Fiber Filters.....	39

	<u>Page</u>
B. Artifact Particulate Nitrate on Glass Fiber Filters.....	39
C. Loss of Particles in the Denuder of the Particulate Nitrate (PN) Sampler.....	40
D. Loss of Non-Volatile Carbon in the Denuder of the Particulate Carbon Sampler.....	41
E. Retention of Carbonaceous Material on Hi-Vol Filter Samples.....	41
VII. Atmospheric Results -- Part I.	
A. Tabulation of Results.....	42
B. Summary of Visibility Results.....	42
C. Diurnal Variation of the Dominant Aerosol Species and Ozone.....	43
D. Size Distribution for Aerosol Constituents.....	43
E. Calculated vs. Observed Ammonium Ion Levels.....	45
F. True Particulate Carbon (PC) and Total Low Volatility Carbon (LVC).....	46
G. Atmospheric Nitric Acid.....	46
VIII. Atmospheric Results -- Part II. Statistical Analyses	
A. Correlation between Pollutant Concentrations.....	48
B. Correlation between Single Pollutant Concentrations and Visibility Parameters.....	48
C. Multiple Regression Analyses between Particle Scattering Coefficients and Pollutant Concentrations.....	49
D. Average Contributions of Aerosol Species to the Scattering and Total Extinction Coefficients.....	51
E. Comparison of Present Results with those for General Motor's Denver Visibility Study.....	52
F. Comparison of the Present Results to those Reported by Trijonis et al(48).....	53

IX. References

Appendices

A. The Impact of Increased Diesel Emissions on Visibility.....	62
B. Operation of the Integrating Nephelometers.....	65
C. Evaluation of Methods for Absorption Coefficient Measurement...	66
D. Calibration of Optical Methods for Elemental Carbon.....	79
E. Measurement of Ambient Temperature and Relative Humidity.....	85
F. Experimental Difficulties with the True Particulate Carbon Measurements.....	86

## FIGURES

<u>Number</u>	<u>Page</u>
1. Light Scattering by Aerosols as a Function of Particle Diameter Computed for Unit Density Spherical Particles of Refractive Index 1.5.....	19a
2. Schematic of Integrating Plate Method (IPM).....	26a
3. Comparison of $b_{ap}$ Measurements at Two Particle Loadings.....	28a
4. Comparison of the Integrating Plate Method and Laser Transmission Techniques for Absorption Coefficient Measurement.....	29a
5. Schematic Diagram of Laser Transmission Method, Viewed From Above.....	30a
6. Comparison of $b_{ap}$ Measurements by the IPM and LTM Methods.....	30b
7. Elemental Carbon by the LTM vs. Reflectance Method.....	34a
8. Relation between Absorption Coefficient and $C_e$ for Denver Winter Aerosol	35a
9. Elemental Carbon by LTM vs. Absorption Coefficients.....	35b
10. Elemental Carbon by the RM vs. Absorption Coefficients.....	35c
11. Mean Elemental Carbon by LTM and RM vs. Absorption Coefficients.....	35d
12. Artifact Sulfate on Glass Fiber Filters, 4-hour Hi-Vol Samples.....	39a
13. Nitric Acid Retention on Glass Fiber Hi-Vol Filters.....	40a
14. Nitric Acid Retention of Glass Fiber Hi-Vol filters.....	40b
15. Nitric Acid Retention of Glass Fiber Hi-Vol Filters.....	40c
16. Nitric Acid Retention of Glass Fiber Hi-Vol Filters.....	40d
17. Loss of Non-Volatile Particles in the Denuder for Nitrate Sampling.....	40e
18. Loss of Non-Volatile Particles in the Denuder of the Particulate Carbon Sampler.....	41a
19. Observed vs. Calculated 16-hour Total Carbon.....	41b
20. Mass Comparisons 1982 ARB Visibility Study.....	43a
21. Comparison of Fine and Total Particulate Sulfate.....	43b
22. Comparison of Fine and Total Particulate Elemental Carbon.....	43c
23. Fine Elemental Carbon vs. Total Carbon in 4-hour Samples.....	43d

<u>Number</u>	<u>Page</u>
24. Fine Particle Mass vs. Fine Particle Elemental Carbon.....	43e
25. Total Particle Mass vs. Fine Particle Elemental Carbon.....	43f
26. Comparison of Filter Collected Carbon with and without a Diffusion Denuder for Carbonaceous Vapors.....	43g
27. B Values San Jose.....	44a
28. B Values Riverside.....	45a
29. B values Los Angeles.....	45b
30. Diurnal Variations in Mean Pollutant Concentrations (San Jose).....	45c
31. Diurnal Variations in Mean Pollutant Concentrations (Riverside).....	45d
32. Diurnal Variations in Mean Pollutant Concentrations (Los Angeles).....	46a
33. Scatter Diagram of Fine Particulate Mass Against the Dry Particle Scattering Coefficient.....	49a
34. Comparison of Calculated and Observed $b'_{ext}$ .....	51a
C-1. Linearity of LTM Detector Response.....	74a
C-2. Comparison of AIHL and Lawrence Berkeley Laboratory LTM Instruments Analyzing the Same Atmospheric Particulate-loaded Millipore Filters.....	76a
D-1. Size distribution for Aged Carbon Particles from a Butane Flame.....	80a
D-2. Calibration of LTM with Aged Carbon Particles.....	80b
D-3. Calibration of LTM with LBL Black Carbon Samples.....	81a
D-4. Light Absorption Efficiency for Graphitic Carbon.....	81b
D-5. Calibration of Reflectance Meter with Aged Carbon Particle Samples.....	82a
D-6. Calibration of Reflectance Meter with Aged Carbon Particle and LBL Black Carbon Samples.....	82b
E-1. Temperature Comparisons 1982 ARB Visibility Study.....	85a
E-2. RH Comparisons 1982 ARB Visibility Study.....	85b

TABLES

<u>Number</u>		<u>Page</u>
1	Summary of Extinction Coefficients per Unit Mass Obtained in Various Regression Studies .....	18a
2	Contribution of the Chemical Species to the Extinction Coefficient, for Denver.....	21a
3	Description of Samplers Employed for Visibility Study ....	25a
4	Analytical Strategy for Visibility Study .....	25c
5	Calibrations of Optical Methods for Elemental Carbon .....	33a
6	Comparison of Total Carbon and Elemental Carbon ( $C_e$ ) Values ( $\mu\text{g}/\text{m}^3$ ) .....	33b
7	Comparison of Elemental Carbon Measurements by General Motors' Combustion and AIHL Optical Methods .....	34b
8	Pearson Correlation Coefficients Between $b_{sw}$ , Pollutant and Meteorological Parameters .....	37a
9	Multiple Regression Analysis Between $b_{sw}$ and Aerosol Constituents .....	38a
10	Summary of Atmospheric Results .....	42a
11	Explanation of Headings Used in Table 10 .....	42c
12	Mean Concentrations of Aerosol Constituents and Meteorological Parameters .....	42d
13	Summary of Optical Measurements at San Jose, Riverside and Los Angeles .....	42e
14	Pearson Correlation Coefficients Between Aerosol Constituents Ozone and Meteorological Parameters .....	48a
15	Correlation Between Fine Aerosol Constituents (or Aerosol Precursors) and $b_{sp}$ .....	48b
16	Pearson Correlation Coefficients Between Visibility Parameters, Individual Pollutants and Meteorological Parameters .....	48c

<u>Number</u>		<u>Page</u>
17	Multiple Regression Analysis Between Aerosol Constituents and $b_{sp}$ .....	50a
18	Average Percent Contributions of Chemical Species to the Particle Scattering Coefficient, $b_{sp}$ and to the Extinction Coefficient, $b'_{ext}$ .....	52a
C-1	Precision of Parallel Sampling for $b_{ap}$ Measurement .....	68a
C-2	Effect on Transmittance of Overlaying Loaded Nuclepore Filter with a Microscope Slide .....	69a
C-3	Effect of Neutral Density Filter on % T of Loaded Filters .....	70a
C-4	Effect of Particle Orientation on % T .....	71a
C-5	Interlaboratory Comparison of IPM (% T) .....	72a
C-6	Batch-to-Batch Variations in Mean Transmittance Values for 0.4 $\mu$ m Pore Size Nuclepore Filters .....	73a
C-7	Influence of Particle Orientation with the IPM and LTM .....	76b
C-8	Influence of Wavelength and the Discrepancy Between the IPM and LTM Methods .....	78a
D-1	Size Distribution for Carbon Particles .....	79a

## I. SUMMARY AND CONCLUSIONS

A laboratory and field study was performed to assess the contribution to visibility reduction at both light-scattering and absorption by air pollutant particles and gases. Gaseous precursors to important visibility-reducing aerosol species were also measured. Emphasis was placed on minimizing sampling artifacts for pollutant particles since preceding visibility studies were generally subject to substantial errors from this source. Optical techniques to measure the particle absorption coefficient and elemental carbon were evaluated.

The aerosol species measured were fine and coarse particulate sulfate, nitrate, elemental carbon and mass. In addition, total particulate organic carbon and ammonium ion were determined. The gases measured were nitric acid,  $\text{NH}_3$ ,  $\text{SO}_2$ ,  $\text{NO}_2$  and  $\text{O}_3$ . Artifact sulfate formation was minimized by using Teflon filters. Particulate nitrate and nitric acid were measured using the denuder difference technique. Particulate organic carbon was sampled with two conventional hi-vol samplers with glass fiber filters, providing both 4-hour and 16 to 24 hr samples. In addition, a diffusion denuder plus a quartz filter and a fluidized  $\text{Al}_2\text{O}_3$  bed were used in an effort to determine particulate carbon while minimizing both positive and negative sampling errors. However, experimental difficulties prevented the development of useful data from this sampler.

The particle absorption coefficient was measured by the integrating plate method using two samplers operating at different particle loading rates. Elemental carbon was measured optically by both a reflectance method and by a method which measured the absorption of a He-Ne laser beam. Two integrating nephelometers operated side-by-side to measure light-scattering by particles with and without heating the incoming air. The difference in results between these instruments was used to approximate light-scattering due to liquid water.

Sampling was done for a total of 109, 4-hour periods, generally between 0800 and 2400 hours, July 10 - August 8, 1982, at San Jose, Riverside and downtown Los Angeles. The mean visual range encountered, as estimated from the calculated extinction coefficients and the Koschmeider equation, were 43 Km at San Jose, 15 Km at Riverside and 13 Km at downtown Los Angeles. The mean four-hour average ozone concentrations ranged from 0.02 to 0.07 ppm. Thus relatively light photochemical smog was experienced.

Light scattering by dry particles was the largest contributor to the total extinction ( $b'_{ext}$ ) at all sites, representing more than half of the extinction coefficient. Light absorption by particles, due almost exclusively to elemental carbon, was relatively unimportant ( $\leq 12\%$  of  $b'_{ext}$ ) in the South Coast Air Basin where high concentrations of sulfate and nitrate were present. At San Jose, however, absorption averaged nearly 22% of  $b'_{ext}$ . The apparent contribution of scattering from liquid water was relatively high at Riverside and Los Angeles but small at San Jose, paralleling the concentrations of the hygroscopic aerosol species, sulfate and nitrate. Light absorption by gases, due only to  $NO_2$ , was small at all sites.

Considering both light scattering and light absorption, and using multiple regression analysis, fine sulfate and fine nitrate (and associated water), fine elemental carbon, and nitrogen dioxide contributed on average, 30%, 36%, 20%, and 8%, respectively, to the total extinction (excluding Rayleigh scattering).

Sulfate, nitrate, elemental carbon, and total carbon were predominately in the fine ( $< 2.5 \mu m$ ) fraction averaging 92%, 60%, 80%, and 62% respectively, measured by comparing results with and without a cyclone preceding the sampler. The percentage of fine total carbon can be compared to the range 56 to 66% previously obtained at three sites using a dichotomous sampler (DS). We previously suggested that the proportion of coarse particle carbon with a DS may be erroneously high

because of the low face velocity for the coarse particle filter (34,40). The present data fail to support this.

Multiple regression analyses between the dry particle scattering coefficient and aerosol species concentrations yielded the relationship:

$$b_{sp} = - 0.14 + 0.051 (FSO_4) + 0.064 (FNO_3) + 0.049 (FC_e) + 0.11 (CSO_4)$$

$$r = 0.95$$

where F = fine

C = coarse

Thus the scattering efficiency per unit mass of nitrate appears to be greater than that for fine sulfate, in contrast to most previous studies. The scattering efficiency for fine elemental carbon ( $C_e$ ) was similar to that for fine sulfate. The results for coarse sulfate are surprising, implying a scattering efficiency twice that for fine sulfate. We believe that some material whose concentration is much higher but proportional to that of coarse sulfate is the actual scattering source. Sea salt chloride, for example, is about seven times the weight concentration of sea salt sulfate. A significant amount of sea salt would be expected in the coarse fraction. Replacing the coarse sulfate concentration with a material seven times more abundant would decrease the scattering efficiency per unit mass by an equal factor of seven (i.e. to  $< 0.02 \times 10^{-4} \text{ m}^{-1} / \mu\text{g}/\text{m}^3$ ). The remaining aerosol species, coarse nitrate, coarse elemental carbon, and organic carbon, did not exhibit a significant scattering efficiency in this evaluation.

Multiple regression analyses between the measured scattering coefficient for liquid water and the concentrations of the hygroscopic aerosol species  $SO_4^{=}$  and  $NO_3^{-}$ , using various functions of relative humidity, showed only moderate correlation ( $r \leq 0.81$ ). This may be

indicative of lack of speciation data for sulfate since, for example,  $\text{H}_2\text{SO}_4$  and  $(\text{NH}_4)_2\text{SO}_4$  differ substantially in hygroscopicity. It may also indicate error in measuring the scattering coefficient for liquid water, since species other than liquid water may be volatilized on entering a heated nephelometer inlet (e.g. organic compounds,  $\text{NH}_4\text{NO}_3$ ).

Artifact particulate nitrate formation on glass fiber filters (prefired Schleicher and Schuell, 1981 EPA Grade) was assessed for both 4-hour and 16-hour atmospheric samples. With the short-term samples, essentially all particulate nitrate and nitric acid was retained, supporting the use of glass fiber as total inorganic nitrate (TIN) collectors. With the long-term samples, however, only at low nitrate levels such as found at San Jose (TIN  $\leq 32 \mu\text{g}/\text{cm}^2$ ) was all TIN retained; at Riverside and Los Angeles with TIN values up to  $147 \mu\text{g}/\text{cm}^2$ , from 24 to 42% of the TIN penetrated the filters, presumably as  $\text{HNO}_3$ .

Expected  $\text{HNO}_3$  concentrations can be calculated from the concentration of  $\text{NH}_3$ , temperature, and corresponding dissociation constant for  $\text{NH}_4\text{NO}_3$ . In general, no correlation between the observed and expected  $\text{HNO}_3$  levels was found. Similarly, the correlation between  $\text{NH}_3$  or  $\text{HNO}_3$  and the particle scattering coefficient remained relatively low.

The principal conclusions from this study are:

1. The light-scattering efficiency of fine particle nitrate appears to exceed that of sulfate in contrast to most previous studies. Since both positive and negative sampling artifacts were minimized we believe these results to be correct.
2. Light absorption by elemental carbon plays a significant role in visibility reduction in California, especially under conditions in which the concentrations of fine sulfate and nitrate are relatively low.

3. Particle-phase water contributed substantially to visibility reduction at sites with relatively high levels of sulfate and nitrate, species which can absorb moisture.

#### Recommendations for Further Studies

1. The significance of true particle phase organic compounds in visibility reduction. Although organic carbon, based on hi-vol filter sampling, was not a statistically significant contributor to visibility reduction, sampling errors may have masked such a contribution.
2. The accuracy of elemental carbon measurement by optical methods. While the elemental carbon measurements reported are consistent with other optical measurements, calibration techniques for elemental carbon measurements by optical methods require more work before their adoption for routine monitoring of elemental carbon can be recommended.
3. The relative significance of aerosol constituents in visibility reduction using the same techniques at other times of the year.
4. Additional statistical analysis of results from the present study to  
a) assess the significance of the aerosol and gaseous pollutants to visibility reduction by site, b) assess the hypothesis that coarse sulfate is functioning as a surrogate for sea salt, and c) assess the impact of co-linearity of variable.

## II. INTRODUCTION

### A. Visibility and Its Relation to Aerosol Constituents

Visual range ( $v_m$ ) is defined as the greatest distance at which an observer can distinguish a contrast between an object and its background. At this distance the contrast of the object has reached its threshold value, which is usually taken to be 2%. With this threshold value, the simple Koschmeider relation for a perfectly black object holds (1):

$$v_m = \frac{3.912}{b_{ext}}$$

The atmospheric extinction coefficient,  $b_{ext}$ , may be written as follows:

$$b_{ext} = b_{ap} + b_{ag} + b_{sp} + b_{sg}$$

where:  $b_{ap}$  = absorption by particles

$b_{ag}$  = absorption by gases (essentially only  $\text{NO}_2$ )

$b_{sp}$  = scattering by particles

$b_{sg}$  = Rayleigh scattering by gases =  $0.12 \times 10^{-4} \text{m}^{-1}$

For a perfectly black object the visual range depends only on the total extinction coefficient,  $b_{ext}$ , and is independent of the ratio of scattering to absorption (2).

Much of the emphasis in atmospheric visibility studies has been to establish the chemical species contributing substantially to

visibility reduction (3-8). Typically  $b_{\text{ext}}$  is approximated by  $b_{\text{sp}}$ , as measured by the integrating nephelometer or as approximated from human observer data. Indeed,  $b_{\text{sp}}$  will often represent more than 2/3 of the total extinction coefficient. Multiple regression analyses are performed with equations of the form:

$$b_{\text{ext}} = b_{\text{sp}} = a + b_1(\text{SO}_4^{--}) + b_2(\text{NO}_3^-) + b_3(\text{R}) + b_4(\text{RH})$$

where  $\text{R} = \text{Remaining aerosol} = \text{TSP} - \text{SO}_4^{--} - \text{NO}_3^-$

$\text{RH} = \text{relative humidity}$

Relative humidity dependence may, alternatively, be incorporated into the sulfate and nitrate terms. In the cases where data on carbonaceous material are available, additional terms [e.g.  $b_5$  (benzene soluble organics)] are added.

Table 1, taken from a recent survey by Trijonis,(3) summarizes the scattering coefficients per unit mass for a series of visibility studies. Principal conclusions that can be reached from these studies are:

1. Sulfates, per unit mass, are the dominant contributor to visibility reduction due to light scattering.
2. Nitrates, per unit mass, can be an important contributor to visibility reduction due to scattering. However, in locations not dominated by photochemical smog, their contribution will be relatively small because of the low nitrate levels.

The contribution of relative humidity as well as organics is illustrated with results from a study by Hidy et al.: (4)

TABLE 1 SUMMARY OF EXTINCTION COEFFICIENTS PER UNIT MASS OBTAINED IN VARIOUS REGRESSION STUDIES.  
(From Trijonis et al. Reference 3)

Locations in California.

LOCATION	EXTINCTION COEFFICIENTS PER UNIT MASS ( $10^4 \text{ m}^{-1}/(\mu\text{g}/\text{m}^3)$ )		
	Sulfates	Nitrates	Remainder of TSP
<u>Other Studies</u>			
SOUTH COAST AIR BASIN			
(White and Roberts 1977)	.07*	.05*	.015*
Various Los Angeles Basin Sites <sup>†</sup>	.06*	.04*	.020*
(Cass 1979)	.17*	NS*	.008
Downtown Los Angeles	.09	.05	NS*
(Grosjean et al. 1976)			
Eastern Los Angeles Basin	.21	.04	NS
(Leaderer and Stolwijk 1979)			
Los Angeles Int. Airport	.16	.03	NS
<u>The Present Study</u>			
SOUTH COAST AIR BASIN			
Burbank	.17*	NS*	NS
	.15*	NS	.008*
Long Beach	.16*	.04*	.011*
	.11	NS	.013
Ontario	.16*	.15*	NS*
	.17	.11	NS
San Bernardino	.12*	NS*	.019*
	.06	.05	.019
SAN FRANCISCO BAY AREA AIR BASIN			
Oakland	.12*	NS*	.014*
	.08	NS	.014
San Jose	NS*	.06*	NS*
	NS	.04	NS
OTHER COASTAL LOCATIONS			
Paso Robles	.08*	.08*	.008*
	.06	.08	.006
San Diego	.19*	.04*	NS*
	.15	.05	NS
SAN JOAQUIN VALLEY AIR BASIN			
Bakersfield	NS*	.09*	NS*
	NS	.07*	NS
Fresno	NS*	.14*	NS*
	NS	.07	NS
SACRAMENTO VALLEY AIR BASIN			
Red Bluff	NS*	.03*	.009*
	NS	.04*	.008
Sacramento	.16*	.05*	.014*
	.15	.03	.014

\* Values marked by an asterisk are based on the nonlinear RH regression model with insertion of average RH. Values not so marked are based on the linear RH model.

<sup>†</sup> Based on nephelometry data rather than airport visibility data.

TABLE 1 SUMMARY OF EXTINCTION COEFFICIENTS PER UNIT MASS  
OBTAINED IN VARIOUS REGRESSION STUDIES (Continued).  
(From Trijonis et al. Reference 3)

Locations in the Northeast and Rocky  
Mountain Southwest.

LOCATION	EXTINCTION COEFFICIENTS PER UNIT MASS ( $10^4 \text{ m}^{-1}/(\mu\text{g}/\text{m}^3)$ )		
	Sulfates	Nitrates	Remainder of TSP
<b>NORTHEAST</b>			
(Trijonis and Yuan, 1978b)			
Chicago	.04*	NS*	NS*
	.03	NS	NS
Newark	NS*	NS*	.026*
	.06	NS	.014
Cleveland	.08	NS*	NS*
	.07	NS	NS
Lexington	.06*	NS*	NS*
	.06	NS	.019*
Charlotte	.11*	NS*	NS*
	.11	NS	NS
Columbus	.12*	.09*	NS*
	.13	.06	NS
(Leaderer and Stolwijk 1979)			
New York <sup>†</sup>	.07	.05	NS
New York	.10	NS	NS
New Haven	.16	NS	NS
St. Louis	.08	NS	NS
<b>ROCKY MOUNTAIN SOUTHWEST</b>			
(Trijonis 1979)			
Phoenix			
County Data	.04	.05	NS
NASN Data	.03	.03	NS
Salt Lake City	.04*	.13*	.004*
	.04	.10	.004

\* Values marked by an asterisk are based on the nonlinear RH regression model with insertion of average RH. Values not so marked are based on the linear RH model.

<sup>†</sup> Based on nephelometry data rather than airport visibility data.

$$10^4 b_{\text{ext}} = 10^4 b_{\text{sp}} = 0.0174(\text{SO}_4^{2-}) + 0.025(\text{NO}_3^-) + 0.049 \mu^2(\text{NO}_3^-) \\ + 0.025(\text{total carbon}) + 0.025(\text{R})$$

$$\text{where } \mu = 1 - \frac{\text{RH}}{100}$$

$$\text{R} = \text{remaining aerosol} = \text{TSP} - \text{SO}_4^{2-} - \text{NO}_3^- - \text{total carbon}$$

Some studies have incorporated relative humidity-dependent sulfate terms as well (3,7).

The dominance of sulfate in contributing to light scattering and the influence of relative humidity on light scattering can be interpreted in relation to Figure 1. Growth caused by pickup of water would be expected to enhance light scattering for sulfate particles initially smaller than 0.5  $\mu\text{m}$  in diameter, since scattering efficiency exhibits a sharp maximum at 0.5  $\mu\text{m}$ . Sulfates in various urban areas around the United States have been reported to have mass median diameters (mmd) ranging from 0.1 to 0.6  $\mu\text{m}$  (9). Nitrate mass median diameters are much more varied. In California's South Coast Basin, 24-hour mean values from 0.3 to 1.6  $\mu\text{m}$  have been reported (9), probably reflecting the proportions of fine  $\text{NH}_4\text{NO}_3$  and coarse  $\text{NaNO}_3$ . Assuming a size distribution for  $\text{NH}_4\text{NO}_3$  similar to that for particulate sulfate, increasing relative humidity would increase the scattering efficiency for this material as well. The limited data on carbonaceous particulates suggest mean diameters of several tenths of a micrometer. For example, mmd values of about 0.3  $\mu\text{m}$  were found for both organic and elemental carbon in Denver (38). This together with their low hygroscopicity may explain their lesser scattering efficiency.

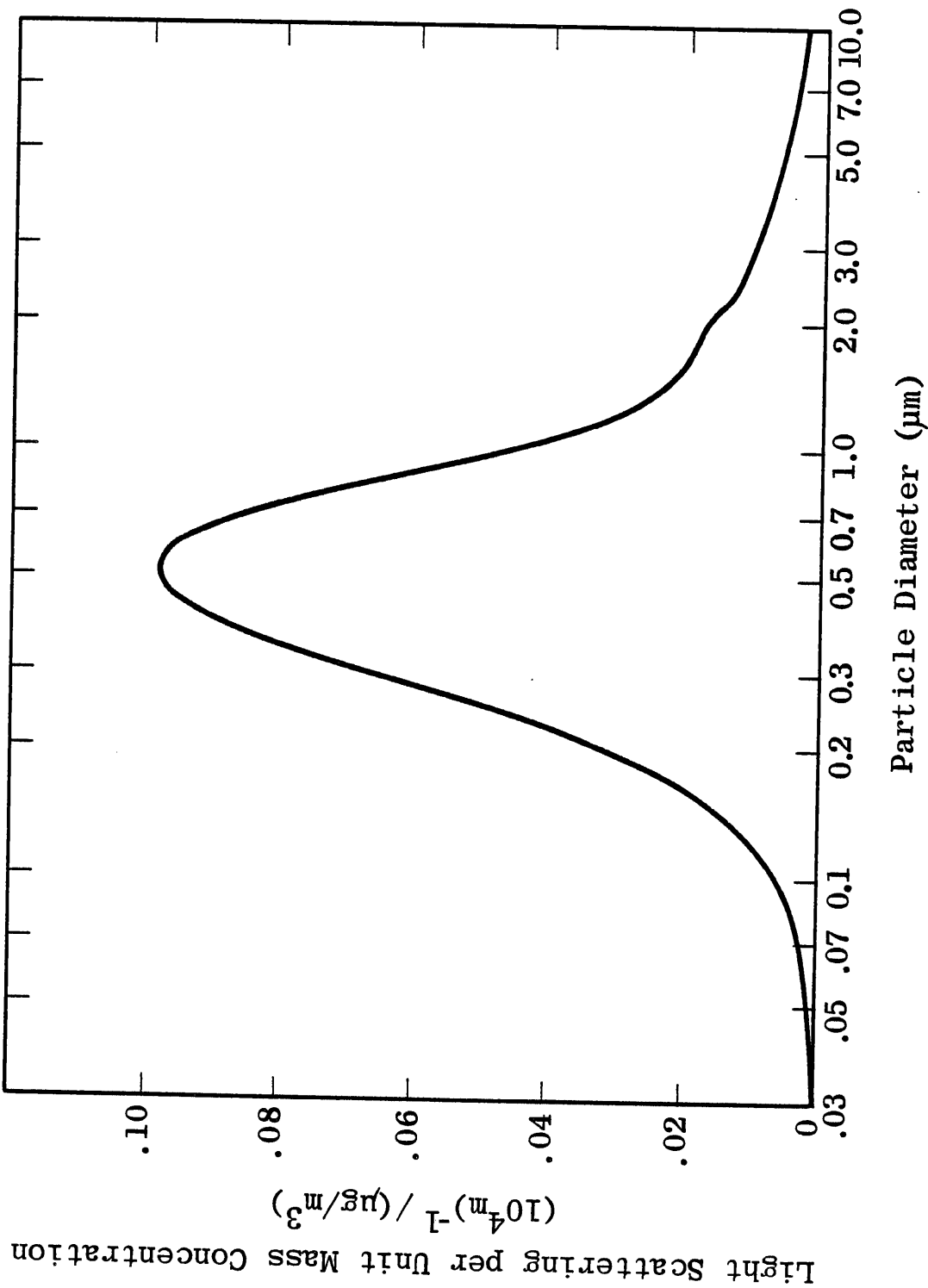


Figure 1. LIGHT SCATTERING BY AEROSOLS AS A FUNCTION OF PARTICLE DIAMETER. COMPUTED FOR UNIT DENSITY SPHERICAL PARTICLES OF REFRACTIVE INDEX 1.5 (White and Roberts 1977)

B. Limitations of Prior Studies

1. Most prior studies have neglected consideration of light absorption by aerosol constituents.
2. Studies based on visual range measurements obtained by a human observer yield daytime visibility at one or two times per day. Attempts to correlate these results with 24-hour average particulate sampling results (e.g. Ref. 7) are subject to substantial error since particulate loadings will generally be higher during daytime hours.
3. Aerosol samples have typically been collected on filters subject to sampling errors. These include artifact particulate sulfate and nitrate employing glass fiber filters, artifact particulate nitrate for those using cellulose ester filters, loss of particulate nitrate ("negative artifact") from inert filters (e.g. Teflon), and positive and negative artifacts with organics common to all studies using filter sampling.
4. The aerosol species measured were generally relatively limited in number.

a. Artifact Particulate Sulfate (16,17,18)

Artifact particulate sulfate results from partial retention of  $\text{SO}_2$  on filters and can yield, with 24-hour atmospheric samples, errors in the range 3 to 6  $\mu\text{g}/\text{m}^3$ . To illustrate the potential effect of this error, the NASN annual geometric mean sulfate value for downtown Los Angeles in 1974 was 8.4  $\mu\text{g}/\text{m}^3$ . A positive error of 4  $\mu\text{g}/\text{m}^3$  in this value would represent about a 50% error. The coefficient for the contribution of sulfate

to  $b_{sp}$  would be expected to be too low by an equal percentage. Perhaps more significant, the variability introduced into sulfate measurements can decrease the correlation with visibility parameters.

The importance of submicron aerosols in visibility reduction by light scattering leads to the desirability of size-segregated particle sampling in visibility-aerosol chemistry correlation studies.

Recent visibility studies have considered more than particle scattering contributions. In urban areas the particle absorption coefficient, due primarily to graphitic carbon, can contribute substantially to  $b_{ext}$  (6,12-14). For example Groblicki et al. (Table 2) reported a mean contribution to  $b_{ext}$  of 31% due to light absorption by particulate carbon for 41 days of sampling in Denver (6). The contribution of light absorption by particles to the total extinction coefficients in California urban areas has only recently been reported (58).

In Denver the dominant source of atmospheric graphitic carbon was concluded to be from the combustion of wood. However, in California urban areas, mobile source emissions, especially from diesel-powered trucks, are the predominant source of graphitic carbon. The increasing use of diesel-powered passenger cars may serve to increase this source of light extinction.

General Motors has estimated that by the year 2000, 25% of all passenger vehicles will be diesel-powered (15). A simple calculation (Appendix A) permits estimation of a  $\geq 12\%$  decrease in mean visual range in downtown Los Angeles by the year 2000, relative to the 1974-1976

TABLE 2 CONTRIBUTION OF THE CHEMICAL SPECIES TO THE  
EXTINCTION COEFFICIENT, FOR DENVER (NOVEMBER - DECEMBER 1978)<sup>a</sup>

<u>Fine Particulate Species</u>		<u>Mean % Contribution</u>
(NH <sub>4</sub> ) <sub>2</sub> SO <sub>4</sub> and associated H <sub>2</sub> O		20.2
NH <sub>4</sub> NO <sub>3</sub> and associated H <sub>2</sub> O		17.2
Organic C		12.5
Elemental C (scattering)	6.5 <sup>b</sup>	
Elemental C (absorption)	<u>31.2</u> <sup>b</sup>	
Elemental C (total)		37.7 <sup>b</sup>
Remainder fine particulate		6.6
NO <sub>2</sub>		<u>5.7</u>
	TOTAL	100.

a. Data of P. J. Groblicki et al., Reference 6.

b. Includes fine and coarse particulate C<sub>e</sub>.

mean (7.5 miles), due only to the associated increase in graphitic carbon, assuming no controls on such emissions.

If used for short-term sampling, glass fiber filters would yield substantially greater artifact sulfate, expressed in  $\mu\text{g}/\text{m}^3$ .

b. Nitrate Sampling Errors

Artifact particulate nitrate results from retention of gaseous  $\text{HNO}_3$ . Under atmospheric conditions, and with 4-hour samples, essentially all  $\text{HNO}_3$  is retained by glass fiber filters resulting in errors which can represent 50% of the observed nitrate (21). As a result, the corresponding nitrate coefficient in regression equations with visibility parameters may be too low by a factor of about two. Similarly, in short term sampling with cellulose acetate filters, 12% retention for  $\text{HNO}_3$  was observed (20) leading to a corresponding negative error in the nitrate coefficient in correlations with visibility.\* Studies employing inert filters (e.g. Teflon) yield nitrate concentrations which are lower limits to the true particulate nitrate values because of complete penetration of  $\text{HNO}_3$ , and the possibility of nitrate loss by volatilization and reaction with strong acid particles (e.g.  $\text{H}_2\text{SO}_4$ ) and gases (e.g.  $\text{HCl}$ ) (21-23). In such cases the nitrate coefficients in the visibility regression equation would be expected to be

---

\*As with sulfate, the coefficient for the remaining aerosol term is also affected.

too high by an amount which depends on meteorological variables and concentrations of airborne acids.

In addition to altering coefficients, the variability in the relationship between true particle nitrate and that measured by simple filter methods can severely decrease correlation coefficients with visibility parameters.

c. Organic Particle Sampling Errors (24-34, 63)

Of the major classes of aerosol constituents least is known about the errors in sampling organics. Many of the organic materials retained on a filter exist in the gas phase as well. The proportion in each phase in the atmosphere probably varies with atmospheric conditions (e.g. temperature and R.H.), the concentration of the pollutants. The contribution of organics to visibility reduction should reflect the fraction of the organics in the particle phase at any moment. Following collection on a filter, volatile organics may be lost depending on the degree of saturation of the air stream with each organic compound. As an opposing source of error, gas phase organics may be retained by sorption on previously collected particulate constituents and on the filter medium. As a result, neither the magnitude nor direction of the error can be estimated without specific measurements.

As with sulfate and nitrate, the variability introduced in filter sampling of organic particles will probably decrease or eliminate correlations with visibility parameters.

### C. Objectives of the Present Study

1. To assess the contribution to visibility reduction of light scattering and absorption by specific pollutant particles and gases, measuring the aerosol species with minimum sampling artifacts.
2. To measure atmospheric visibility by determining the total light extinction coefficient due to light scattering and absorption in the San Francisco Bay Area, and Los Angeles Basin.
3. To measure gaseous precursors to important visibility-reducing aerosols species to aid in data interpretation and assessment of air quality.
4. To provide further field trials of techniques to measure aerosol species with minimum errors.

### D. Strategy

This study included both a laboratory phase and a field sampling and sample analysis phase. The former focused on the setup, calibration and evaluation of techniques to measure  $b_{ap}$  and elemental carbon ( $C_e$ ). Atmospheric sampling was performed at San Jose, Riverside and downtown Los Angeles for nine, 16-hour days at each site, during the summer of 1982. Table 3 summarizes the sampling scheme. Fine and total sulfate samples were collected minimizing artifacts using Teflon filters. True fine particle nitrate (FPN) was measured with a cyclone plus acid gas denuder and total inorganic nitrate collector (21,36). Total fine nitrate (particle plus gas phase), FN, was measured the same way as for FPN but without the denuder. Nitric acid was then obtained by difference, FN-FPN.

True particulate carbon was sampled with a denuder, intended to remove the gas phase component of relatively non-volatile organic

compounds, followed by a particle filter and a fluidized bed of  $\text{Al}_2\text{O}_3$ . A second unit without the denuder was intended to measure the total of particle plus gas phase components of such relatively non-volatile carbonaceous materials (40). Two hi-vol samplers were operated to provide both short and long-term samples of carbonaceous material. They were also analyzed for sulfate and nitrate for measurement of sampling artifacts.

Samplers 9 and 10 (Table 3) collected fine particulate matter on 25 mm and 47 mm Nuclepore filters, provided samples for the integrating plate method (41) differing by a factor of about five in filter loading per unit area. Sampler 11 provided a sample for measuring  $b_{ap}$  and  $C_e$  with the laser transmission method (42). Two integrating nephelometers were used, one operating at ambient temperature and the second with the inlet air heated above ambient. The difference provided an upper limit estimate of  $b_{sw}$ , the scattering coefficient due to liquid water. The limitations of this approach are discussed in Section V. Appendix B details the calibration and operation of these nephelometers. The analytical strategy, totaling 2,826 determinations, is shown in Table 4.

TABLE 3 DESCRIPTION OF SAMPLERS EMPLOYED FOR VISIBILITY STUDY

<u>Sampler No.</u>	<u>Sampler</u>	<u>Sampling Rate (LPM)</u>	<u>Filter Size</u>	<u>Time (Hr)</u>	<u>Species Measured</u>
2	Cyclone, acid-gas denuder, <sup>c</sup> Teflon and NaCl/W41 filter	20	47mm	4	True fine particle NO <sub>3</sub> <sup>-</sup> , SO <sub>4</sub> <sup>=</sup>
1 <sup>d</sup>	Cyclone, teflon and NaCl/W41 filter	20	47mm	4	Fine particle NO <sub>3</sub> <sup>-</sup> + HNO <sub>3</sub> , SO <sub>4</sub> <sup>=</sup> , fine mass
3 <sup>a</sup>	Teflon and NaCl/W41 filter	20	47mm	4	TSP, total particle NO <sub>3</sub> <sup>-</sup> + HNO <sub>3</sub> , True total SO <sub>4</sub> <sup>=</sup>
4	Organics denuder, quartz filter, Al <sub>2</sub> O <sub>3</sub> fluidized bed	9.5	37mm	12	True particulate carbon, C <sub>e</sub>
5	Quartz filter <sup>e</sup> , Al <sub>2</sub> O <sub>3</sub> fluidized bed	9.5	37mm	12	Particulate + low v.p. gaseous carbon, C <sub>e</sub>
6	Quartz filter <sup>f</sup> , 2 oxalic acid impregnated filters <sup>g</sup>	20	47mm	4	NH <sub>4</sub> <sup>+</sup> , NH <sub>3</sub>
7	Hi-vol (prefired glass fiber) <sup>h</sup>	40 (cfm)	20 X 25cm	4	SO <sub>4</sub> <sup>=</sup> , NO <sub>3</sub> <sup>-</sup> , C <sub>o</sub> , C <sub>e</sub> , C <sub>t</sub> <sup>i</sup>
8	Hi-vol (prefired glass fiber)	40 (cfm)	20 X 25cm	16-24	SO <sub>4</sub> <sup>=</sup> , NO <sub>3</sub> <sup>-</sup> , C <sub>o</sub> , C <sub>e</sub> , C <sub>t</sub>
9 <sup>a</sup>	Cyclone plus Nuclepore filter <sup>j</sup>	8	25mm	4	b <sub>ap</sub> (integrating plate method)
10 <sup>d</sup>	Cyclone plus Nuclepore filter	8	47mm	4	b <sub>ap</sub> (integrating plate method)
11	Cyclone, quartz <sup>k</sup> filter	27.5	47mm	4	b <sub>ap</sub> (laser transmission method), C <sub>e</sub>
	Nephelometer, (MRI 1560)	28 (cfm)		continuous	b <sub>sp</sub> at ambient temperature
	Nephelometer, heated (MRI 1560)	5 (cfm)		continuous	b <sub>sp</sub> for dry particles
	Dew point and Ambient Temperature	--		continuous	Relative humidity and temperature
	Hygrothermograph	--		continuous	Relative humidity and temperature

TABLE 3 DESCRIPTION OF SAMPLERS EMPLOYED FOR VISIBILITY STUDY  
(Cont'd)

<u>Sampler No.</u>	<u>Sampler</u>	<u>Sampling Rate (LPM)</u>	<u>Filter Size</u>	<u>Time (Hr)</u>	<u>Species Measured</u>
--	Dasibi Model 1003AH O <sub>3</sub> Analyzer			continuous	O <sub>3</sub>
--	Teco Model 14B/E			continuous	NO, NO <sub>2</sub>
--	Teco Model 43			continuous	SO <sub>2</sub>

- <sup>a</sup> Samplers 3 and 9 sampled from the same Teflon-lined AIHL cyclone, with combined flow rate 28 Lpm (50% cut-point for unit density spheres, 2.2 μm).  
<sup>b</sup> 2 μm pore size Ghia Zefluor filters.  
<sup>c</sup> NaCl-impregnated Whatman 41 (cellulose) filter.  
<sup>d</sup> Samplers 1 and 10 sampled from the same Teflon-lined cyclone, with combined flow rate 28 Lpm (50% cut-point for unit density spheres, 2.2 μm).  
<sup>e</sup> Prefired Pallflex 2500 QA0 quartz filters.  
<sup>f</sup> Prefired Pallflex 2500 QAST quartz filters.  
<sup>g</sup> Oxalic acid impregnated glass fiber (prefired Schleicher and Schnell 1981 EPA Grade).  
<sup>h</sup> Prefired Schleicher and Schnell 1981 EPA Grade glass fiber filters.  
<sup>i</sup> C = elemental C, C<sub>o</sub> = organic C, C<sub>t</sub> = total C  
<sup>j</sup> 0.4 μm pore size.  
<sup>k</sup> An all Teflon cyclone with total flow rate 28 Lpm. The collection efficiency of this cyclone for 3.5 μm particles was about 80%.  
<sup>l</sup> Sampled through a 15 cm long, 3.2 cm I.D. polycarbonate tube on to a filter in a Nuclepore open face filter holder.

Table 4 ANALYTICAL STRATEGY FOR VISIBILITY STUDY

Sampler No.	Medium	Mass	SO <sub>4</sub> <sup>=</sup>	NO <sub>3</sub> <sup>-</sup>	NH <sub>4</sub> <sup>+</sup>	b <sub>ap</sub> and C <sub>e</sub> LPM	bap IPM	C <sub>t</sub>	Reflectance C <sub>e</sub>
1	Teflon	108	108	108					
1	NaCl/W41			108					
2	Teflon	108	108	108					
2	NaCl/W41			108					
3	Teflon		108	108					
3	NaCl/W41			108					
4	QAQ Quartz							36	36
4	Al <sub>2</sub> O <sub>3</sub>							36	36
5	QAQ Quartz							36	36
5	Al <sub>2</sub> O <sub>3</sub>							36	36
6	QAST Quartz				108				
6	Oxalic/glass fiber				108				
7	Baked glass fiber		108	108				216	
8	Baked glass fiber		18	18				36	
9	Nuclepore						108		
10	Nuclepore						108		
11	2500 QAQ					108			108
Totals:		216	450	774	216	180	216	396	180

### III. MEASUREMENT OF THE PARTICLE ABSORPTION COEFFICIENT ( $b_{ap}$ )

#### A. The Integrating Plate Method (IPM)

The measurement of  $b_{ap}$  is most commonly done with samples collected on an appropriate filter medium using the integrating plate method (IPM) developed by Lin et al. at the University of Washington (41,43). The IPM method is fast, simple, inexpensive, reported to be relatively insensitive to the geometry of the measuring device, and has received rather wide use (44,45). In the IPM, a collimated light beam ( $\lambda = 500 \text{ nm}$ ) is directed onto a filter, normal to the filter surface, with the particulate matter facing the beam (Figure 2). A piece of opal glass beneath the filter diffuses the transmitted and forward-scattered light. The resulting isotropic light flux emitted from the opposite side of the opal glass is measured with a photodetector. The transmittance of a loaded filter,  $T$ , is measured relative to that of a blank filter (set equal to 100%). The purpose of the neutral density filter will be discussed later.

Particulate matter on the filter both absorbs and scatters light, the latter principally in the forward direction. The integrating plate (i.e. the opal glass) is intended to permit measurement of the sum of transmitted and scattered light. If effective, the decrease in transmittance is related only to the absorbance of the particulate matter. The absorption coefficient is then measured by:

$$\frac{T(\%)}{100} = \frac{I}{I_0} = e^{-L \cdot b_{ap}}$$

Where:  $I$  = light intensity measured with loaded filter

$I_0$  = light intensity measured with blank filter

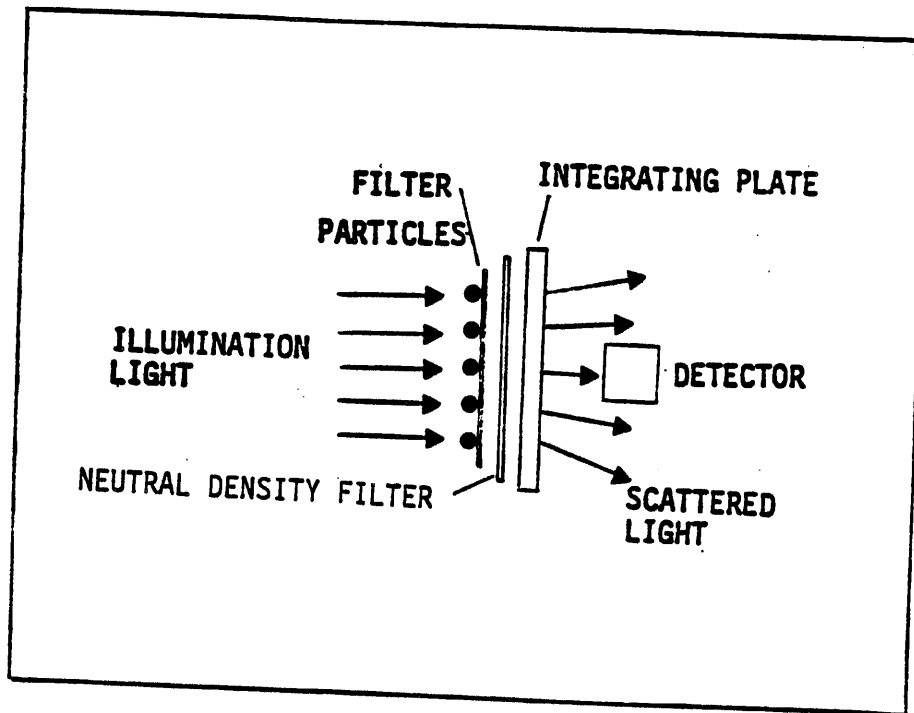


Figure 2. Schematic of Integrating Plate Method (IPM).

L = the ratio of the air volume sampled to the particulate deposit area on the filter

$$\text{Thus: } b_{ap} = \frac{\ln I_0/I}{L} \text{ in the units (distance)}^{-1}$$

To yield accurate absorption coefficients, it is necessary that the incident beam strikes each particle only once, and that light absorbing particles not be shielded by other particles. Accordingly, particle loadings < 20  $\mu\text{g}/\text{cm}^2$  have been recommended. Use of a filter with minimal absorbance also should increase the precision of measuring  $b_{ap}$ . The Lin procedure uses Nuclepore filters, which provide low absorbance, a refractive index similar to that of atmospheric particles, and minimal penetration of particles into the filter so that multiple absorption is minimized.

The Lin procedure is subject to error due to multiple reflection between the upper surface of the opal glass and the Nuclepore filter. This multiple reflection provides an opportunity for multiple absorption of light by the particulate matter. To minimize this effect, a neutral density (ND) optical filter was inserted between the Nuclepore filter and opal glass (43). The ND filter attenuates the multiply-reflected light.

In support of this technique, Lin reported (41) that a Nuclepore filter loaded with non-absorbing NaCl aerosol exhibited a transmittance of 99%, indicating that the light scattered from these particles still reached the detector. Since no neutral density filter was employed with this experiment, and the particles faced away from the light source, this value may have limited relevance to the IPM as currently done.

A more recent evaluation (45) with a non-absorbing aerosol  $(\text{NH}_4)_2\text{SO}_4$ , as well as mixtures of absorbing and non-absorbing materials, also done without an ND filter, revealed a small

apparent absorption for  $(\text{NH}_4)_2\text{SO}_4$ , about 1% of that for an equal mass of carbon (soot).

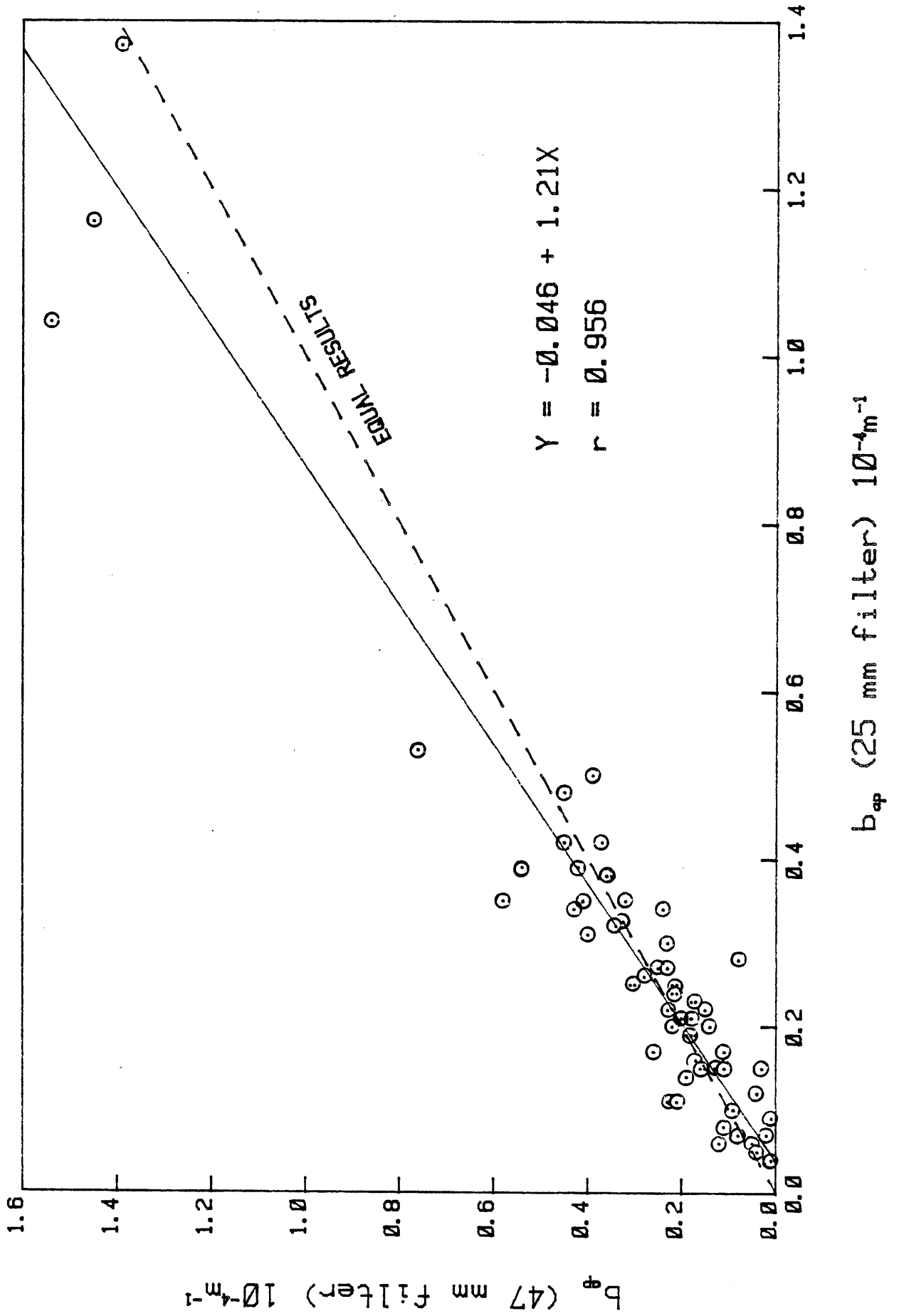
For the present study our objectives were (1) to evaluate the sensitivity of the technique to wavelength and geometry, (2) to evaluate and improve, if necessary, the precision of the method, (3) to evaluate factors influencing the accuracy of the method (e.g. the use of neutral density filter), and (4) to compare results with those obtained by University of Washington personnel with the same samples. Appendix C details these evaluations.

The precision of the IPM method with loaded filters was found to be 0.3 to 1.4% coefficient of variation (C.V.). In parallel atmospheric sampling, the C.V. between samplers was  $\leq 1.7\%$ . A comparison with the University of Washington yielded % transmittance (T) values for loaded Nuclepore filters which agreed within 1 to 2% T.

The accuracy and precision of the method varied with loading. Very lightly loaded samples gave reduced precision. However, samples with particle loadings  $> \text{ca. } 20 \mu\text{g}/\text{cm}^2$  no longer approximate the requirements for the IPM method. Accordingly, in the present study, parallel atmospheric samples were collected with 25 mm and 47 mm filters at the same flow rate (8 Lpm) to obtain particle loadings per unit area differing by about a factor of five. It was intended that at least one of the sample pairs would provide an appropriate sample. In this sampling, the loadings on the 47 mm filter samples were  $\leq 16 \mu\text{g}/\text{cm}^2$ , and, except at San Jose, most of the 25 mm samples exceeded  $20 \mu\text{g}/\text{cm}^2$  loadings.

Figure 3 compares  $b_{ap}$  determinations for the 47 and 25 mm filter samples. Samples yielding  $b_{ap}$  values  $< 0.04$  have been excluded. The data show good correlation and a ratio of mean values, 47 mm: 25 mm filters, of 1.04. Nevertheless, the least squares slope and intercept differ significantly from 1.0 and zero, respectively ( $p = 0.99$ ). We consider the  $b_{ap}$  values  $< 0.1$  to be more reliably

Figure 3. Comparison of  $b_{ap}$  Measurements at Two Particle Loadings



measured by the 25 mm filter. Values > 0.6 are considered to be more reliably measured with the 47 mm filter.

B. A Laser Transmission Method (LTM)

Rosen et al., at the Lawrence Berkeley Laboratory, have devised a version of the IPM which measured the transmission of light from a He-Ne laser (632.8 nm) passing through atmospheric particulate-loaded filters (42). In this system the integrating plate is eliminated and the filter, itself, is used to provide uniform intensity to all forward-scattered light. In addition, a large lens immediately behind the sample filter is used to focus the light onto the detector, increasing the sensitivity of the measurement and possibly decreasing errors due to light scattering. The decreased light intensity reaching a detector relative to that with a blank filter, is assumed to be due to light absorption by the particles.

The reported advantages of the LTM compared to the IPM, are its applicability to more heavily loaded samples, and the suitability of filter media other than Nuclepore, including quartz fiber. The latter would also permit combustion analysis for total, organic and elemental carbon. Accordingly, this technique was included in the present study.

Figure 4 compares University of Washington IPM and LBL LTM results for co-collected samples (46). The LTM method was used with both Millipore cellulose ester membrane filters and prefired Pallflex quartz filters. The LTM method showed reasonable agreement for the two filter types but differed by, on average, a factor of 2.5 from the IPM. R. Weiss (47) believes that the factor of 2.5 higher results by LTM is due to multiple absorption because particles penetrate substantially beneath the cellulose ester and quartz filter surfaces. Within the filter matrix, each particle could intercept the incident light more than once as the light is scattered by surfaces. Since the IPM has been reported to measure  $b_{ap}$  with an

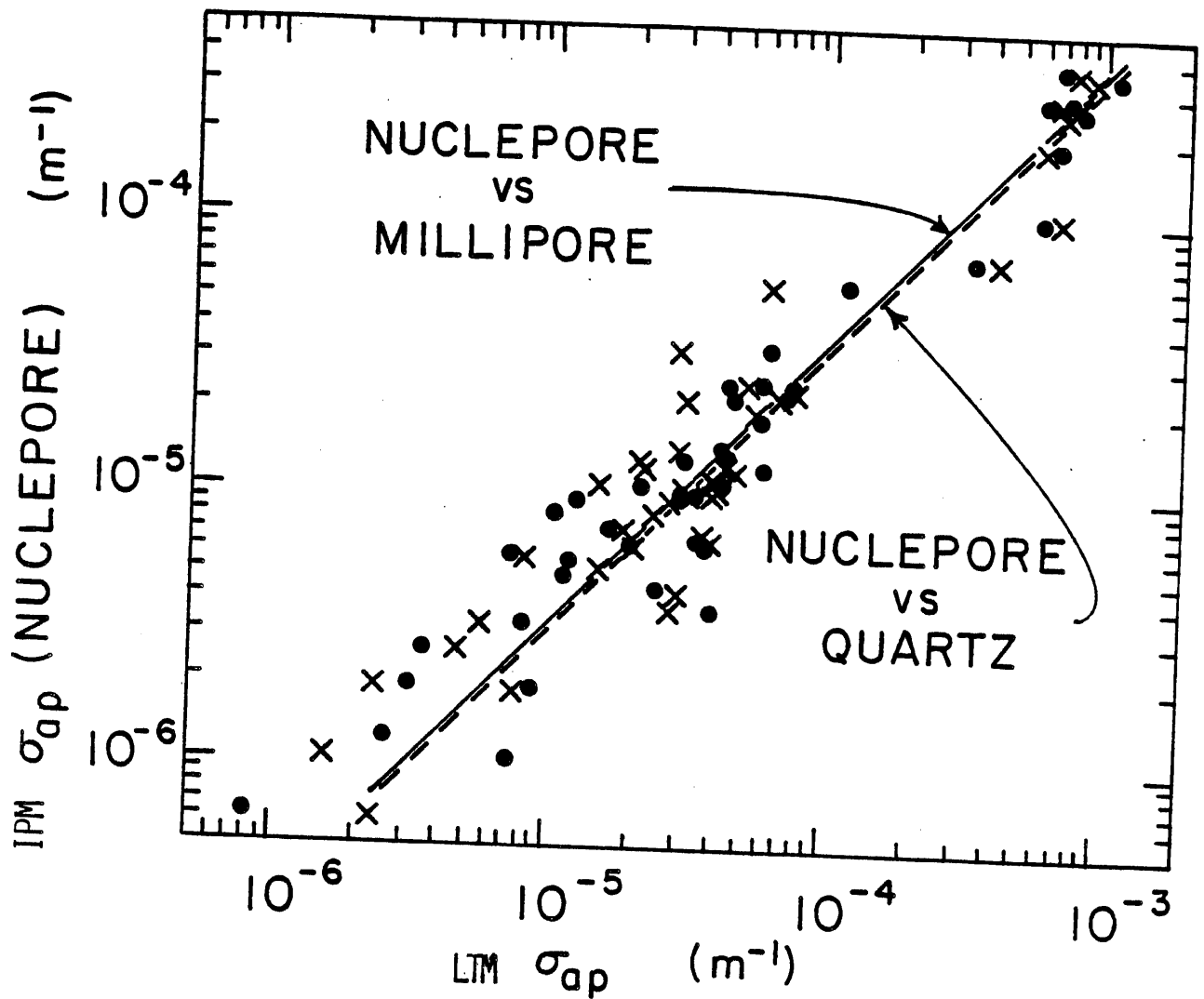


Figure 4 Comparison of the Integrating Plate Method and Laser Transmission Techniques for Absorption Coefficient Measurement (x = Millipore, • = Quartz)

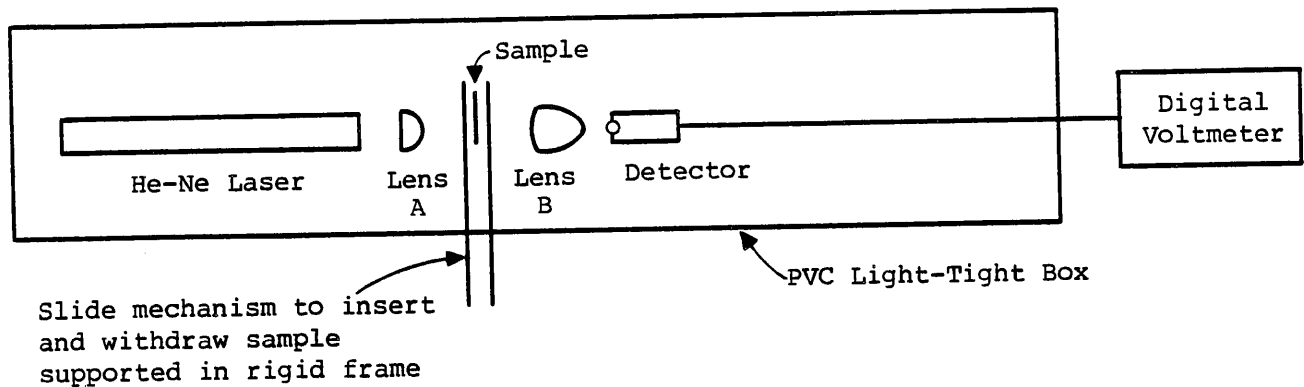
error of  $\pm 15\%$ , (43) the  $b_{ap}$  measurements by the LTM would require substantial correction. However the LTM was also compared to a photoacoustic method and showed almost perfect agreement (45). When compared to a similar photoacoustic method, the IPM gave higher results by a factor of 1.3. Given these inconsistencies, the factor of two uncertainty in absorption coefficient measurements estimated elsewhere (45, page 28) seems prudent.

Figure 5 is a diagram of an LTM apparatus as constructed at AIHL. The unit differs from the LBL apparatus principally in the detector, a photodiode/op amp in place of a photomultiplier tube. Our initial evaluation of this technique considered: (1) Linearity of the detector response with change in light intensity, (2) precision, (3) effect of filter medium, (4) effect of particulate orientation (toward or away from the light source), (5) comparison with the IPM for  $b_{ap}$  measurement, (6) the influence of wavelength, and (7) comparison of LTM results by AIHL and LBL.

As detailed in Appendix C, linearity was excellent throughout the range relevant to loaded quartz filter samples. The precision of  $b_{ap}$  measurements was 2 and 4.4% (C.V.) for Millipore and quartz filters, respectively. Analyses of the same filter samples by AIHL and LBL showed high correlation ( $r = 0.9999$ ).

C. Comparison of  $b_{ap}$  Determinations by The IPM and LTM

Figure 6 compares results by the two methods for the atmospheric samples collected at the three sampling sites in the current field study. For this comparison, IPM results with 25 mm and 47 mm parallel filter samples were averaged, except where one or both  $b_{ap}$  values was  $< 0.04 \times 10^{-4} \text{ m}^{-1}$ . For such low absorption coefficients, the higher face velocity results (i.e., those for 25 mm filters) were considered more accurate. The results are highly correlated. The ratio of mean values LTM:IPM is 2.72. Since the preponderance of current data suggests the IPM to be more accurate for the measurement



Laser: 632.8nm, 0.5mW, Spectraphysics Model 155, random polarization.

Lens A: 12.4mm diameter, 14.3mm focal length, plano-convex lens to expand beam to a 1.2cm diameter disc on the filter sample.

Lens B: 60mm diameter, 39mm focal length, aspheric lens, Rolyon optics.

Detector: EG & G Model HUV-1000B silicon photovoltaic detector/operational amplifier combination, positioned at focal point of lens B.

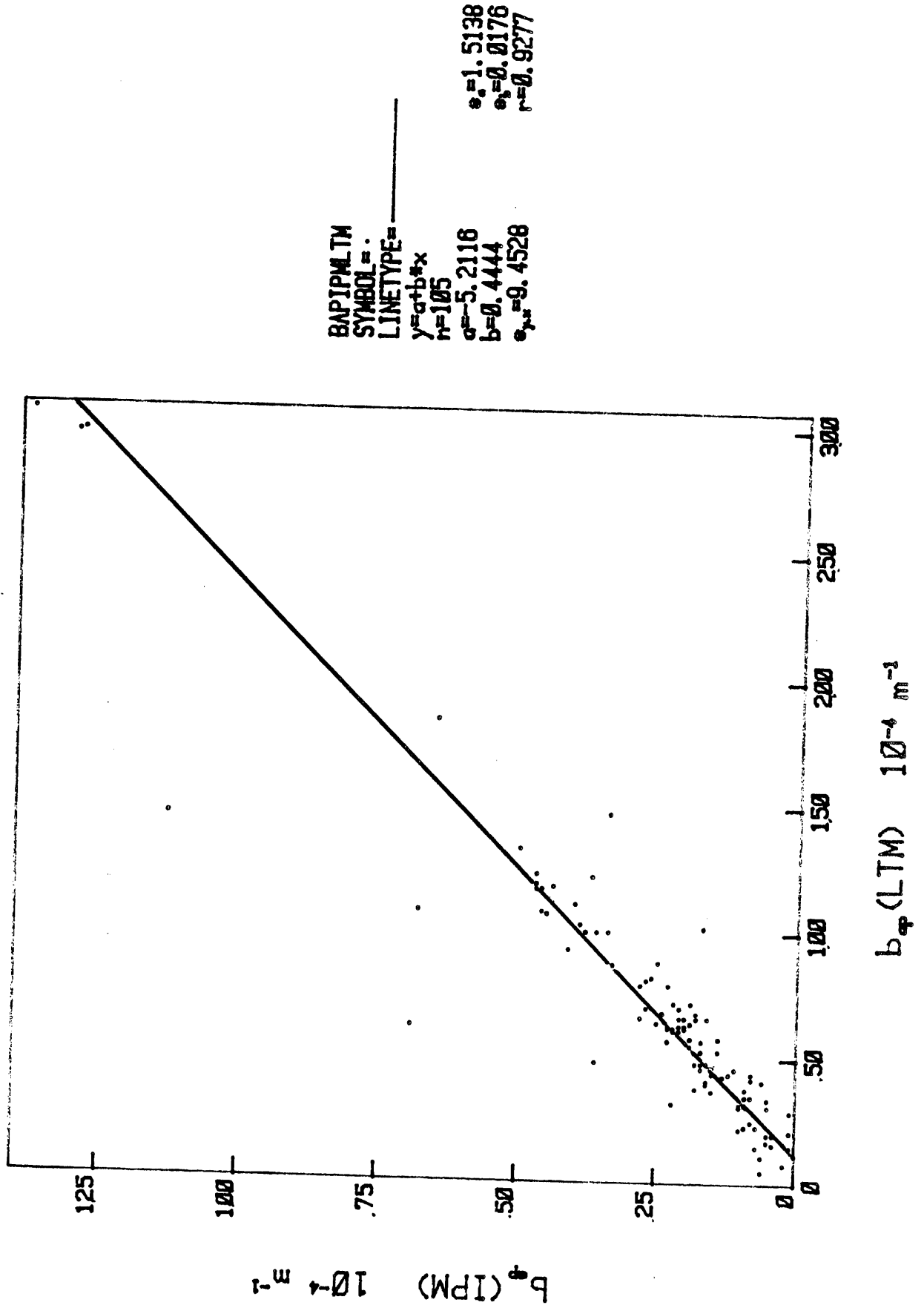
DVM: Fluke Model 8000A digital multimeter.

Base: 1/2" flat steel plate optical bench permitting use of clamps with magnetic bases.

Enclosure: 1/2" PVC sheet.

Figure 5. Schematic Diagram of Laser Transmission Method, Viewed From Above.  
(not to scale)

Figure 6. Comparison of  $b_{ap}$  Measurements by the IPM and LTM Methods



of  $b_{ap}$ , the LTM was judged potentially suitable only for elemental carbon measurement.

#### IV. DETERMINATION OF ELEMENTAL CARBON ( $C_e$ )

##### A. Introduction

Elemental or black carbon is the major contributor to the particle absorption coefficient,  $b_{ap}$ . However, discrimination between organic and elemental carbon ( $C_e$ ) is difficult. A selective combustion method (SCM) and a reflectance method (RM) were previously used for this purpose (34). The former gave results which were believed to be in error by ca. 20%. The RM yielded results which, with 24-hr hi-vol filter samples, were too low by a factor of two. While more accurate, the SCM is slow and relatively difficult. Accordingly, an effort was made to improve the calibration of the RM. In addition, the laser transmission method (LTM) was calibrated for use in measuring  $C_e$ .

As detailed in Appendix D, for the current study the LTM as well as the RM were calibrated with butane flame-derived soot of known particle size distribution prior to collection. In addition, calibration employed samples supplied by LBL including diesel soot, atmospheric particulates and vehicle tunnel air particulate samples. The LBL samples were analyzed for elemental carbon by a thermal analysis technique correcting for decomposition (60). The RM calibration appeared to be relatively insensitive to the source of the carbon standard whereas the LTM calibration showed great variation.

##### B. The Laser Transmission Method for $C_e$ (42).

LBL has used the LTM technique to measure black or elemental carbon.

$$C_{total} = [C_{black}] + [C_{organic}]$$

Thus by measuring total C and black C, organic C can be obtained by difference (correcting for carbonate C if necessary). If black

carbon is assumed to be proportional to the absorbance of a loaded filter:

$$\begin{aligned}C_{\text{black}} &= \frac{1}{K} [-100 \ln (I/I_0)] \\ &= \frac{1}{K} [\text{Attn}]\end{aligned}$$

Where: Attn = Attenuation =  $-100 \ln (I/I_0)$

K = a constant

The attenuation per unit mass of  $C_{\text{total}}$ , or specific attenuation,  $\sigma$ , is defined by:

$$\sigma = \frac{\text{Attn}}{[C_{\text{total}}]} = \frac{K[C_{\text{black}}]}{[C_{\text{total}}]}$$

Employing laboratory-generated and ambient air elemental carbon samples, the LBL group determined a mean value for K of  $20 \frac{\mu\text{g}}{\text{cm}^2}$  when deposited on a Millipore filter. Thus:

$$C_{\text{black}} (\mu\text{g}/\text{cm}^2) = \frac{\text{Attn}}{20}$$

### C. Intermethod and Interlaboratory Comparisons

Calibrations results are summarized in Table 5. For ease in identification, the calibrations were coded as shown. Elemental carbon values obtained with these calibration for ten fine particulate atmospheric samples are compared to the corresponding total carbon values in Table 6. Samples identified with the letters J - Q were collected in Riverside and the remaining, in downtown Los Angeles.

Comparing ratios of mean values, elemental carbon calculated from LTM-1 (i.e. the LTM using the aged butane flame carbon) yielded

TABLE 5

## CALIBRATIONS OF OPTICAL METHODS FOR ELEMENTAL CARBON

Carbon Source	Reflectance Method (RM) <sup>a</sup>	Code for RM Calibration	Laser Transmission Method (LTM) <sup>b</sup>	Code for LTM Calibration
Butane Flame	a = 0.0309, b = 1.68 (r = 0.957)	-----	a = 5.59, b = 6.88 (r = 0.992)	LTM-1
LBL Carbon Samples	a = 0.0366, b = 1.62 (r = 0.99)	-----	a = 11.1, b = 23.1 (r = 0.964)	LTM-2
LBL Samples and Butane Flame	a = 0.0337, b = 1.65 (r = 0.974)	RM-4	-----	

a. Slope, intercept and correlation coefficient for the equation  $\log y = \log a + b \log x$ , where:  $y = (100-R)/200R$  and  $x = \text{elemental or black carbon, } \mu\text{g/cm}^2$ . R = % Reflectance.

b. Slope, intercept and correlation coefficient for the equation  $-100 \ln (I/I_0) = a + b (C)$ , where I and  $I_0$  are light intensity through loaded and clean filters, respectively, and  $C_e$  is elemental or black carbon,  $\mu\text{g/cm}^2$ .

TABLE 6

COMPARISON OF TOTAL CARBON AND ELEMENTAL CARBON ( $C_e$ ) VALUES ( $\mu\text{g}/\text{m}^3$ )<sup>a</sup>

Sample ID	Total C	$C_e$ (LTM-1)	$C_e$ (LTM-2)	$C_e$ (RM-4)	Mean $C_e$ <sup>b</sup>
J1159Q11	25.15	28.55	5.87	5.41	5.64 ± .33
M1176Q011	18.03	6.62	1.61	1.40	1.51 ± .15
01183Q011	13.89	12.37	2.73	2.44	2.59 ± .21
01185Q011	12.0	11.51	2.56	2.12	2.34 ± .31
P1186Q011	16.50	22.88	4.76	4.35	4.56 ± .29
Q1192Q011	13.80	9.24	2.12	1.83	1.98 ± .21
T1202Q011	17.02	25.6	5.30	3.98	4.64 ± .93
U1209Q011	4.46	7.57	1.79	1.01	1.40 ± .55
W1214Q011	36.16	59.34	11.83	11.00	11.42 ± .59
X1221Q011	13.54	10.03	3.99	3.01	3.50 ± .69
Ratio of Means:	1.00	1.13	0.25	0.21	0.23

a. The terms LTM-1, LTM-2 and RM-4 are defined in Table 5.

b. Mean of results by LTM-2 and RM-4 methods.

values which averaged 13% higher than the total carbon. Thus this calibration was rejected as inappropriate. The remaining techniques yielded  $C_e$  values averaging 21 to 25% of the total C. This compares to an average of 20% reported elsewhere by similar optical techniques (59). The results by the laser method (LTM-2) were higher by, on average, 19%, compared to those by reflectance.

Figure 7 is a scatter diagram of  $C_e$  determinations by LTM-2 against those by RM-4 for about 100 fine particulate samples from the current program. Symbols A,B,C,D indicate 1,2,3,4 data points, respectively, at the same locations. The results are highly correlated, show a negligible intercept, and average 15.5% higher by the LTM.

Eight respirable particle samples which, by our optical methods, ranged in  $C_e$  loading from 1 to 8  $\mu\text{g}/\text{cm}^2$ , were analyzed by the General Motors Research Laboratory. In the GM technique (49) filter samples are dropped into a furnace at 950° in helium. The evolved pyrolysis products are subsequently converted to  $\text{CO}_2$  and analyzed by a non-dispersive infra-red method to yield "apparent organic carbon". Oxygen is then introduced into the furnace section containing the sample and the resulting  $\text{CO}_2$  is used to measure "apparent elemental carbon". The method is believed to be subject to error from charring during analysis which would yield elevated  $C_e$  values.

Table 7 lists the AIHL and GM results. The AIHL values show  $C_e$  obtained by the LTM, RM and mean values by those techniques. In addition to  $C_e$  results, GM's values for organic carbon are also given. The optical methods were highly correlated with the GM values ( $r \geq 0.95$ ) but yielded results which were about 25% lower. Given the uncertainty in defining organic and elemental carbon in atmospheric samples, none of these methods can as yet be considered to be more nearly "correct".

Figure 7. Elemental Carbon by the LTM vs. Reflectance Method

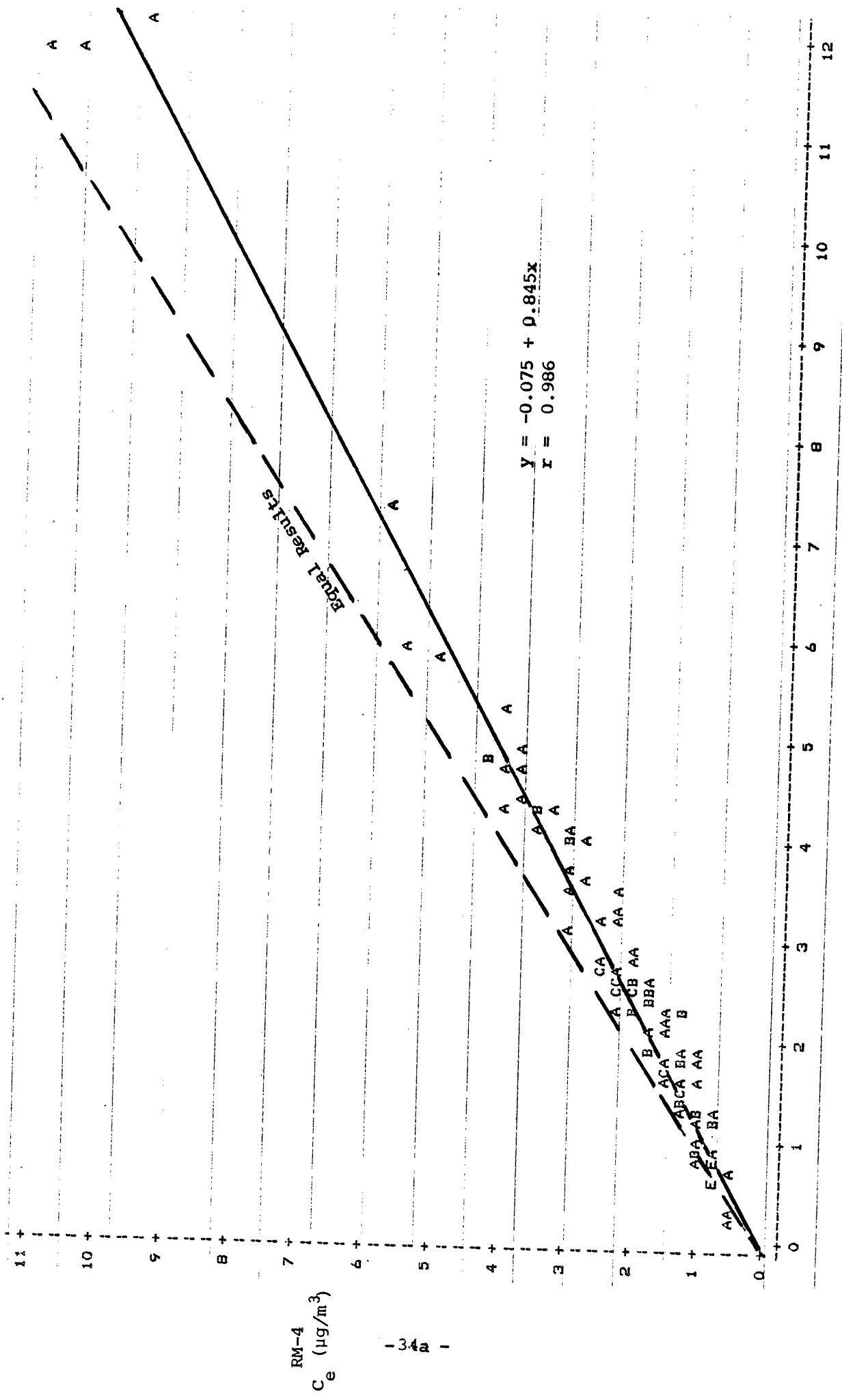


TABLE 7

COMPARISON OF ELEMENTAL CARBON MEASUREMENTS BY  
GENERAL MOTORS' COMBUSTION AND AIHL OPTICAL METHODS ( $\mu\text{g}/\text{m}^2$ )

Sample	$C_e$				$C_o$
	LTM <sup>a</sup>	RM <sup>b</sup>	Mean $C_e$ <sup>c</sup>	GM	GM
J1161Q011	2.92	2.49	$2.70 \pm 0.03$	$3.9 \pm 0$	$12.4 \pm 0.4$
L1169Q011	1.07	0.94	$1.01 \pm 0.09$	$2.4 \pm 0.1$	$9.1 \pm 0.3$
R1194Q011	2.67	1.95	$2.31 \pm 0.51$	$3.5 \pm 0.1$	$9.5 \pm 0.5$
R1196Q011	1.20	0.82	$1.01 \pm 0.27$	$2.3 \pm 0.3$	$7.6 \pm 0.4$
V1210Q011	8.35	6.55	$7.45 \pm 1.27$	$11.0 \pm 0.4$	$18.1 \pm 0.8$
W1217Q011	3.32	2.63	$2.97 \pm 0.49$	$3.2 \pm 0.1$	$8.7 \pm 0.4$
X1218Q011	8.01	7.16	$7.59 \pm 0.60$	$8.6 \pm 0.1$	$15.2 \pm 0.8$
X1219Q011	5.05	3.96	$4.51 \pm 0.77$	$7.1 \pm 0.3$	$17.8 \pm 1.5$
Blank	0	0	0	< 0.1	$1.8 \pm 0.8$
Regression Equations:		Mean $C_e = -0.141 + 0.748$ (GM $C_e$ )		$r = 0.956$	
		LM $C_e = -0.36 + 0.845$ (GM $C_e$ )		$r = 0.969$	
		RM $C_e = -0.375 + 0.702$ (GM $C_e$ )		$r = 0.947$	

- a. Laser transmission method.  
b. Reflectance method.  
c. Mean results by the LTM and RM.

D. Comparison of  $C_e$  by Optical Methods with Particle Absorption Coefficient Results

Since  $C_e$  is the nearly exclusive source of light absorption in suspended atmospheric particles, and since most of the  $C_e$  is in the fine particle fraction, a linear correlation is expected between fine particle concentration  $C_e$  and the light absorption coefficient ( $b_{ap}$ ). For example, Figure 8 shows General Motors' results for Winter Denver aerosol (6). The mean slope was  $11.8 \text{ m}^2/\text{g}$  ( $0.118 \times 10^{-4} \text{ m}^2/\mu\text{g}$ ) and correlation coefficient, 0.93. The  $b_{ap}$  values for the Denver study were obtained by the integrating plate method (IPM), (but without a neutral density filter as employed in the present study)\* and  $C_e$ , by General Motors' controlled combustion technique (49). The latter yielded results equal, within experimental variability, to the interlaboratory mean values for  $C_e$  and organic carbon  $C_o$  by combustion methods with 24-hr hi-vol samples, in the GM Round Robin comparison.

Figures 9 - 11 are scatter diagrams for about 100 atmospheric samples from the present study plotting,  $C_e$  (LTM-2),  $C_e$  (RM-4) and mean fine particle  $C_e$  values against means  $b_{ap}$  values by the IPM. The intercepts are negligible in all cases, and the mean slopes are 11.1, 12.9 and  $12.0 \text{ m}^2/\text{g}$ , respectively. Thus the results are similar to those by GM in Denver, implying reasonable agreement between our optical methods and GM's selective combustion technique.

These values for atmospheric  $C_e$  may be compared to the absorption coefficient per unit mass for soot. Heitzenberg reports a value of

---

\*Better accuracy is expected for the IPM with N.D. filter. The GM  $b_{ap}$  values are inferred to be 5-10% too high (50).

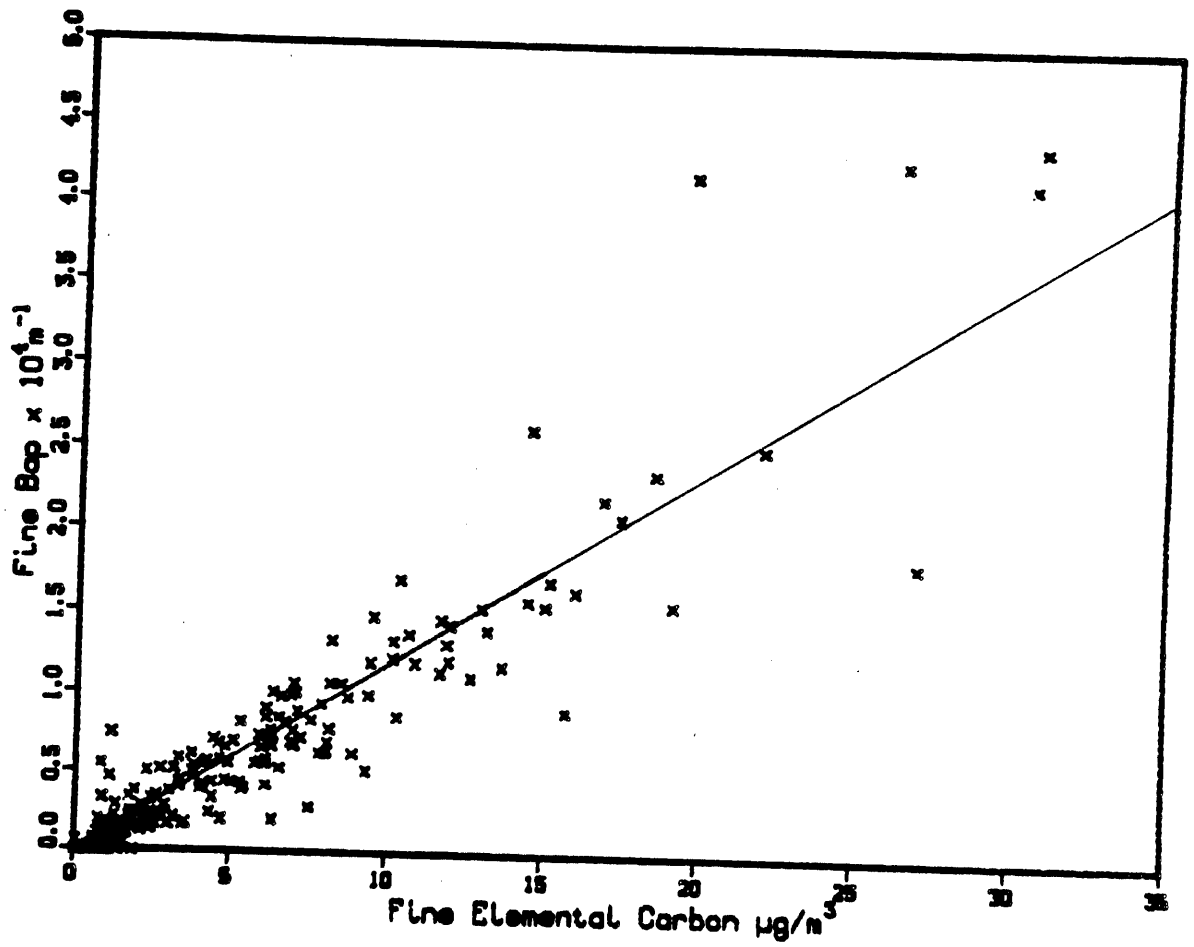
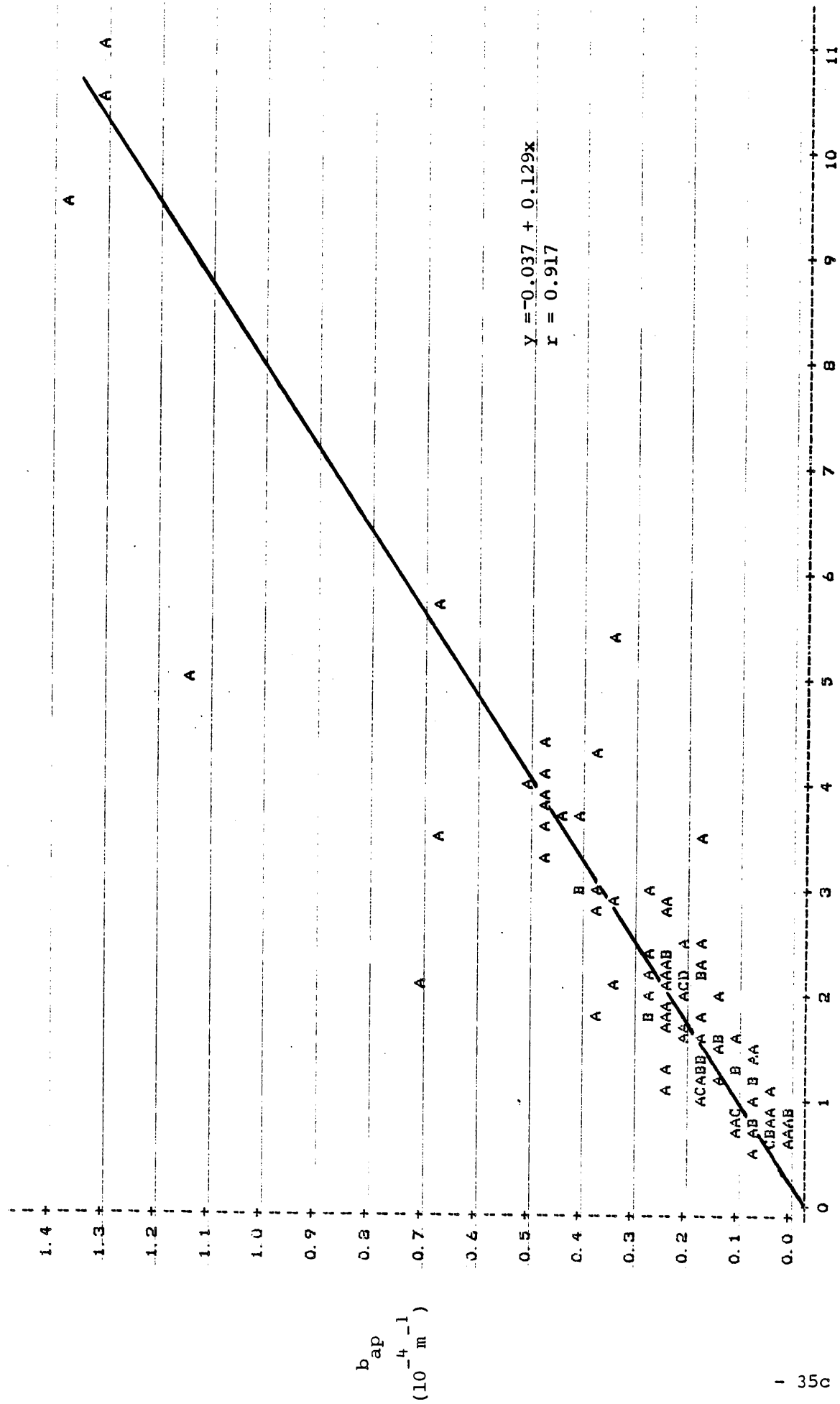


Figure 8. Relation between Absorption Coefficient and  $C_e$  for Denver Winter Aerosol (Ref. 6)

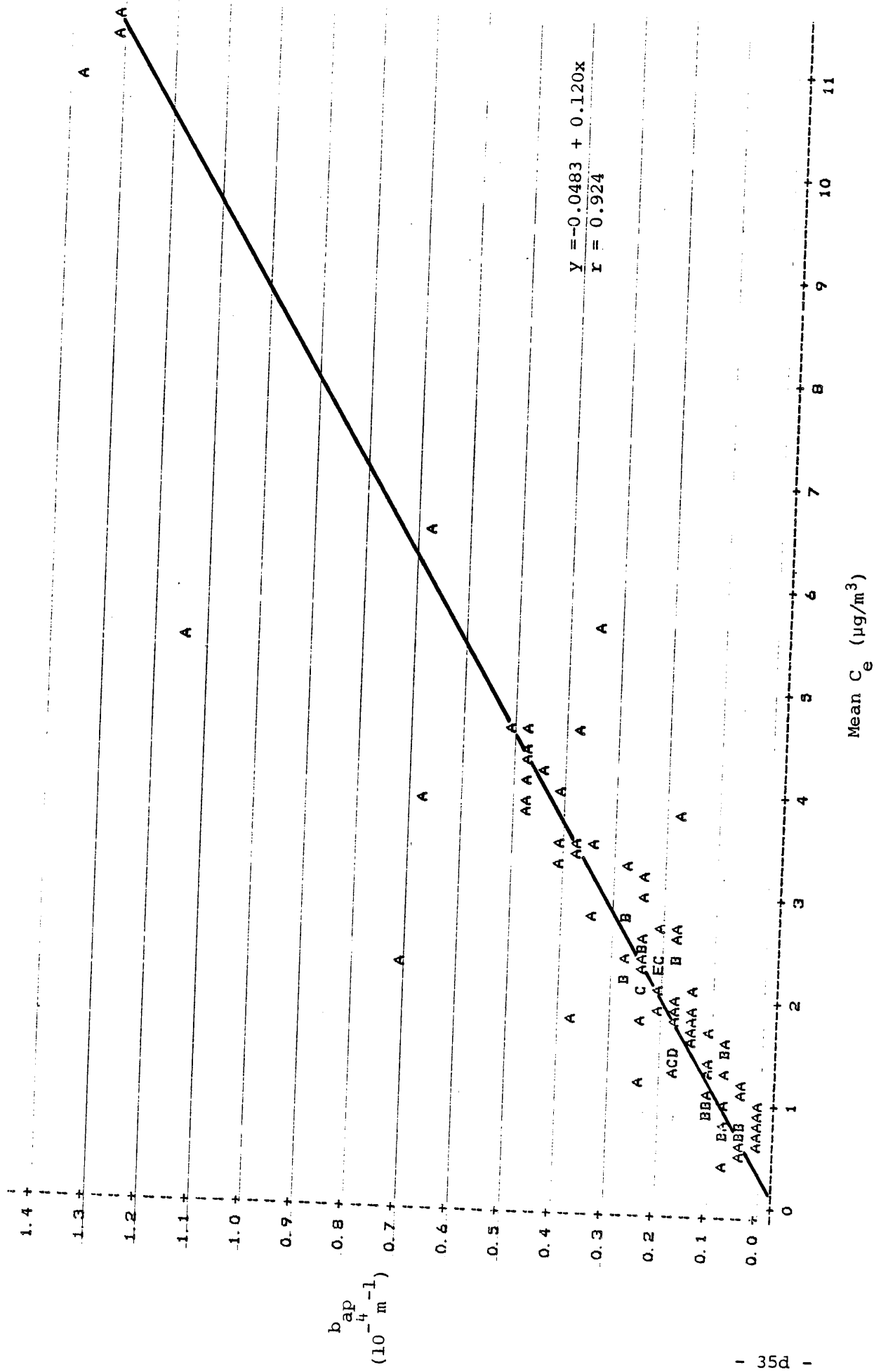


Figure 10 Elemental Carbon by the RM vs. Absorption Coefficients



RM-4 C<sub>e</sub> (µg/m<sup>3</sup>)

Figure 11. Mean Elemental Carbon by LTM and RM vs. Absorption Coefficients



These values for atmospheric  $C_e$  may be compared to the absorption coefficient per unit mass for soot. Heitzenberg reports a value of  $9.7 \text{ m}^2/\text{g}$  (13) but notes that in mixtures with non-absorbing material, the value increases. Clarke and Waggoner (50) report a mean value of  $10.1 \pm 2.1 \text{ m}^2/\text{g}$  ( $n = 4$ ) for soot collected on Nuclepore filters.

Previous studies showed measurable absorption by coarse as well as fine particle  $C_e$ . Employing mean  $C_e$  values and multiple regression analysis for 104, four-hour periods yields the equation (in units  $10^{-4} \text{ m}^{-1}$ ):

$$b_{ap} = -0.048 \pm 0.15 + 0.116 \pm 0.008 (C_e)_{\text{fine}} + 0.02 \pm 0.029 (C_e)_{\text{coarse}}$$

$$r = 0.925.$$

Thus the absorption efficiency for coarse  $C_e$ , per unit mass concentrations, is not significantly different from zero. Furthermore, the addition of coarse  $C_e$  does not significantly improve the correlation with  $b_{ap}$  ( $r = 0.924$ , Figure 11). However, as will be shown in Section VIII A, fine and coarse elemental carbon show a relatively strong linear correlation ( $r = 0.81$ ). As a result, the standard deviations for the coefficients in the multiple regression with  $b_{ap}$  are increased. Thus coarse elemental carbon may have a relatively small but real contribution to light absorption.

## V. MEASUREMENT OF THE SCATTERING COEFFICIENT FOR LIQUID WATER

### A. Introduction

Water is a significant constituent of suspended particulate matter and contributes to light extinction by light scattering. To estimate the contribution of such scattering, two integrating nephelometers were operated side-by-side (Appendix B) with the incoming sample of one unit heated  $16 \pm 3^\circ \text{C}$  above ambient, following the recommendation of A. Waggoner, to dehydrate the aerosol. The scattering coefficient for water,  $b_{sw}$ , can be calculated as the difference  $(b_{sp})_{\text{ambient}} - (b_{sp})_{\text{heated}}$ . In principle, this technique is subject to error since other aerosol constituents, including organic compounds,  $\text{NH}_4\text{NO}_3$  and halide salts, might volatilize as well. However, it should provide an upper limit for the scattering coefficient for particle-bound water.

### B. Method Evaluation and Correlation with Aerosol Constituents

The water content of atmospheric aerosols should vary with relative humidity as well as the aerosol composition, since both sulfate and nitrate aerosols are hygroscopic. Table 8 lists Pearson correlation coefficients between  $b_{sw}$ , pollutant and meteorological parameters as well as visibility parameters as measured in the current study. The highest correlations (0.6 - 0.7) were found between  $b_{sw}$ , fine sulfate, ammonium, fine mass, and  $b_{ag}$ , the absorption coefficient for  $\text{NO}_2$ . If volatilization of organic compounds was an important contributor to  $b_{sw}$ , as measured by the difference method, then a higher correlation between  $b_{sw}$  and  $C_o$  would be expected compared to the 0.32 observed.

To assess the combined influence of RH and aerosol constituents  $b_{sw}$  data were fit to equations of the form:

Table 8

PEARSON CORRELATION COEFFICIENTS BETWEEN  $b_{sw}$ ,  
 POLLUTANT AND METEOROLOGICAL PARAMETERS<sup>a</sup>

<u>Parameter<sup>b</sup></u>	<u>r</u>
$FSO_4^-$	0.74
$CSO_4^-$	0.54
$FNO_3^-$	0.48
$CNO_3^-$	0.43
$HNO_3$	0.29
$NH_4^+$	0.73
$NH_3$	0.05 <sup>c</sup>
$FC_e$	0.27
$CC_e$	0.31
$C_o$	0.32
F Mass	0.64
$O_3$	0.19
RH	0.41
T	- 0.06
$b_{ag}$	0.67
$b_{sp}$	0.58
$b_{ap}$	0.18

a. n = 107 - 109

b. F = fine, C = coarse

c. Not significantly different from zero

$$b_{sw} = a + \frac{b(\text{SO}_4^-)}{(1 - \mu)^x} + \frac{c(\text{NO}_3^-)}{(1 - \mu)^x} \quad (1)$$

and

$$b_{sw} = a + b(\text{SO}_4)\mu^y + c(\text{NO}_3)\mu^y \quad (2)$$

Where x and y are constants between 0 and 2, and  $\mu = \% \text{ RH}/100$ .

The results shown in Table 9 indicate a general improvement in correlation relative to linear regression with two parameters. However employing equation 1, the addition of a relative humidity factor shows only a small improvement in the correlation with little change for  $x = 0.5$  to  $1.0$ . Similarly, using the other equations shown in table 9, there is relatively little change for x or  $y = 0.67$  to  $2.0$ . The range in the variance,  $r^2$ , with equations including humidity dependence was only  $0.63$  to  $0.66$ . Based on the criterion of maximizing  $r^2$ , clearly the choice of a specific model from the six listed is not crucial. For simplicity we have employed equation 9-2 with  $y = 1.0$ , although most recent studies have used equation (1).

The correlation obtained here ( $r^2 = 0.66$ ) compares to a value  $r^2 = 0.87$  observed in Denver with equation 9-1,  $x = 1$  and  $r^2 = 0.17$  with the same equation in the eastern U.S. (51). Poor correlation was suggested to be due to the lack of speciation of sulfates since  $\text{H}_2\text{SO}_4$ , for example, is more hygroscopic than  $(\text{NH}_4)_2\text{SO}_4$ .

Table 9

MULTIPLE REGRESSION ANALYSIS BETWEEN  $b_{sw}$  AND AEROSOL CONSTITUENTS

Equation <sup>a</sup>	X	Y	a <sup>b</sup>	b	c	r	r <sup>2</sup>
9-1	0.0	--	- 0.029	0.046	0.023	0.76	0.58
	0.5	--	- 0.039	0.031	0.019	0.79	0.63
	0.7	--	- 0.034	0.026	0.018	0.80	0.64
	1.0	--	- 0.015	0.019	0.015	0.81	0.65
9-2	--	0.67	- 0.031	0.069	0.047	0.81	0.66
	--	1.0	- 0.012	0.081	0.062	0.81	0.66
	--	2.0	0.083	0.125	0.115	0.78	0.61
9-3	--	0.5	- 0.039	0.044	0.040	0.78	0.60
	--	1.0	- 0.038	0.042	0.063	0.79	0.62
	--	2.0	- 0.011	0.040	0.125	0.79	0.63
9-4	0.5	--	- 0.039	0.044	0.019	0.77	0.60
	1.0	--	- 0.04	0.042	0.015	0.78	0.61
	2.0	--	- 0.017	0.040	0.0073	0.79	0.62
9-5	--	0.5	- 0.034	0.066	0.024	0.79	0.62
	--	1.0	- 0.030	0.090	0.026	0.80	0.65
	--	2.0	- 0.010	0.152	0.029	0.81	0.66
9-6	0.5	--	- 0.037	0.033	0.024	0.79	0.62
	1.0	--	- 0.032	0.021	0.026	0.80	0.64
	2.0	--	0.0037	0.0076	0.031	0.79	0.62

$$^a \text{Equation 9- 1: } b_{sw} = a + \frac{b(SO_4)}{(1 - \mu)^x} + \frac{c(NO_3)}{(1 - \mu)^x}$$

$$\text{Equation 9- 2: } b_{sw} = a + b (SO_4) \mu^y + c (NO_3) \mu^y$$

$$\text{Equation 9-3: } b_{sw} = a + b (SO_4) + c (NO_3) \mu^y$$

$$\text{Equation 9- 4: } b_{sw} = a + b (SO_4) + \frac{c (NO_3)}{(1 - \mu)^x}$$

$$\text{Equation 9- 5: } b_{sw} = a + b (SO_4) \mu^y + c (NO_3)$$

$$\text{Equation 9- 6: } b_{sw} = \frac{a + bSO_4}{(1 - \mu)^x} + c (NO_3)$$

<sup>b</sup>None are significantly different from zero at  $p = 0.95$ .

## VI. ASSESSMENT OF SAMPLING ARTIFACTS

### A. Artifact Particulate Sulfate on Glass Fiber Filters

Glass fiber hi-vol filters (Schleicher and Schuell, 1981 EPA Grade fired at 450°C) were used to collect samples for analysis of carbonaceous materials. However, these were also analyzed for sulfate and nitrate to assess what difference in sampling artifacts resulted from the firing at 450°C relative to the filters as received. In addition, glass fiber filters were assessed for HNO<sub>3</sub> retention with varying doses.

Figure 12 is a scatter diagram of blank-corrected sulfate results on 4-hour hi-vol glass fiber filter samples against those on Teflon filters obtained in an open face 47 mm filter holder (i.e., without deliberate particle size segregation). Riverside and Los Angeles data were fit with a single line, and the San Jose data, with a second line of markedly higher slope. Results on glass fiber are significantly higher. The average difference (glass fiber)-(Teflon), was 4.9 µg/m<sup>3</sup>. Thus, although the sulfate artifact is smaller than expected for short term samples (52) the positive artifact clearly persists.

### B. Artifact Particulate Nitrate on Glass Fiber Filters

Previous studies with 4-hour hi-vol sampling have indicated that at least for short term sampling, glass fiber filters serve as total inorganic nitrate (TIN) collectors, retaining both particulate and gaseous nitric acid (21). The present study repeated this comparison at San Jose, Riverside and Los Angeles and, in addition, evaluated 16 to 24-hour hi-vol filters (prefired S & S glass fiber filters) as TIN collectors. For this purpose, NO<sub>3</sub><sup>-</sup> on glass fiber filters was compared to the sum of the nitrate retained by Teflon filter and a NaCl-impregnated filter sampling in tandem.

Figure 12. Artifact Sulfate on Glass Fiber Filters, 4 Hr. Hi-Vol Samples

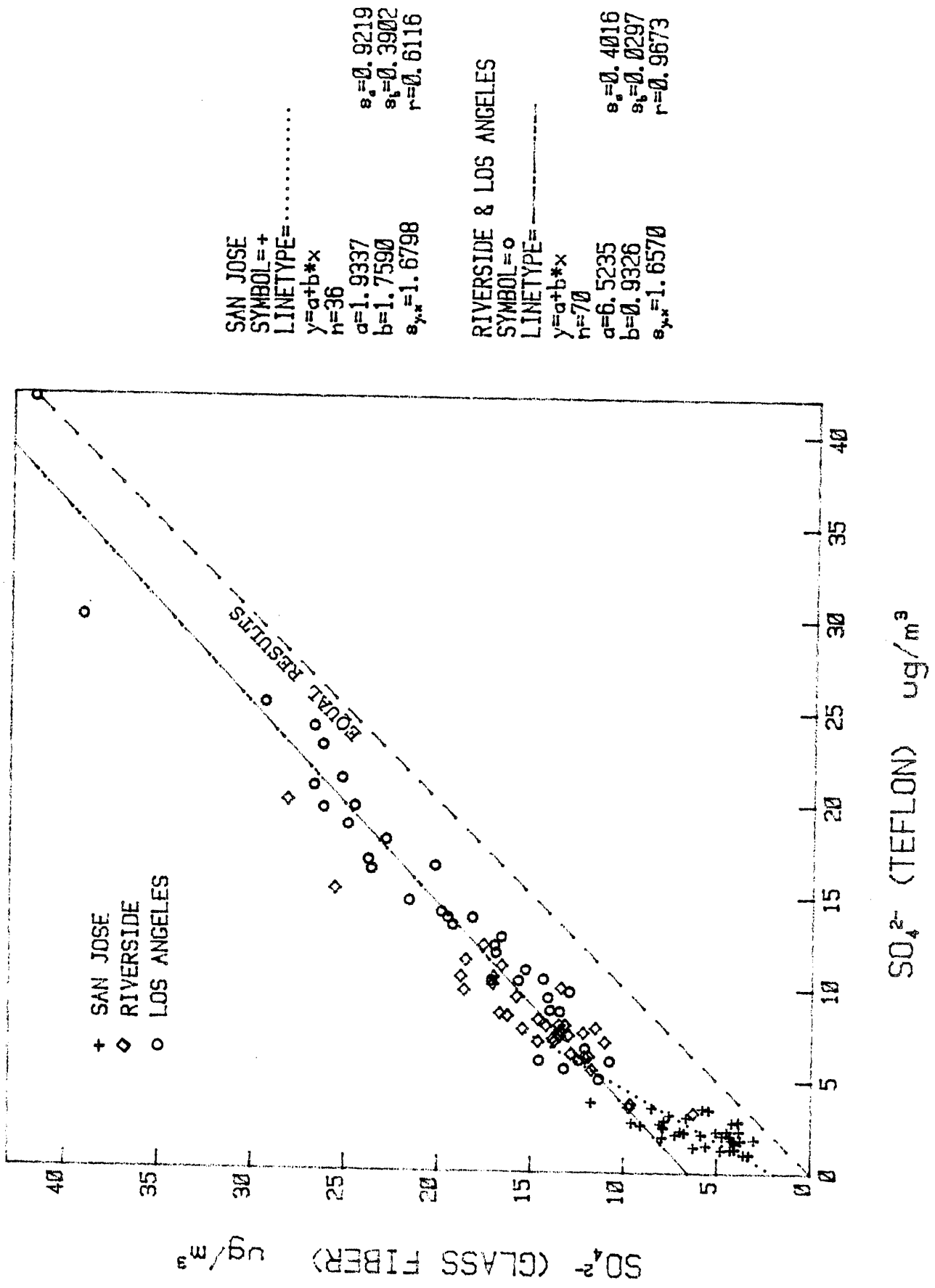


Figure 13 compares 4-hour results for the three sites. The results are highly correlated, with a ratio of means (glass fiber  $\text{NO}_3^-$ )/TIN of 0.997. Thus these data also support glass fiber filters as TIN samplers.

The 16 to 24-hour hi-vol filter nitrate data are compared to the corresponding TIN values calculated from 4-hour samples in Figures 14-16. Only at San Jose, which exhibited low nitrate levels (TIN  $< 32 \mu\text{g}/\text{cm}^2$ ) did the glass fiber filters continue to approximate TIN samplers (ratio of mean, glass fiber/TIN = 1.03). At Riverside and Los Angeles, an average of 24 to 42% of the nitrate (presumably  $\text{HNO}_3$ ) penetrated the filters. The difference in results with location probably results from the much higher nitrate dose in the Los Angeles basin ( $< 147 \mu\text{g}/\text{cm}^2$  TIN).

C. Loss of Particles in the Denuder of the Particulate Nitrate (PN) Sampler

Previous studies have suggested that coarse particle nitrate may be lost in transit through the diffusion denuder employed to remove  $\text{HNO}_3$  from particulate nitrate leading to negative errors in measuring PN. To minimize such errors the present study measured fine particle nitrate, excluding coarse nitrate and other aerosols from the denuder with a cyclone. Loss of  $< 2.5 \mu\text{m}$  nitrate was not expected to be significant. However, if it occurred, it would produce a negative error in the fine particulate nitrate measurements.

To measure the loss of fine particle constituents in the denuder, it is necessary to compare concentrations of a stable species collected on a filter with and without a preceding denuder. Sulfate collected on Teflon filters was used for this purpose. Figure 17 compares results for sampler 3 (with denuder) to those for sampler 1 (no denuder), and indicates very high correlation of results and no significant loss of sulfate in the denuder. Although sulfate

FIGURE 13 Nitric Acid Retention on Glass Fiber Hi-Vol Filters, (4 Hr. Samples)

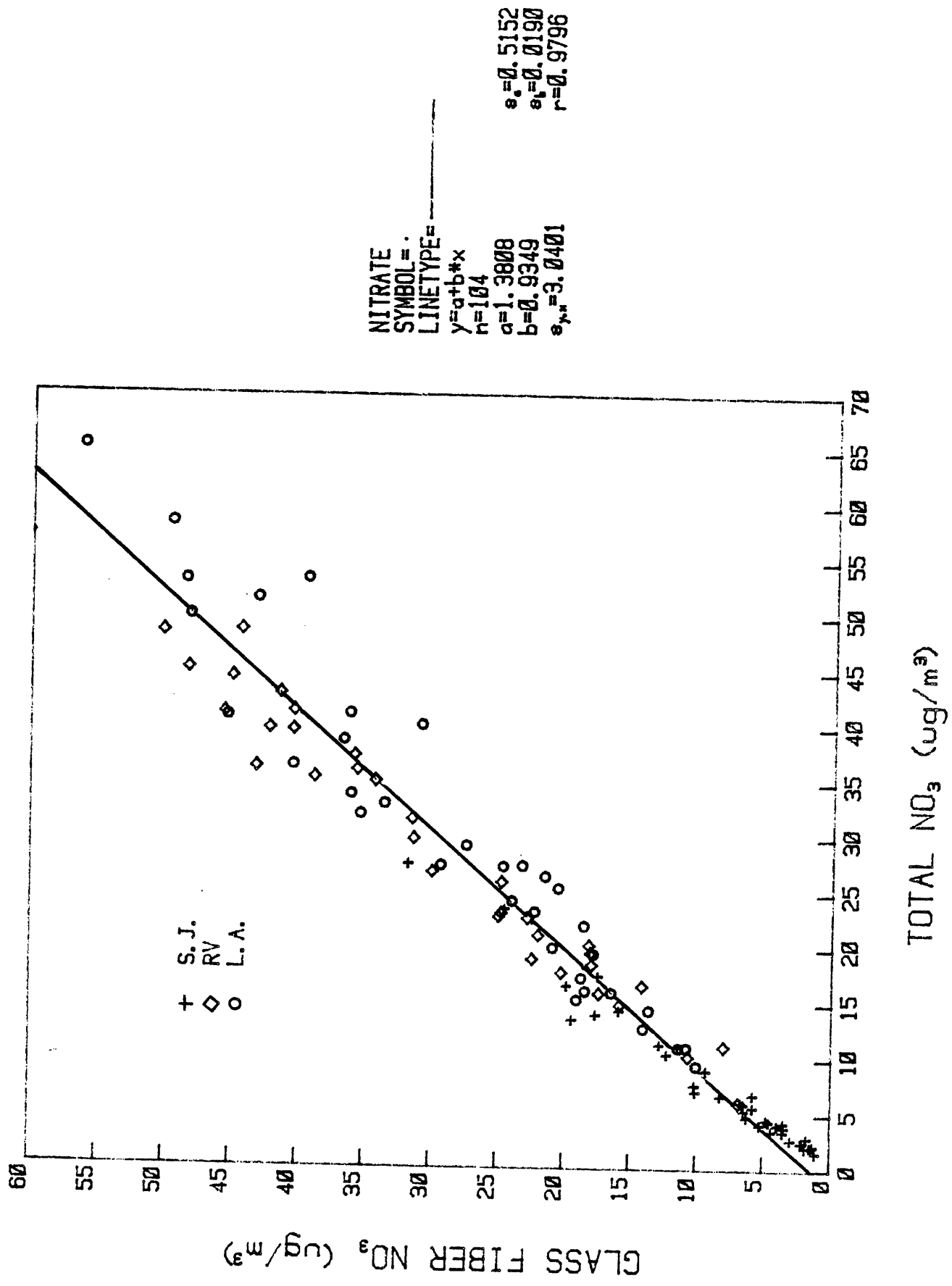


Figure 14. Nitric Acid Retention on Glass Fiber Hi-Vol Filters (San Jose, 16-24 hr Samples)

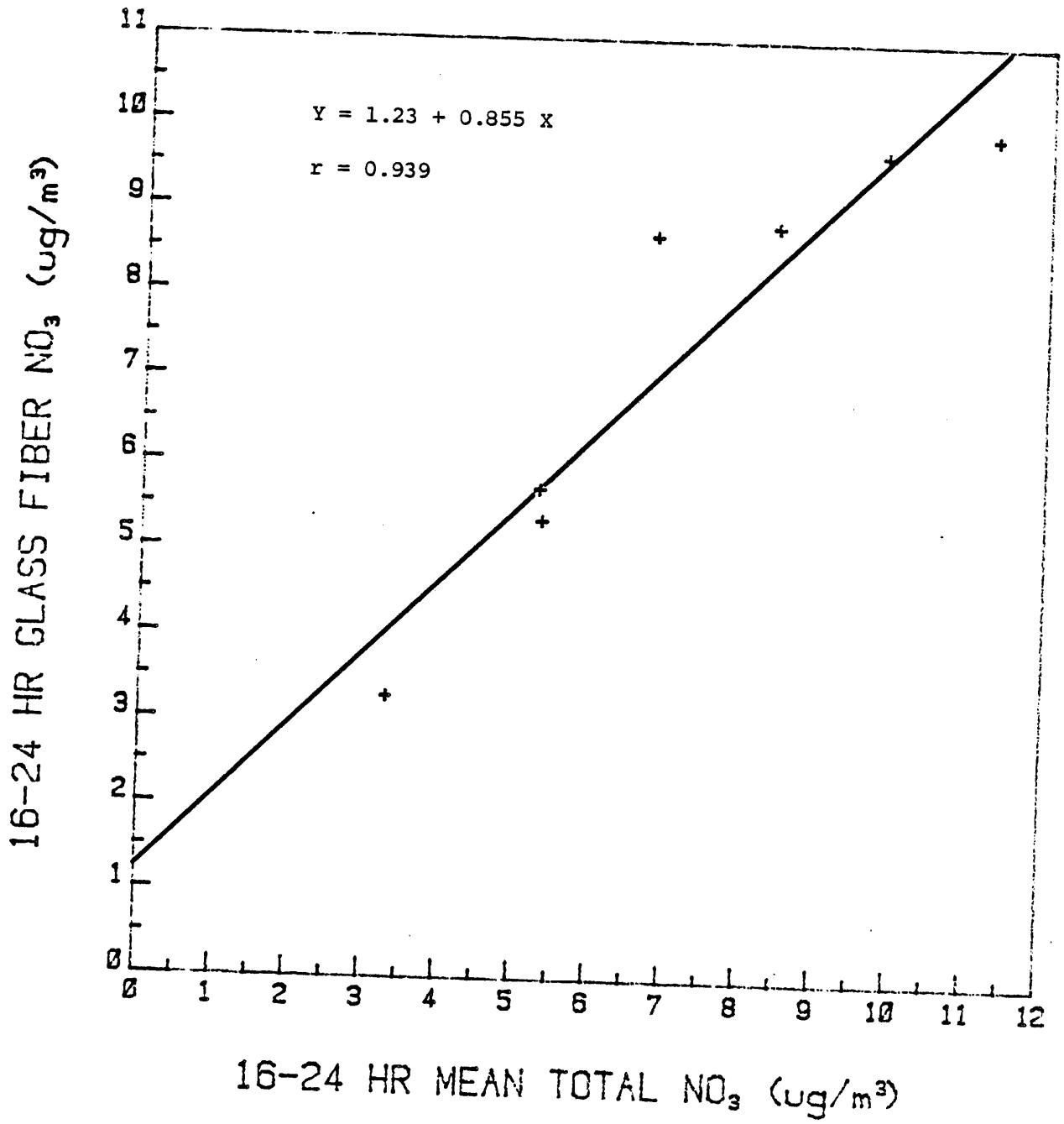


Figure 15. Nitric Acid Retention on Glass Fiber Hi-Vol Filters (Riverside, 16-24 hr Samples)

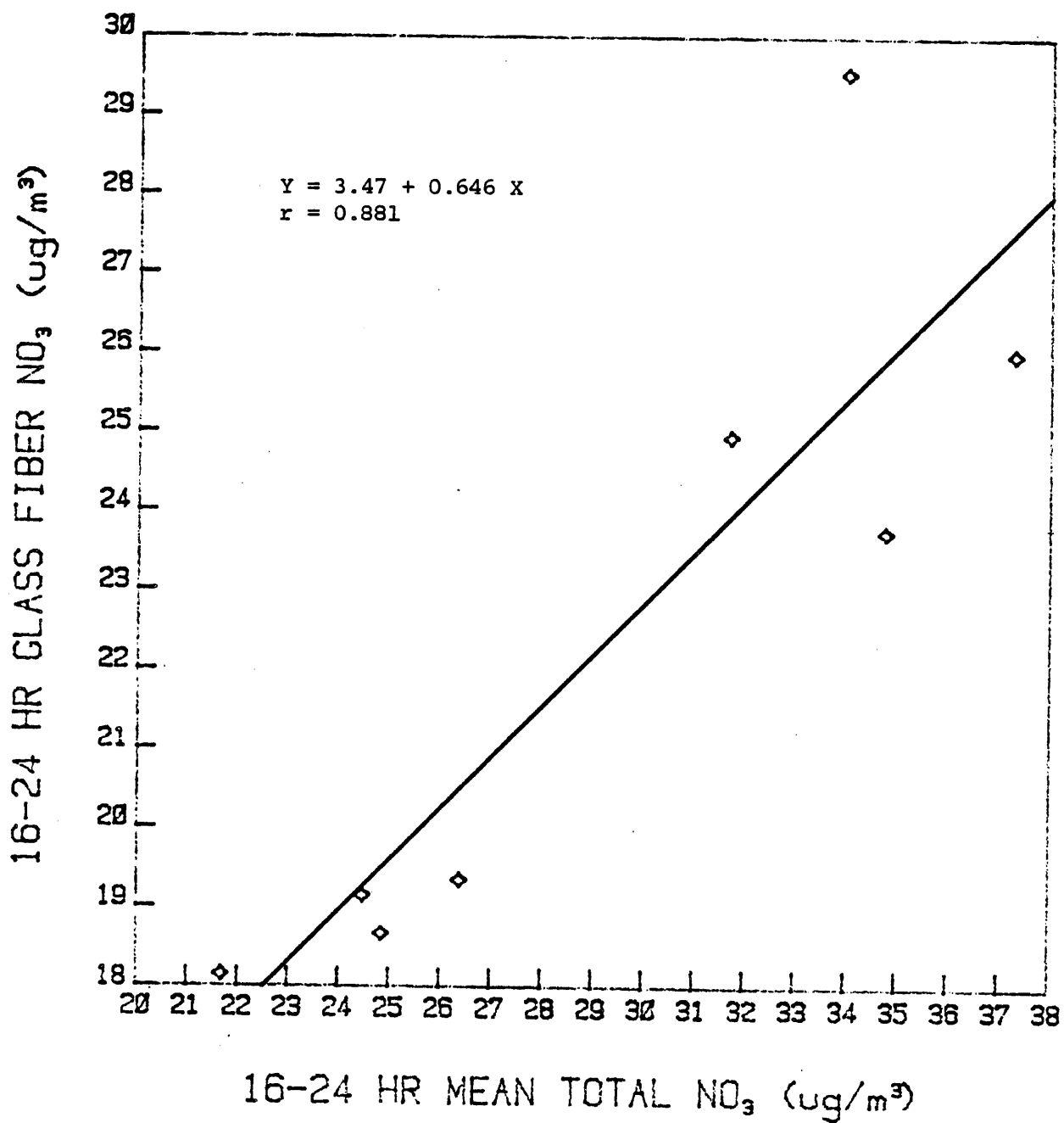


Figure 16. Nitric Acid Retention on Glass Fiber Hi-Vol Filters (Los Angeles, 16-24 hr Samples)

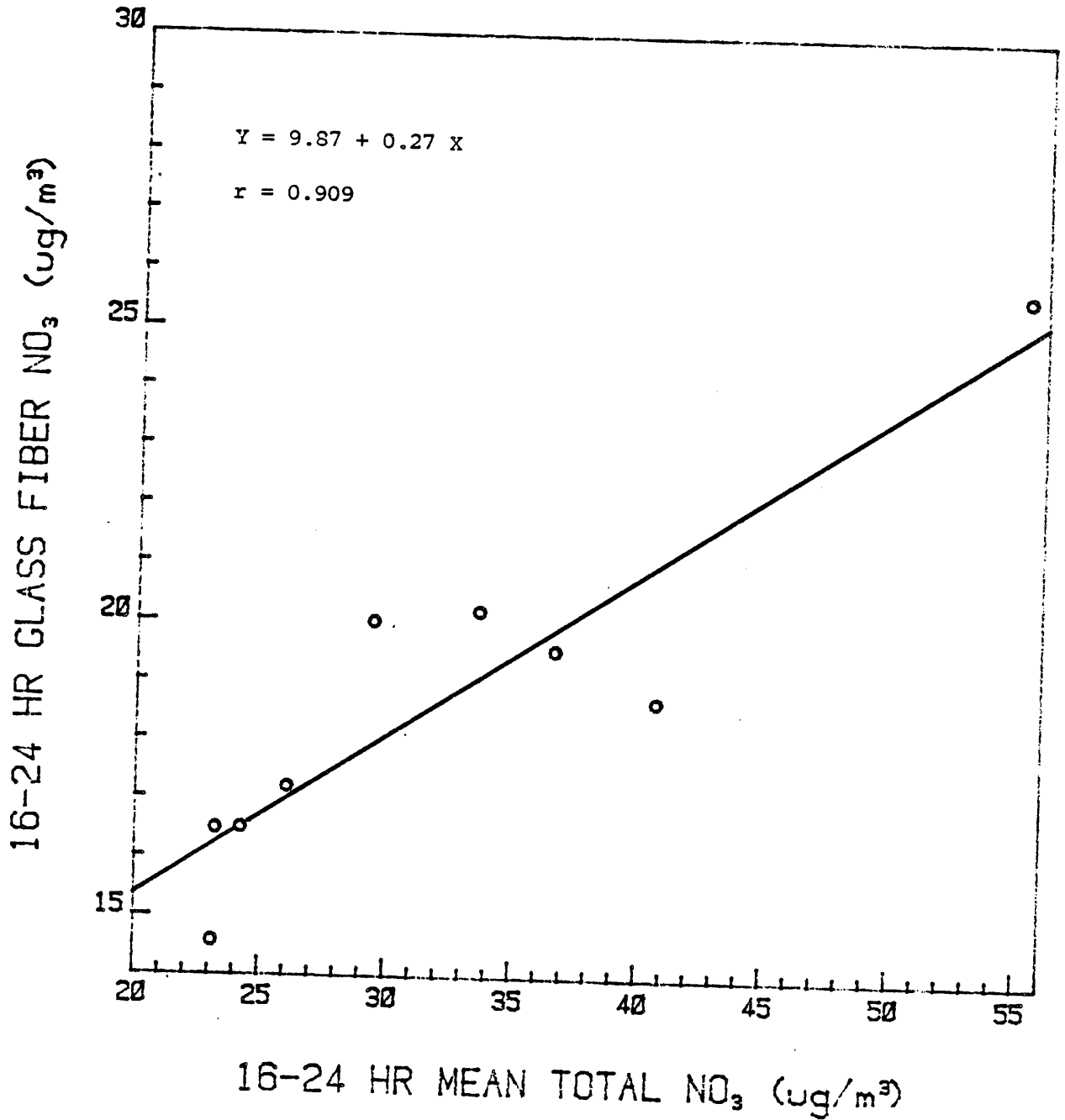
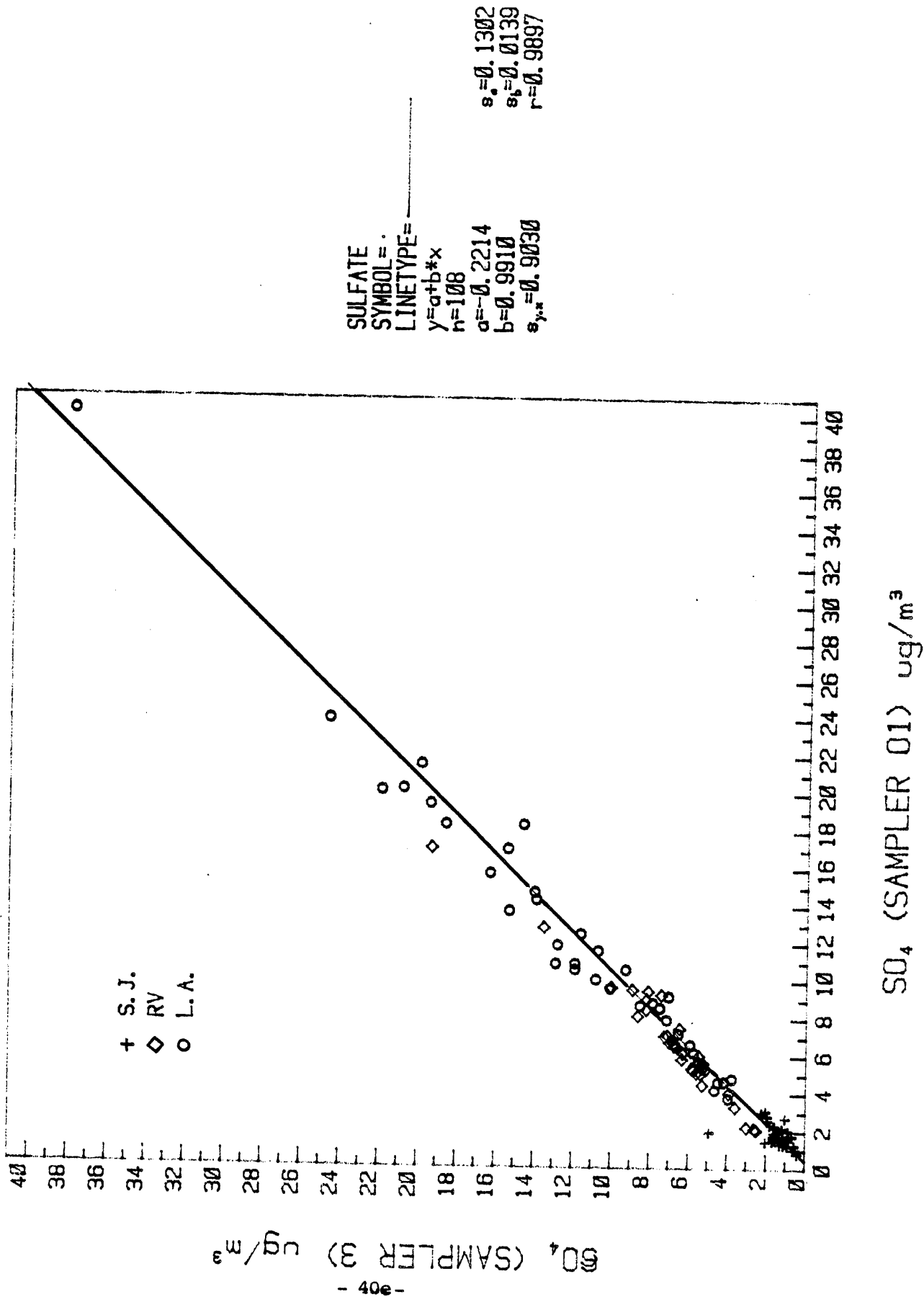


Figure 17. Loss of Non-Volatile Particles in the Denuder for Nitrate Sampling



particles are expected to be somewhat smaller than nitrate (9) and, therefore, not the ideal surrogate to estimate  $\text{NO}_3^-$  loss, these results do not support a significant error in particulate nitrate measurement due to particle loss.

D. Loss of Non-Volatile Carbon in the Denuder of the Particulate Carbon Sampler

To assess the extent of loss of non-volatile particles in the  $\text{Al}_2\text{O}_3$ -coated denuder of the true particulate carbon sampler, the quartz fiber filters from samplers 4 and 5 were analyzed and compared for elemental carbon by the reflectance method (RM-4), discussed previously. Figure 18 is a scatter diagram of the  $C_e$  results, on the two samplers. On average the loss of  $C_e$  was negligible.

E. Retention of Carbonaceous Material on Hi-Vol Filter Samples

The retention of carbonaceous material on filters is the net result of adsorption of gaseous organic compounds on filters and on previously collected particles, and volatilization from the filter of initially particle-phase materials. Some insight into the relative significance of such errors is obtained by comparing results for a single long-term filter sample with a series of short-term samples. Figure 19 compares observed total carbon values for samples collected for 16 hours against 16-hour average values calculated from four, successive 4-hour samples. Calculated values are consistently higher, suggesting that adsorption of gaseous species on relatively fresh filter surfaces and/or volatilization from filters during prolonged sampling were important. Adsorption of gaseous material on previously collected particles, which would yield 16-hour sample results higher than those calculated from the short-term samples, appears to be less significant.

Figure 18. Loss of Non-Volatile Particles in the Denuder of the Particulate Carbon Sampler.

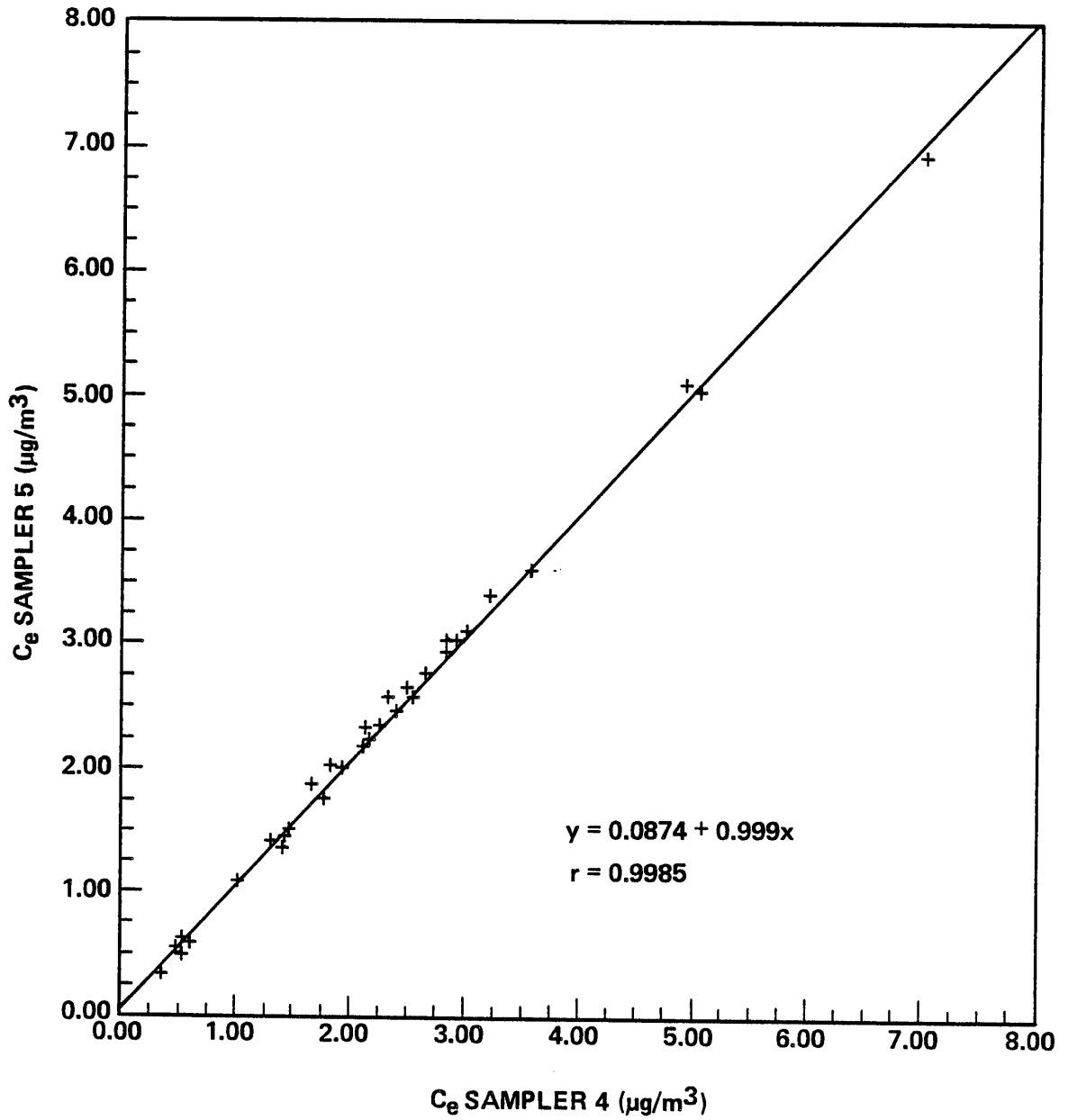
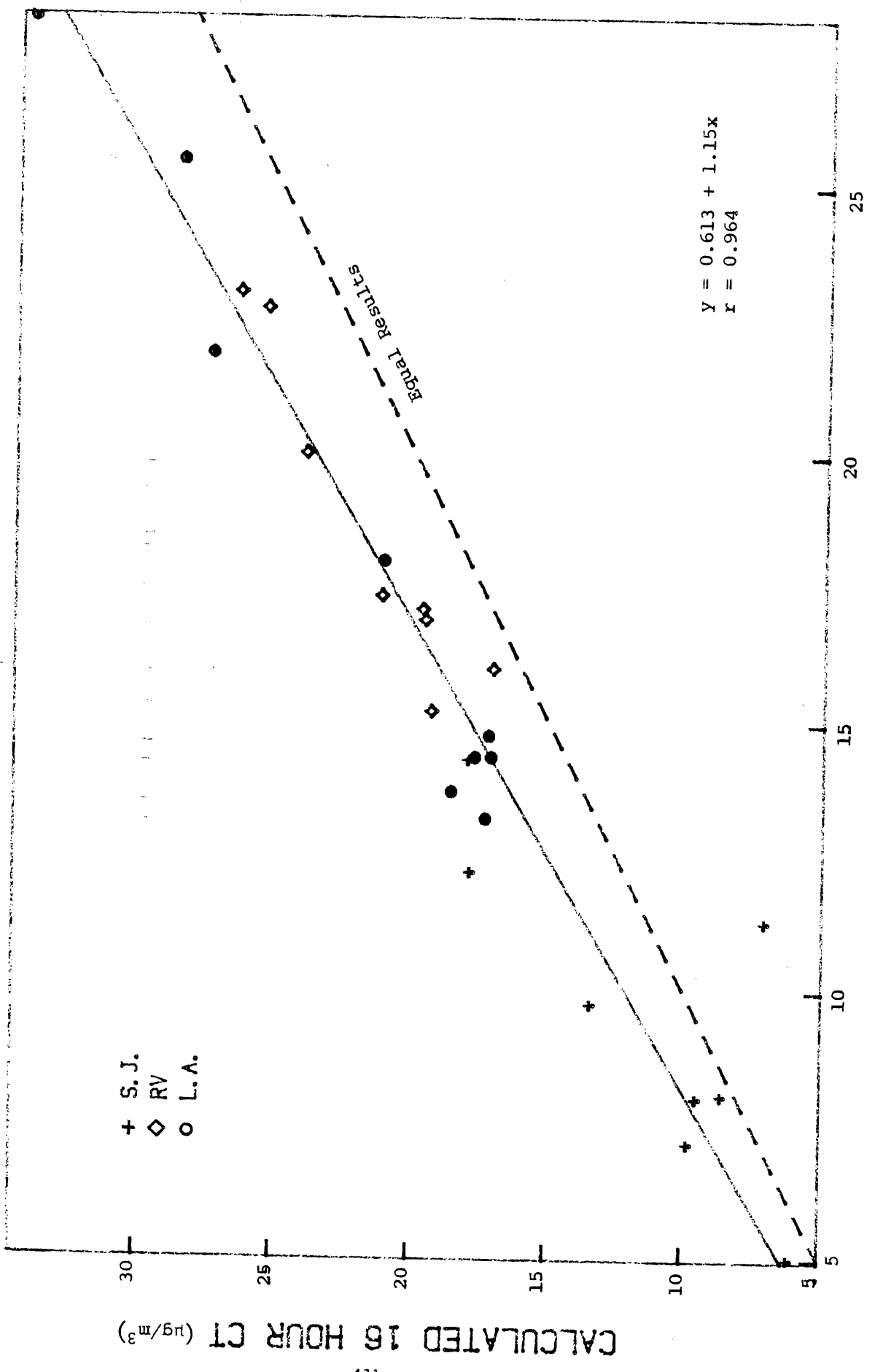


Figure 19 Observed vs. Calculated 16-Hour Total Carbon

# 1982 ARB VISIBILITY STUDY



OBSERVED 16 HOUR CT (µg/m³)

## VII. ATMOSPHERIC RESULTS, PART-- I

### A. Tabulation of Results

Aerosol collection was done for 109, 4-hour periods. Table 10 compiles results for the more significant parameters measured directly or indirectly for aerosol and gaseous pollutants. Except as noted all chemical species are listed in  $\mu\text{g}/\text{m}^3$ . Table 11 explains the meaning of the headings used. Table 12 provides mean concentrations for the chemical species and meteorological parameters. The downtown Los Angeles site shows highest average levels for sulfate and carbonaceous material. Riverside exhibited the highest particulate nitrate.

### B. Summary of Visibility Results

Table 13 lists mean and maximum values measured for visibility parameters at the three sampling sites. Mean values are for 30 to 36, 4-hour periods at each site.

Light scattering by dry particles (i.e.,  $b_{sp}$  as measured by an integrating nephelometer heated  $16 \pm 3^\circ\text{C}$  above ambient temperature) was the largest contributor to the total extinction at all sites, representing somewhat more than half of the extinction coefficient,  $b'_{ext}$ . Light absorption by particles, which can be related almost exclusively to elemental carbon (42), was relatively small at sites in the Los Angeles basin where high concentrations of efficient light scattering species were present. However, at San Jose absorption averaged nearly one-fourth of the  $b'_{ext}$ . Conversely, the apparent contribution of water was relatively high at Riverside and Los Angeles and small at San Jose. This is consistent with the relatively high sulfate and nitrate concentrations in the L.A. basin, species which can absorb and retain water. The light absorption calculated for  $\text{NO}_2$ ,  $b_{ag}$ , remained relatively insignificant at all sites. The daily changes in the values of



Table 10. Summary of Atmospheric Results (continued)

TIME	FINE SO4	COARSE SO4	FINE NO3	COARSE NO3	HNO3	NH4	NH3	FINE CE	COARSE CE	TOTAL CN	FINE MASS	TOTAL MASS	R FTNE	BAG E-4/M	O3 PPB	RH %	TEMP C	BSP E-4/M	BSW	BAP
723072520	17.12	2.24	12.06	9.96	14.39	11.05	18.62	1.51	0.84	23.34	68.08	134.75	6.90	0.18	150.0	38.80	32.54	0.54	0.19	
725072524	12.98	2.31	22.10	12.35	0.88	12.56	18.24	1.71	0.25	20.00	75.00	138.99	7.57	0.21	67.5	47.00	27.39	2.52	0.88	0.11
7250872612	8.78	1.86	16.86	7.35	13.04	5.59	16.79	3.24	0.16	13.83	54.00	109.80	11.63	0.23	40.0	54.30	25.72	2.33	0.71	0.25
7251272616	2.55	0.71	0.99	0.39	9.79	0.79	8.63	0.63	0.14	7.84	20.50		6.43	0.12	45.0	36.00	32.94	0.31	0.13	0.05
7251672620	9.73	0.85	11.47	16.45	1.83	6.50	18.22	2.33	0.67	21.52	63.24	103.77	14.12	0.18	110.0	36.00	32.50	0.90	1.32	0.20
7252072624	7.44	1.91	5.20	12.31	3.57	5.01	17.35	2.33	0.32	15.97	44.91	103.13	5.90	0.25	25.0	43.00	27.11	0.90	0.55	0.20
7270872712	6.40	1.61	26.77	10.13	11.72	11.42	48.10	4.55	0.64	19.26	63.85	159.39	11.28	0.32	57.5	39.00	26.00	1.66	1.27	0.36
7271272716	9.54	1.69	12.49	10.35	12.21	7.24	23.20	2.42	0.67	24.58	58.99	136.84	10.97	0.18	130.0	33.80	33.50	2.13	1.16	0.24
7271672720	9.80	1.59	10.19	10.60	1.92	5.66	19.95	2.34	0.58	19.35	59.75	117.05	15.22	0.28	16.3	38.30	27.22	1.14	0.22	0.19
7290872812	6.03	1.40	11.00	5.55	15.03	4.45	9.58	4.56	0.94	15.86	48.56	115.92	12.53	0.32	45.0	40.80	26.00	1.21	0.47	
7291272816	6.22	0.88	16.00	4.67	6.09	4.89	19.25	2.30	0.51	19.82	60.32	126.22	15.11	0.18	117.5	31.80	32.67	2.11	0.24	
7291672820	6.22	0.88	16.00	4.67	6.09	4.89	19.25	2.30	0.51	19.82	60.32	126.22	15.11	0.18	117.5	31.80	32.67	2.11	0.24	
7292072824	2.61	0.96	1.83	3.57	0.67	0.80	13.49	1.03	0.35	10.25	22.88	54.35	4.84	0.20	15.0	42.30	27.50	0.27	0.15	0.10
7290872912	3.74	1.27	5.58	4.25	12.27	13.76		4.05	1.22	14.47	31.08	109.56	2.33	0.27	37.5	43.50	26.56	0.85	0.31	0.40
7291272916	5.65	0.78	21.11	4.98	13.64	6.52	36.42	2.36	1.12	22.08	43.47	125.05	1.43	0.18	110.0	32.50	33.78	1.33	1.34	0.20
7291672920	4.88	1.42	7.87	9.24	8.69	4.62	27.54	1.98	0.68	21.16	39.51	111.73	1.29	0.19	75.0	33.30	33.22	0.75	0.63	0.17
7292072924	2.59	1.04	3.20	6.39	0.65	1.55	22.45	1.59	0.60	14.35	23.67	77.25	-0.34	0.20	22.5	35.60	28.06	0.42	0.25	0.13
7310873112	14.25	2.15	13.83	12.66	12.15	8.55	4.78	3.46	0.82	19.48	83.12	132.40	18.42	0.28	52.5	58.50	25.56	2.55	1.00	0.34
7311273116	21.52	1.57	8.01	48.23	-4.76	9.86	4.60	2.75	0.99	23.95	87.12	132.40	17.85	0.18	135.0	45.30	30.29	2.22	0.99	0.26
7311673120	16.99	1.78	4.12	7.48	12.56	5.00	2.96	1.48	0.64	16.45	56.43	98.12	6.82	0.20	82.5	55.30	27.39	1.41	1.18	0.08
7312073124	18.30	-0.37	8.63	1.66	9.73	7.18	3.25	1.77	0.46	16.45	92.69	107.66	31.85	0.24	27.5	70.00	22.78	3.18	0.20	0.14
8010801116	27.93	2.07	9.91	9.91	28.44	8.56	2.10	2.43	0.58	18.32	79.29	125.72	9.93	0.23	102.5	65.00	27.33	2.34	2.11	0.19
8011280116	40.18	1.64	12.68	-0.40	28.44	17.44	4.90	2.20	0.48	19.36	108.17	120.70	20.08	0.16	67.5	56.50	25.83	1.96	1.58	0.28
8011690120	23.95	1.41	2.77	2.47	10.85	5.72	1.55	1.11	0.50	12.14	61.36	83.47	11.60	0.16	67.5	56.50	25.83	1.96	1.58	0.28
8012090124	20.25	1.06	6.69	4.35	4.26	7.11	0.59	1.52	0.18	11.14	58.11	82.49	10.44	0.16	67.5	56.50	25.83	1.96	1.58	0.28
802080212	18.26	1.41	8.62	5.08	13.68	6.39	1.57	4.64	0.88	18.72	64.85	118.83	7.57	0.28	27.5	61.00	22.67	1.78	1.74	0.50
8021280216	19.36	1.55	5.28	-0.06	27.71	6.47	1.81	2.81	0.94	20.01	52.45	122.03	-2.42	0.22	67.5	47.30	26.56	1.62	0.94	0.33
8021580220	13.70	3.16	3.65	6.75	9.10	3.53	0.70	1.50	0.36	12.02	48.47	76.48	12.77	0.20	42.5	53.00	25.28	1.06	0.93	0.18
8022080224	10.60	2.84	2.67	8.66	1.41	2.46	0.69	0.98	0.33	6.45	33.48	58.12	9.00	0.19	22.5	70.30	20.44	0.83	1.03	0.07
803080312	11.90	2.79	8.29	7.94	13.03	5.18	2.24	4.11	1.31	17.31	58.58	111.41	12.02	0.28	25.0	55.00	24.25	1.49	1.29	0.47
8031280316	10.92	3.22	5.61	11.23	10.46	3.62	1.59	1.78	0.71	15.50	43.54	91.21	6.98	0.21	45.0	47.50	24.28	1.01	0.62	0.17
8031680320	10.87	2.91	3.54	11.15	7.31	3.69	1.19	1.86	0.51	14.12	55.81	81.43	20.54	0.23	15.0	68.30	21.05	1.02	1.09	0.15
8032080324	10.08	2.69	3.80	10.17	0.42	3.63	1.19	1.40	0.31	10.30	41.63	71.34	11.39	0.25	15.0	68.30	21.05	1.02	1.09	0.15
804080412	15.74	4.11	28.07	22.69	14.42	14.09	2.05	10.81	2.39	36.73	132.94	210.33	32.42	0.41	40.0	57.30	24.25	4.21	1.55	1.38
8041280416	20.14	3.91	8.12	18.83	33.09															
8041680420	9.59	1.40	4.55	8.74	13.14	3.12	1.55	3.42	0.85	25.04	78.16	130.45	14.55	0.18	80.0	48.30	27.67	2.54	0.47	0.36
8042080424	4.63	1.44	3.91	6.58	0.94	1.24	2.16	2.06	0.70	15.30	46.33	73.20	10.94	0.19	80.0	48.30	27.67	2.54	0.47	0.36
805080512	7.94	1.88	13.85	-4.50	30.40	6.42	3.80	11.42	0.39	11.18	33.20	62.33	16.62	0.20	30.0	43.00	26.00	2.37	0.70	1.29
8051280516	10.64	1.55	4.82	6.51	16.11	2.03	1.95	3.34	0.95	21.90	57.44	97.30	10.94	0.20	32.5	33.00	30.28	1.49	0.64	0.41
8051680520	6.19	0.55	4.82	6.51	16.11	2.03	1.95	3.34	0.95	21.90	57.44	97.30	10.94	0.20	32.5	33.00	30.28	1.49	0.64	0.41
8052080524	4.82	1.29	4.72	9.25	1.98	2.22	3.67	4.23	0.88	16.38	38.66	102.82	3.37	0.20	15.0	51.30	24.72	0.67	0.36	0.44
806080612	9.18	1.18	15.33	9.32	28.49															
8061280616	8.84	1.53	11.92	82.92	-8.54	4.76	7.17	6.54	2.47	34.21	76.14	169.44	12.03	0.25	72.5	31.00	33.89	2.31	0.72	0.65
8061680620	12.54	1.31	8.11	11.73	38.56	6.48	1.84	3.79	0.97	24.53	68.20	125.93	11.29	0.25	57.5	39.00	30.44	1.66	0.48	0.45
8062080624	7.20	1.60	6.99	13.13	3.26	3.83	6.71	3.50	1.08	17.49	44.42	119.88	2.25	0.22	8.0	55.00	25.72	0.87	0.53	0.33
807080712	6.62	2.11	11.04	14.83	15.27	4.52	4.54	4.34	0.84	19.87	61.97	136.79	12.88	0.20	25.0	60.00	24.61	1.17	0.68	0.47
8071280716	8.69	1.82	8.12	-21.38	26.51	2.93	4.19	1.90	0.32	17.41	46.53	89.02	6.98	0.14	40.0	37.30	29.89	1.02	0.06	0.17
8071680720	8.57	0.91	5.11	6.88	13.46	2.80	2.90	1.53	0.35	13.44	40.97	73.18	7.30	0.15	32.5	41.30	29.33	0.79	0.32	0.17
8072080724	4.64	0.44	3.48	6.41	1.15	1.35	3.66	2.40	0.47	12.10	36.90	80.12	10.01	0.15	9.0	66.30	22.78	0.69	0.48	0.27
808080812	14.69	1.89	17.33	5.58	13.46	4.21	3.32	3.54	0.61	18.24	71.69	118.35	11.74	0.15	30.0	58.60	24.83	2.53	1.15	0.59
8081280816	11.57	0.73	7.33	-2.38	28.84	4.21	3.32	2.12	0.56	18.32	54.79	87.58	12.34	0.15	45.0	42.50	28.89	1.67	0.45	0.22
8081680820	4.21	1.85	3.93	1.85	11.49	1.52	4.32	1.34	0.43	12.11	33.55	67.92	9.42	0.15	25.0	41.50	28.89	1.67	0.45	0.22
8082080824	3.77	1.87	3.23	5.92	0.25	1.38	4.01	2.72	0.53	11.11	34.57	71.60	-23.79	0.19	8.8	61.00	23.06	0.56	0.17	0.18

Table 11

## Explanation of Headings Used in Table 10

<u>Heading</u>	<u>Meaning</u>
Time	Designates the date and time of the 4-hr period. For example, 7101571019 indicates a starting date of July 10, starting time of 1500 hours, ending date July 10, at 1900 hours.
Fine SO <sub>4</sub>	Sulfate collected on a Teflon filter downstream of a cyclone with cutoff at 2.2 μm. μg/m <sup>3</sup> .
Coarse SO <sub>4</sub>	Coarse sulfate calculated as the total SO <sub>4</sub> <sup>=</sup> collected on a Teflon filter without preceding cyclone less fine SO <sub>4</sub> . μg/m <sup>3</sup> .
Fine NO <sub>3</sub>	True particulate respirable nitrate measured with a Teflon-coated cyclone plus acid gas diffusion denuder ahead of Teflon and NaCl-impregnated cellulose filters. μg/m <sup>3</sup> .
Coarse NO <sub>3</sub>	Total inorganic nitrate (TIN) collected with a Teflon and NaCl-impregnated filter less fine nitrate collected with a TIN sampler preceded by a cyclone (cutoff 2.2 μm). μg/m <sup>3</sup> .
HNO <sub>3</sub>	Measured with a TIN sampler plus cyclone less Fine NO <sub>3</sub> . μg/m <sup>3</sup> .
Fine CE	Fine elemental C. Mean results by RM and LTM methods on samples collected with quartz filters preceded with a cyclone (cutoff ca. 2.5 μm). μg/m <sup>3</sup> .
Total CO	Total organic carbon. Total carbon measured on hi-vol filter samples with baked glass fiber filters less mean C <sub>e</sub> by the RM and LTM on hi-vol samples. μg/m <sup>3</sup> .
Fine Mass	Mass concentrations measured on Teflon filters preceded by a cyclone (cutoff 2.2 μm). μg/m <sup>3</sup> .
Total Mass	Mass concentrations measured on Teflon filters without cyclone. μg/m <sup>3</sup> .
BAG	Light absorption coefficient due to gases (i.e. NO <sub>2</sub> ) in unit 10 <sup>-4</sup> m <sup>-1</sup> .
BSP	Light scattering coefficient due to particles measured with a heated integrating nephelometer at 550 nm, in units 10 <sup>-4</sup> m <sup>-1</sup> .
BSW	Light scattering coefficient for water estimated as the difference between the reading of a nephelometer at ambient temperature and BSP, in units 10 <sup>-4</sup> m <sup>-1</sup> .
BAP	Light absorption coefficient measured by the IPM in units 10 <sup>-4</sup> m <sup>-1</sup> .

Table 12

MEAN CONCENTRATIONS OF AEROSOL CONSTITUENTS  
AND METEOROLOGICAL PARAMETERS<sup>a</sup>

<u>Species</u> <sup>b</sup>	<u>San Jose</u>	<u>Riverside</u>	<u>Los Angeles</u>	<u>Overall</u>
$\text{FSO}_4^-$	1.66	6.97	13.04	7.17
$\text{FNO}_3^-$	3.38	13.54	7.88	8.27
$\text{FC}_e$	1.54	2.50	3.34	2.46
$\text{CSO}_4^-$	0.61	1.46	1.80	1.29
$\text{CNO}_3^-$	2.11	8.28	7.93	6.07
$\text{NH}_4^+$	0.30	6.09	5.18	3.80
$\text{CC}_e$	0.25	0.60	0.86	0.57
$\text{C}_o$	9.44	17.58	18.31	15.03
FMass	22.26	47.47	61.49	43.54
TSP	51.49	115.70	107.16	90.85
$\text{NH}_3$	4.33	24.54	3.20	10.63
$\text{HNO}_3$	2.13	7.41	16.74	8.69
$\text{O}_3$ (ppb)	24	72	42	49
$\text{NO}_2$ (ppb)	18.79	50.44	47.05	38.58
RH (%)	46.90	39.84	51.73	46.15
T (°C)	23.66	29.59	26.03	26.40

a. Except as noted, concentrations in  $\mu\text{g}/\text{m}^3$ . Sampling between July 10 and August 8, 1982, generally during the hours 0800 - 2400.

b. F = fine, C = coarse

Table 13

SUMMARY OF OPTICAL MEASUREMENTS AT SAN JOSE, RIVERSIDE and LOS ANGELES ( $10^{-4} \text{ m}^{-1}$ )

Parameter	San Jose			Riverside			Los Angeles		
	Mean	% of $b'_{\text{ext}}$	Max. Value	Mean	% of $b'_{\text{ext}}$	Max. Value	Mean	% of $b'_{\text{ext}}$	Max. Value
$b_{\text{ap}}$	0.17 ± 0.23	21.8	1.13	0.21 ± 0.10	8.6	0.47	0.36 ± 0.32	12.0	1.38
$b_{\text{sp}}$	0.47 ± 0.27	60.0	1.15	1.44 ± 0.70	59.3	2.75	1.61 ± 0.86	53.7	4.21
$b_{\text{sw}}$	0.050 ± 0.12	6.4	0.44	0.58 ± 0.45	23.9	1.34	0.32 ± 0.53	27.3	2.25
$b_{\text{ag}}$	0.090 ± 0.05	11.5	0.29	0.20 ± 0.05	8.2	0.32	0.21 ± 0.06	7.0	0.41
$b'_{\text{ext}}$	0.78 ± 0.38			2.43 ± 0.84			3.00 ± 1.06		

each component of  $b_{ext}$  are illustrated in Figures 20-22. These plots show, in general, that diurnal changes are correlated among the four coefficients, with the poorest correlation for  $b_{ag}$ ; this probably reflects the relatively small changes experienced in the concentration of  $NO_2$ . The onset of a relatively polluted period in Los Angeles, beginning August 4 is clearly seen.

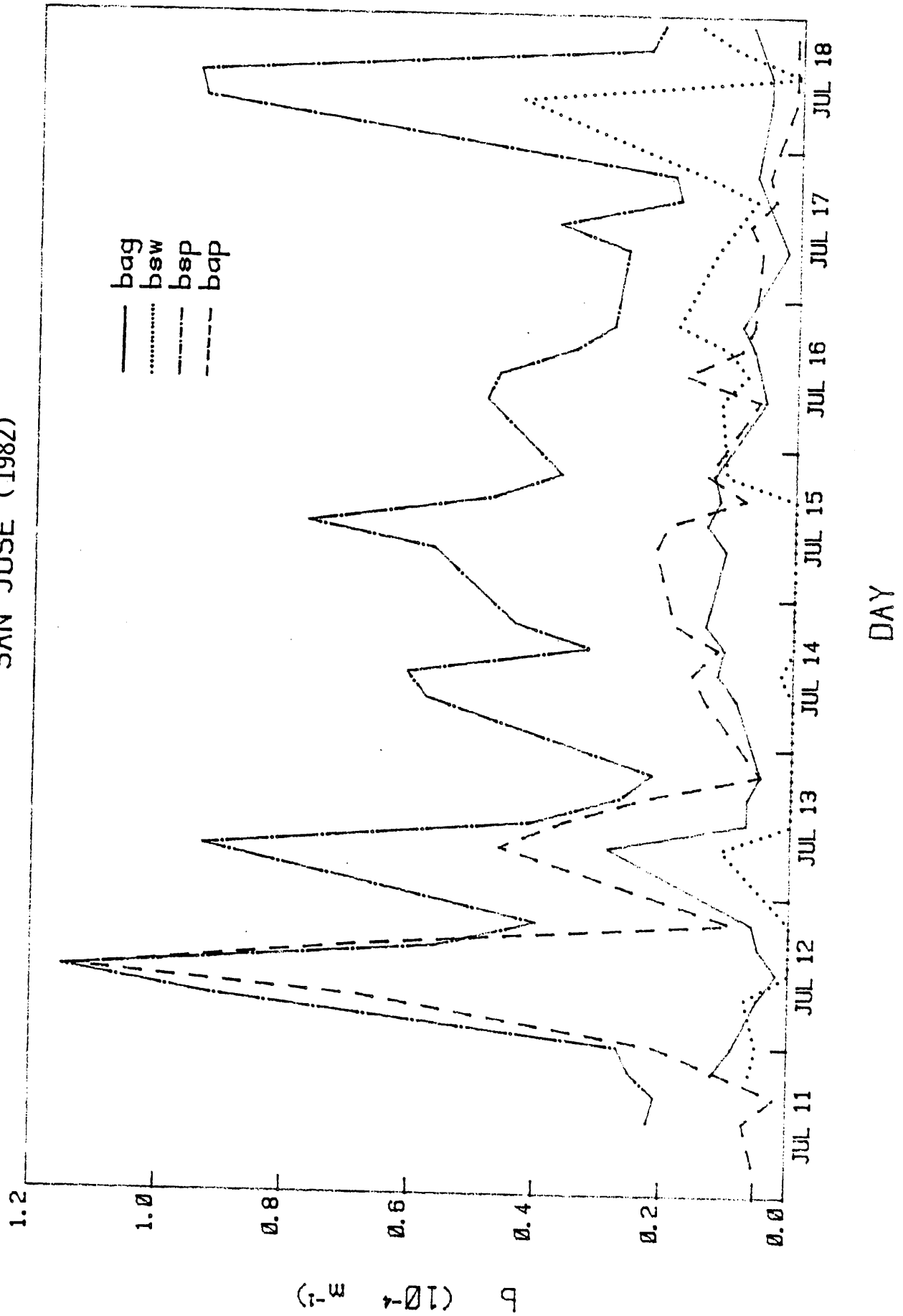
C. Diurnal Variations for the Dominant Aerosol Species and Ozone

Figures 23-25 show the average diurnal concentrations for all sampling days for the pollutants  $SO_4^{=}$ ,  $NO_3^-$ ,  $C_e$ , and  $O_3$  at each site. In Riverside, two 24-hour runs were performed. The data points shown at 0200 and 0600 hours are means for these two episodes only. Thus conclusions drawn based on differences between these data points and those for other time periods averaged over eight days may be in error because of a statistical bias. At both San Jose and Riverside, sulfate concentrations showed relatively little diurnal change. In Los Angeles the sulfate concentration was higher and exhibited a sharp maximum in mid-afternoon, paralleling that for ozone, and similar to previous observations (21). At both Los Angeles and Riverside fine particle nitrate exhibited a morning maximum. This contrasts with earlier findings (9) which found a large particle  $NO_3^-$  maximum in the morning and a fine  $NO_3^-$  ( $< 0.5 \mu m$ ) maximum in the afternoon. This earlier study was hampered by both positive and negative sampling errors for nitrate, a factor which might account for this difference. Four-hour average ozone maxima at the sampling sites were, 0.03, 0.13 and 0.08 ppm at San Jose, Riverside and Los Angeles, respectively. Thus the study was performed during periods of generally light photochemical smog.

D. Size Distribution for Aerosol Constituents

Figure 26 compares mass measurements with the fine ( $< 2.2 \mu m$ ) and total particulate samplers. The data show moderate correlation

Figure 20 B VALUES  
SAN JOSE (1982)



B (10<sup>-1</sup> m<sup>-1</sup>)

Figure 21 B VALUES  
RIVERSIDE (1982)

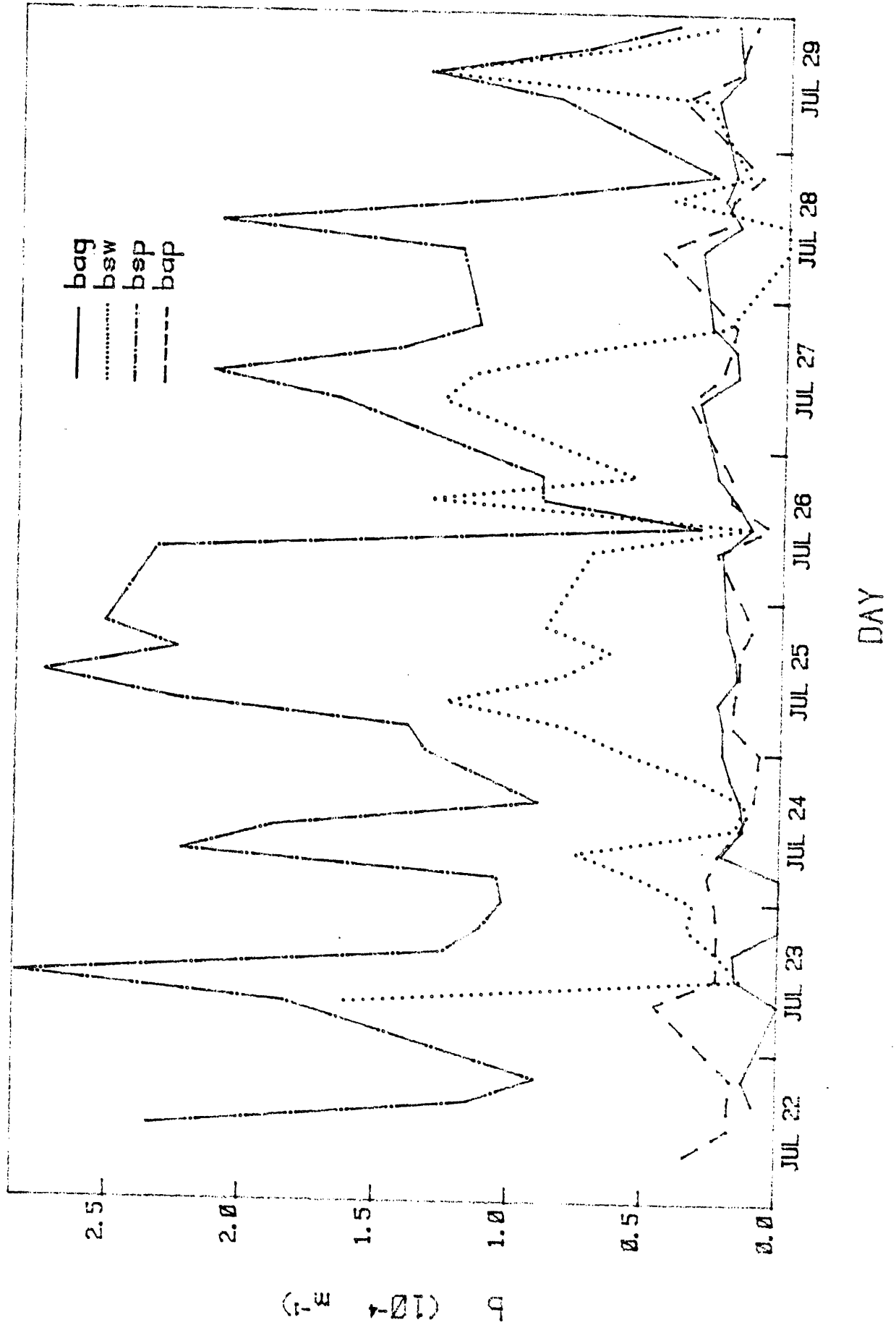


Figure 22 B VALUES  
LOS ANGELES (1982)

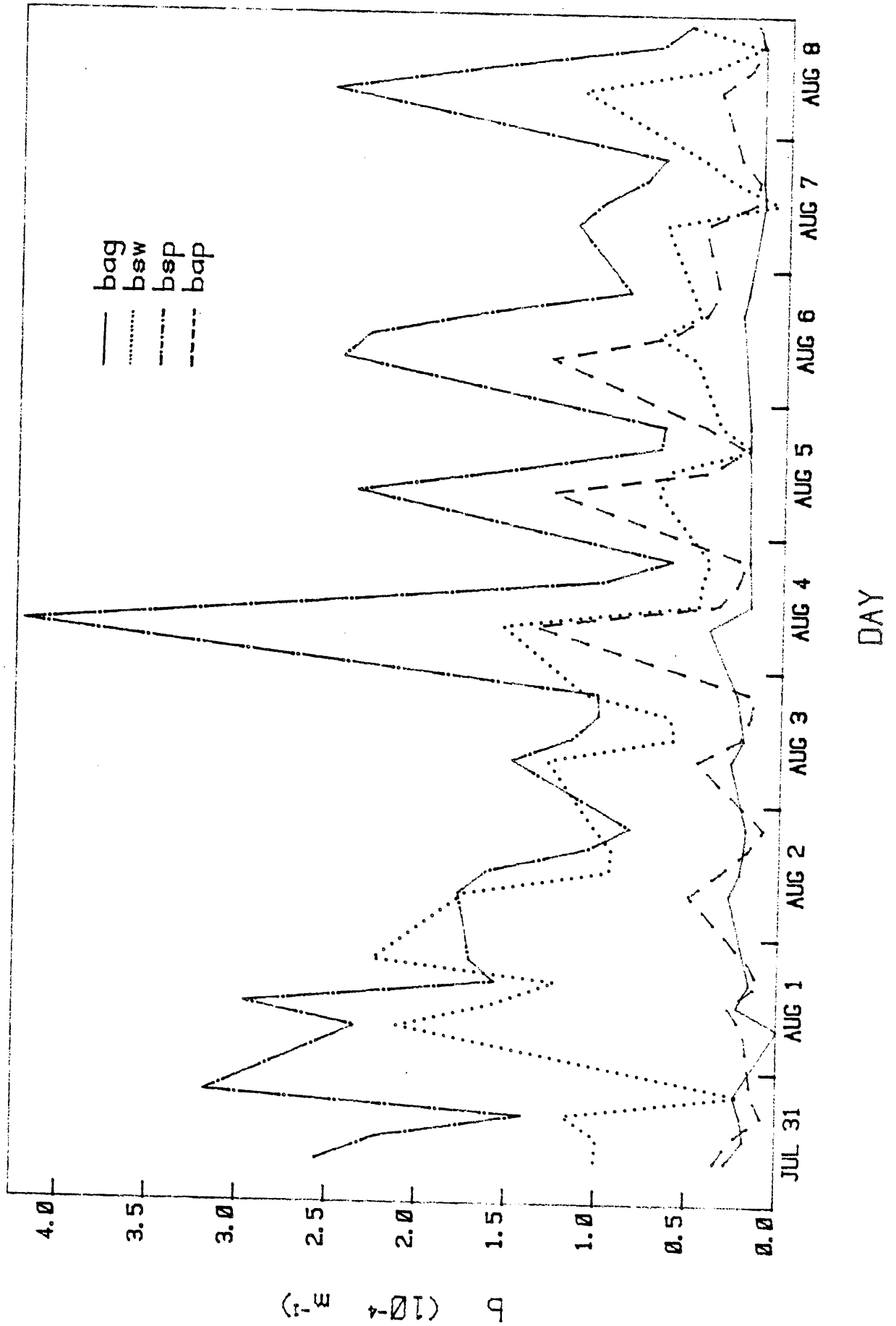


Figure 23 Diurnal Variations in Mean Pollutant Concentrations (San Jose)

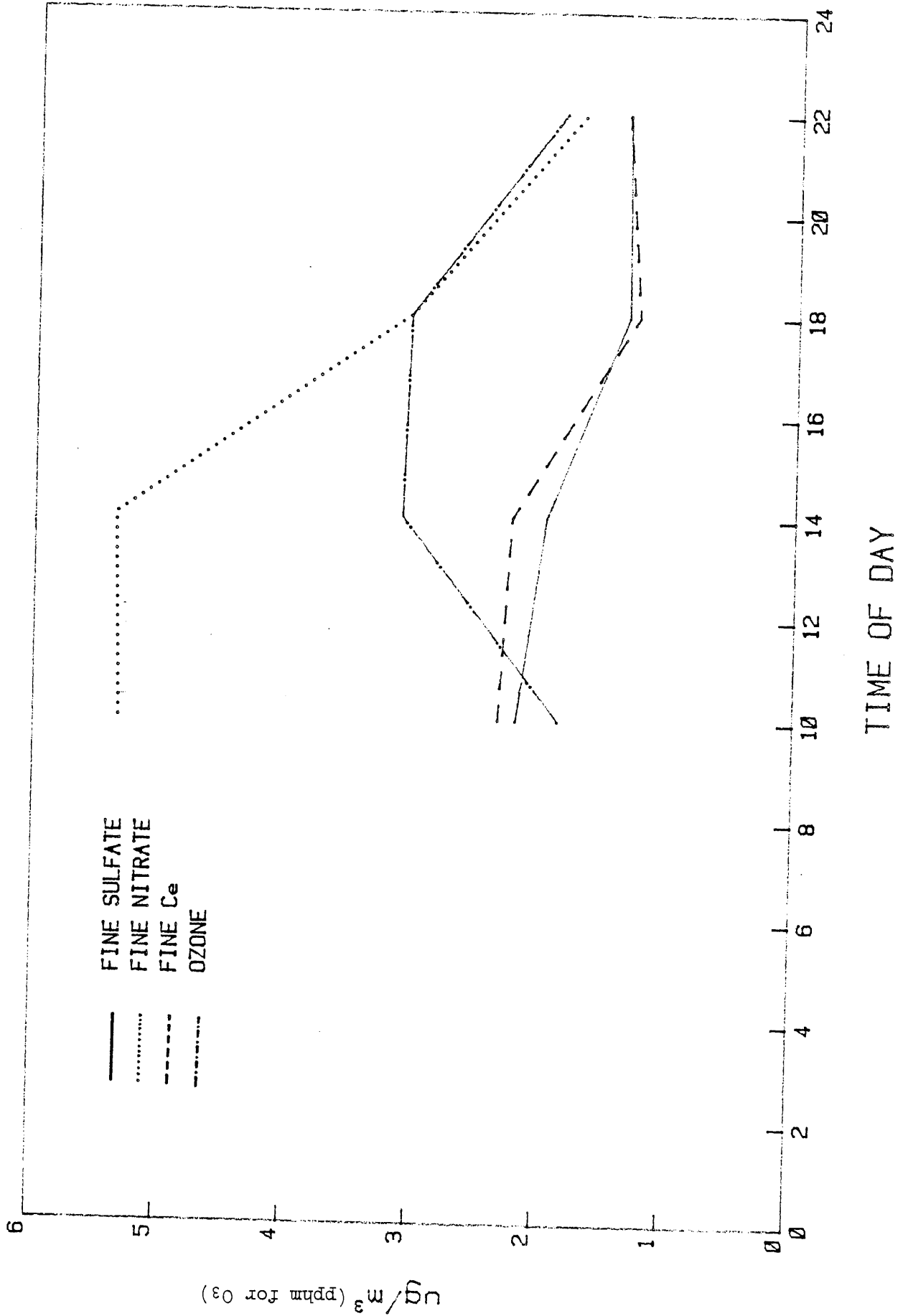


Figure 24 Diurnal Variations in Mean Pollutant Concentrations (Riverside)

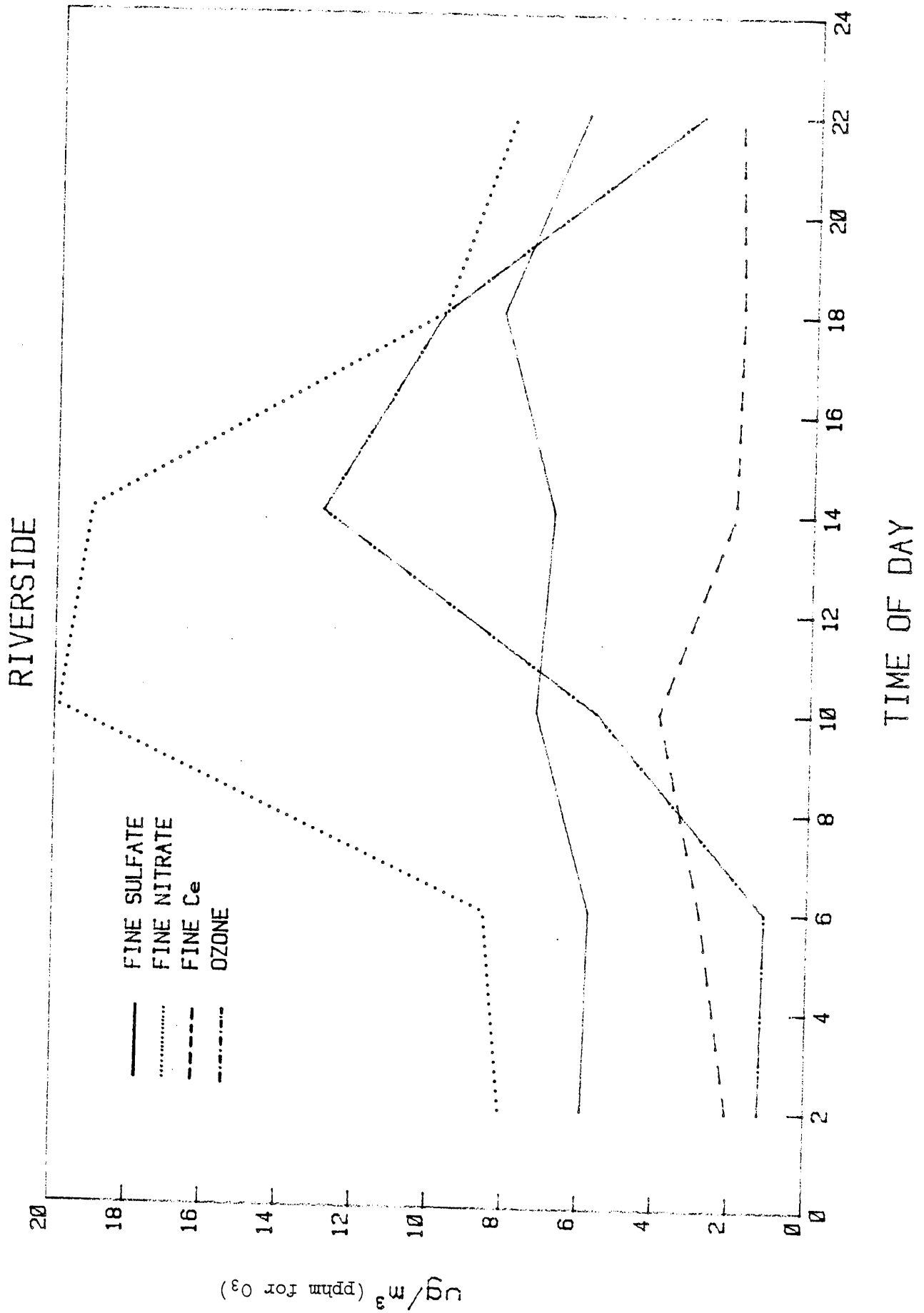


Figure 25 Diurnal Variations in Mean Pollutant Concentrations (Los Angeles)

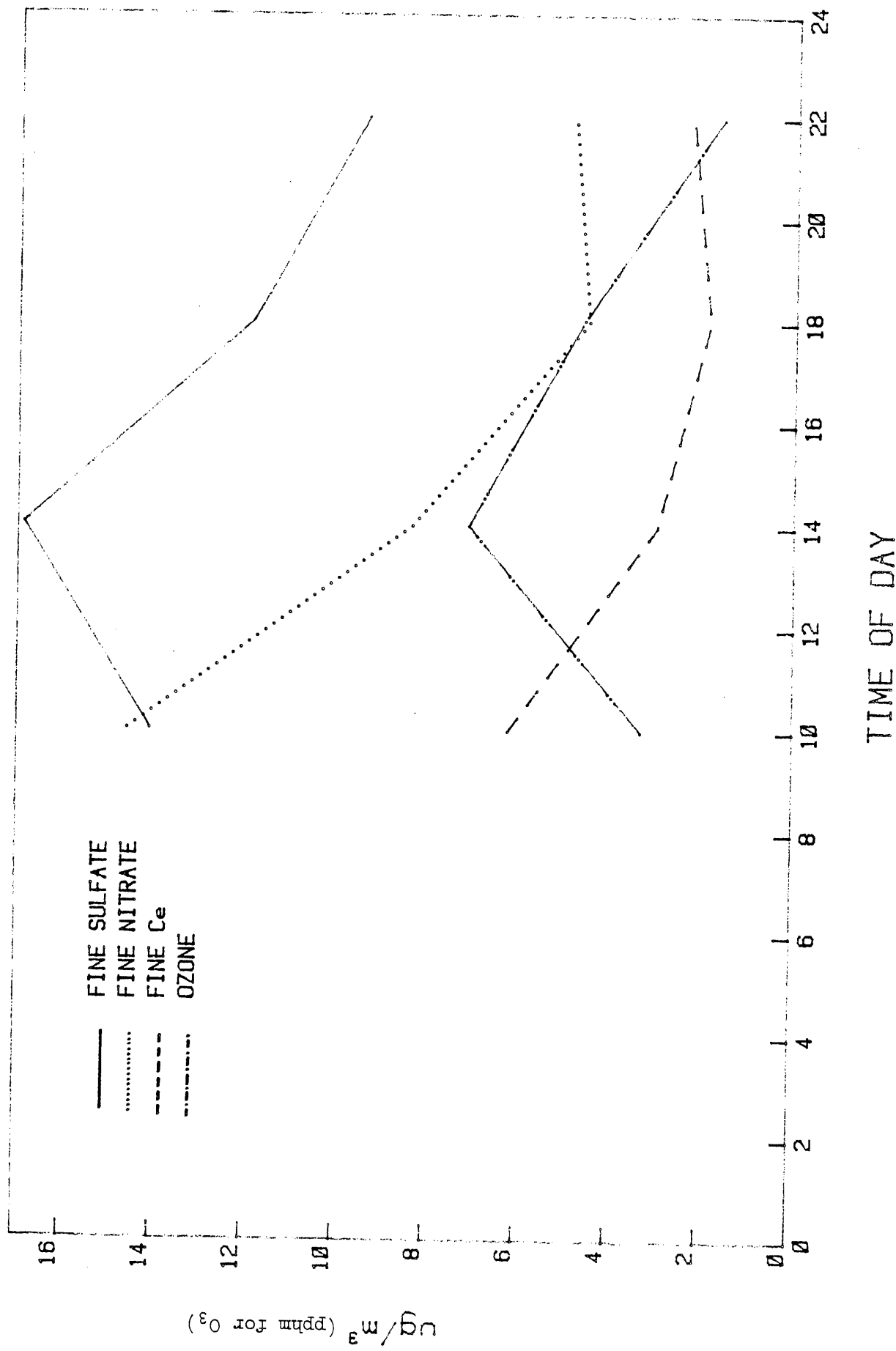
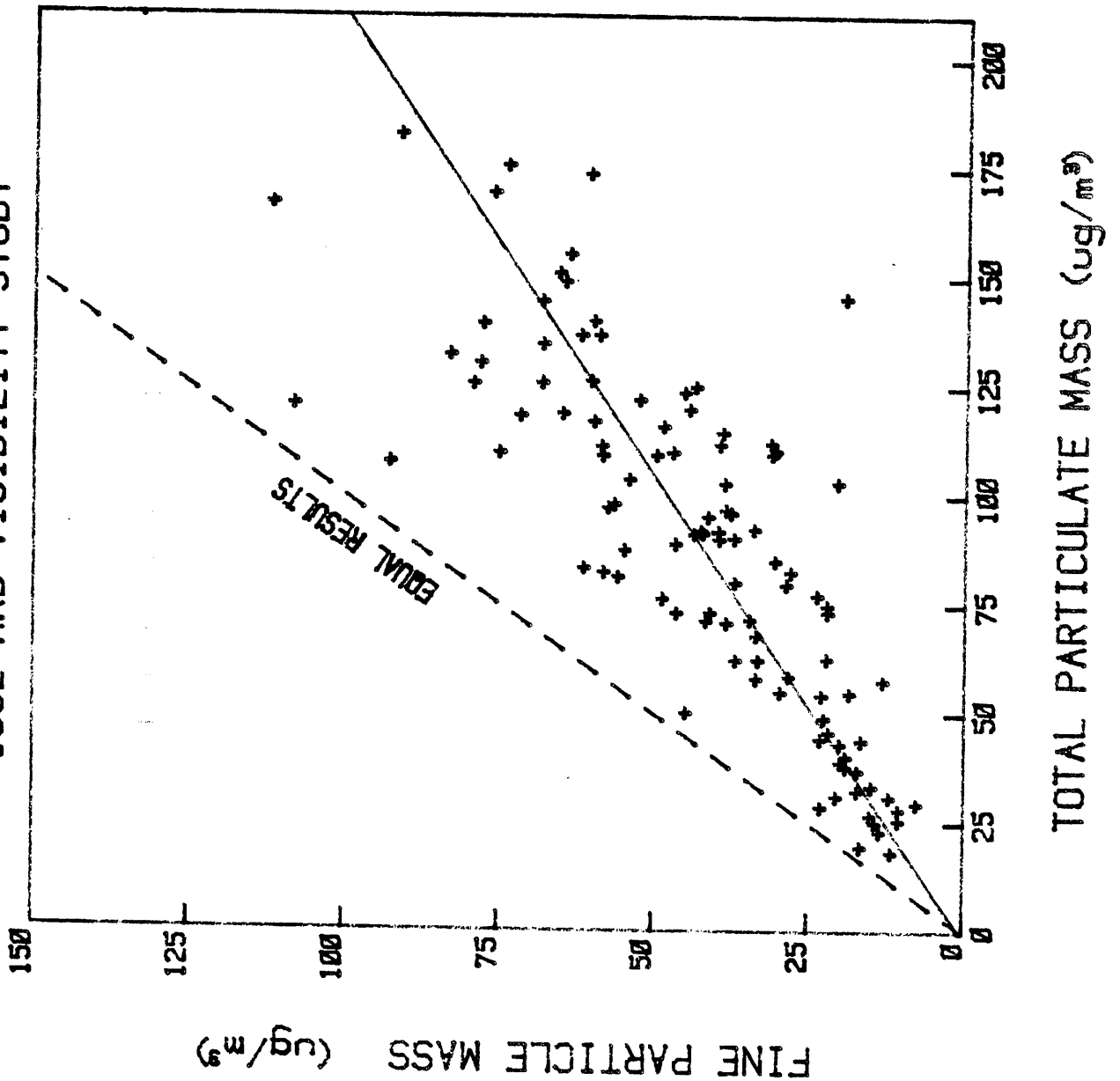


Figure 26

# MASS COMPARISONS 1982 ARB VISIBILITY STUDY



( $r = 0.82$ ). Higher correlation cannot generally be expected since the proportion of coarse particles can vary with meteorological conditions. On average, the fine fraction represented about half of the total particulate mass.

The proportion of the total sulfate which was in the fine fraction was assessed in similar manner (Figure 27). More than 90% of the total sulfate collected with Teflon filters was in the fine fraction. Thus either fine or total particulate sulfate could be employed for data analysis in assessing contributors to light scattering. With nitrate, however, a substantially larger fraction of coarse nitrate was observed. Linear regression between fine and total particulate nitrate yielded the equation:

$$\begin{aligned} \text{Fine NO}_3^- &= -0.625 + 0.620 (\text{Total NO}_3^-) \\ &= 0.917 \end{aligned}$$

Thus nearly 40% of the nitrate was coarse material.

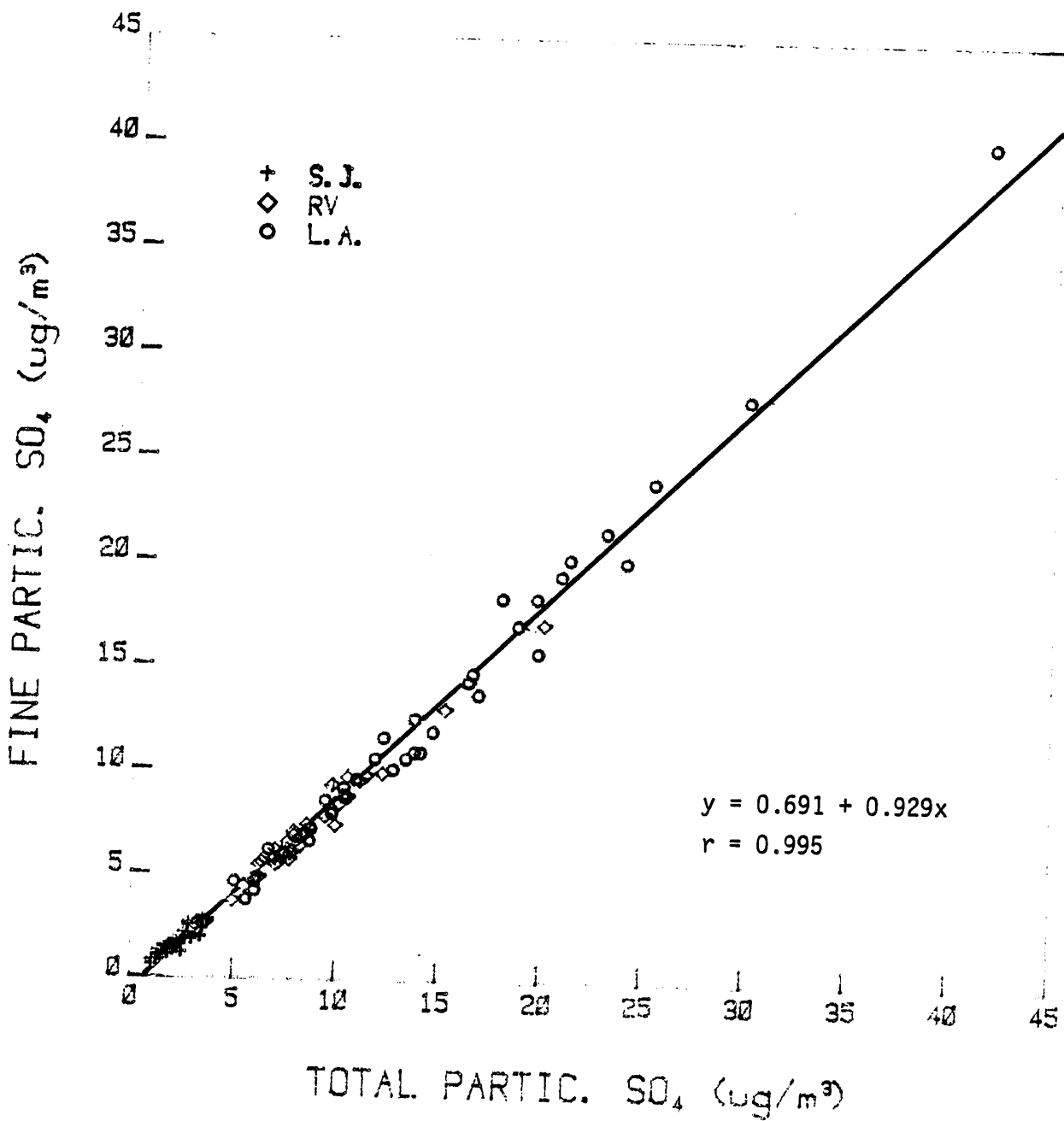
Samples collected on pre-fired Pallflex quartz 2500QA0 filters following a cyclone (cutpoint about  $2.5 \mu\text{m}$ ) were compared for total carbon retained to that on pre-fired glass fiber filters using a conventional hi-vol sampler. The face velocities for the two units were nearly identical (49 cm/sec for the fine particle sampler, 47 cm/sec for the hi-vol). Assuming no significant difference in carbon retention by the quartz and glass fiber filters, differences reflect directly the proportion of carbon in the fine fraction.

For ten paired samples collected in Riverside and downtown Los Angeles the fine fraction carbon ( $\mu\text{g}/\text{m}^3$ ) averaged  $62 \pm 13\%$  of that in the total particulate (hi-vol) sample. Linear regression yielded the result:

$$\text{Fine C} = -3.93 + 0.789 (\text{Total C})$$

$$r = 0.962$$

Figure 27 Comparison of Fine and Total Particulate Sulfate



The results for percent fine carbon compare to the range 56 to 66% obtained with dichotomous samplers at three sites.

Preceding results suggested that the proportion of coarse particle carbon obtained with dichotomous sampler may be erroneously high because of the relatively low face velocity for the coarse particle filter (34). The present data fail to support this. The proportion of  $C_e$  in the fine fraction can be assessed from Figure 28 which plots fine against total  $C_e$ . The results are highly correlated and indicate about 20% of the elemental carbon to be in the coarse fraction. The fine  $C_e$  is compared to the total carbon, measured by combustion in Figure 29. The results suggest, on average, about 18% of the total carbon to be elemental carbon.

Figures 30 and 31 test linear regressions between fine particle  $C_e$ , fine and total suspended particle mass, respectively. The moderate correlations observed ( $r = 0.69 - 0.73$ ) suggests that elemental carbon represented about 6% of the fine particle mass.

E. Calculated vs. Observed Ammonium Ion Levels

If one assumes all fine particle  $SO_4^{=}$  to be  $(NH_4)_2SO_4$  and true, fine particle nitrate to be  $NH_4NO_3$ , then expected concentrations of  $NH_4^+$  can be calculated. Regression equations relating observed and calculated  $NH_4$  values are as follows:

$$\text{San Jose} \quad \text{Calc. } NH_4^+ = 1.66 + 1.77 (\text{obs. } NH_4^+) \quad r = 0.81$$

$$\text{Riverside} \quad \text{Calc. } NH_4^+ = 2.56 + 0.96 (\text{obs. } NH_4^+) \quad r = 0.96$$

$$\text{Los Angeles} \quad \text{Calc. } NH_4^+ = 3.92 + 0.98 (\text{obs. } NH_4^+) \quad r = 0.95$$

In all cases, calculated values exceed observed values. At Riverside and Los Angeles where high correlations were observed, the difference was relatively constant at 2.5 to 4  $\mu g/m^3$ . This

Figure 28 Comparison of Fine and Total Particulate Elemental Carbon

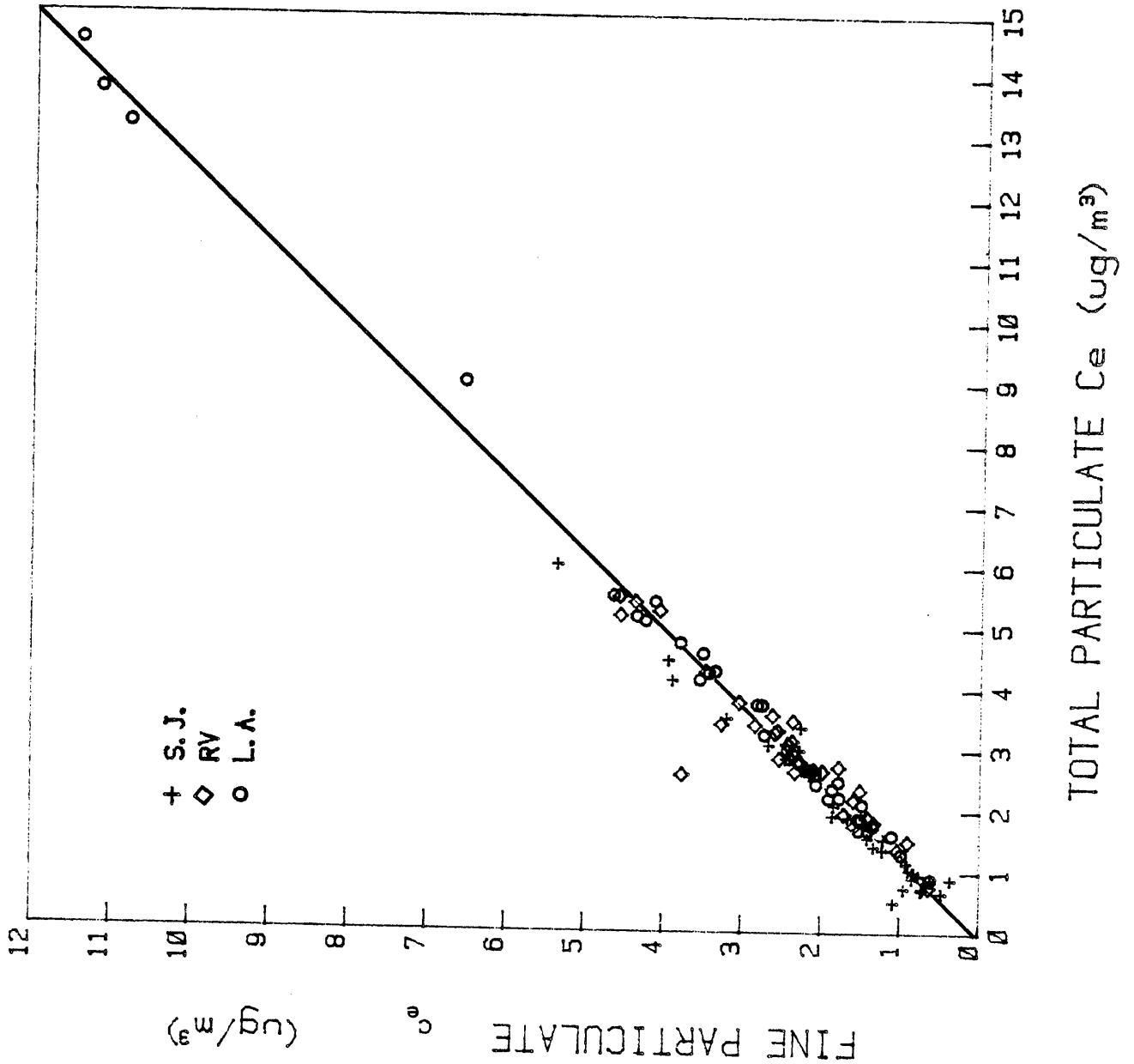


Figure 29 Fine Elemental Carbon vs. Total Carbon in 4-Hour Samples

# VISIBILITY STUDY

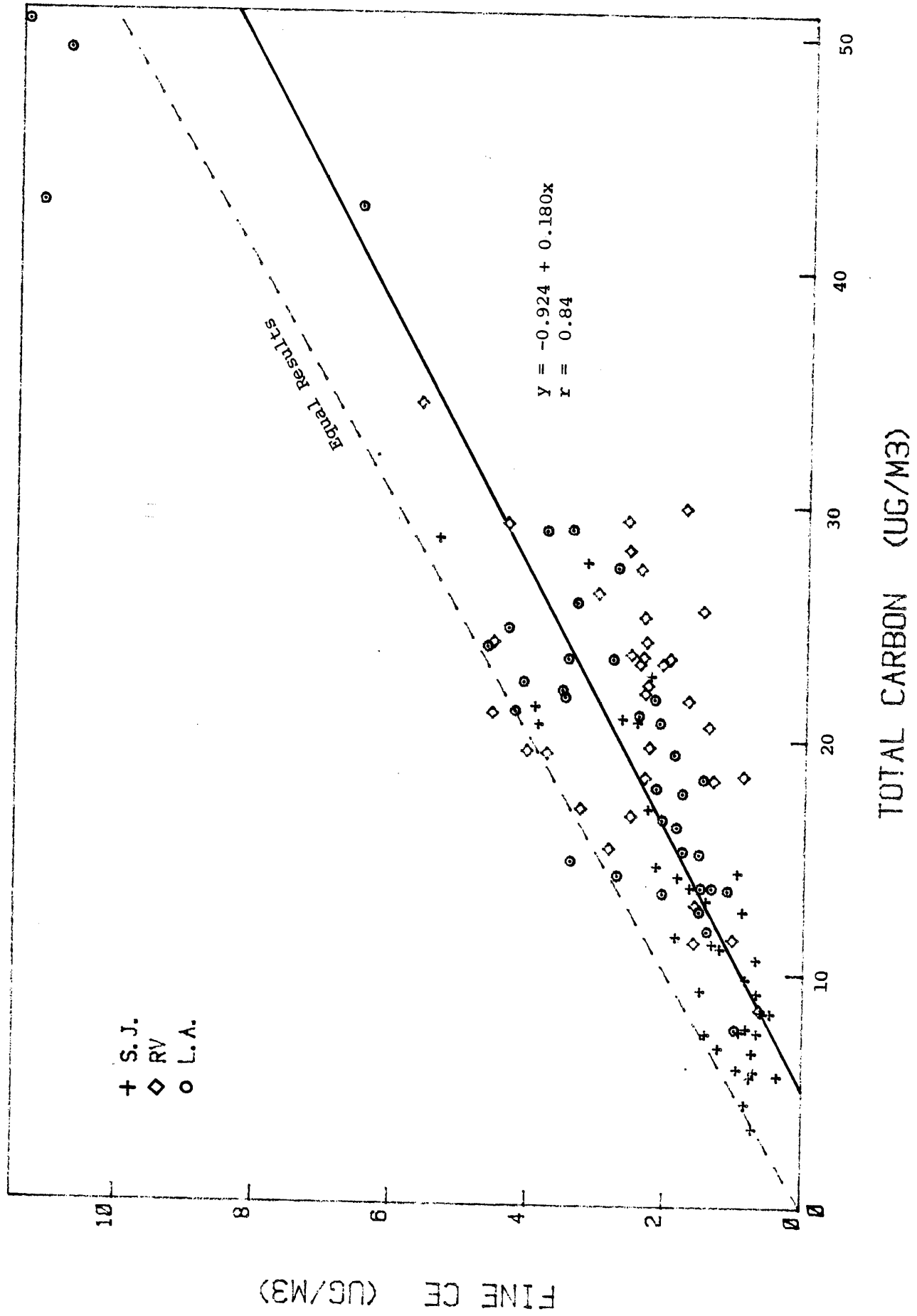


Figure 30 Fine Particle Mass vs. Fine Particle Elemental Carbon

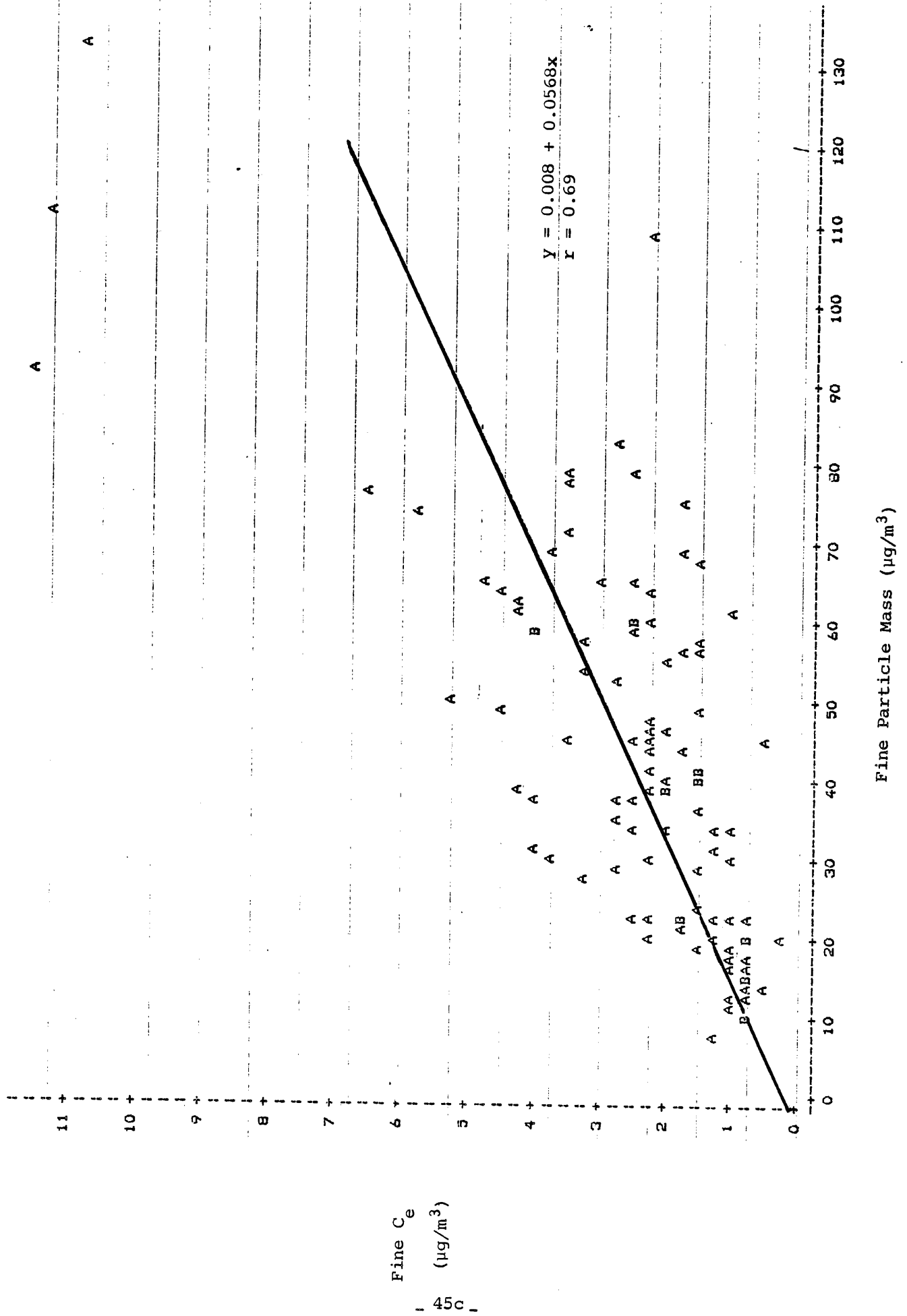
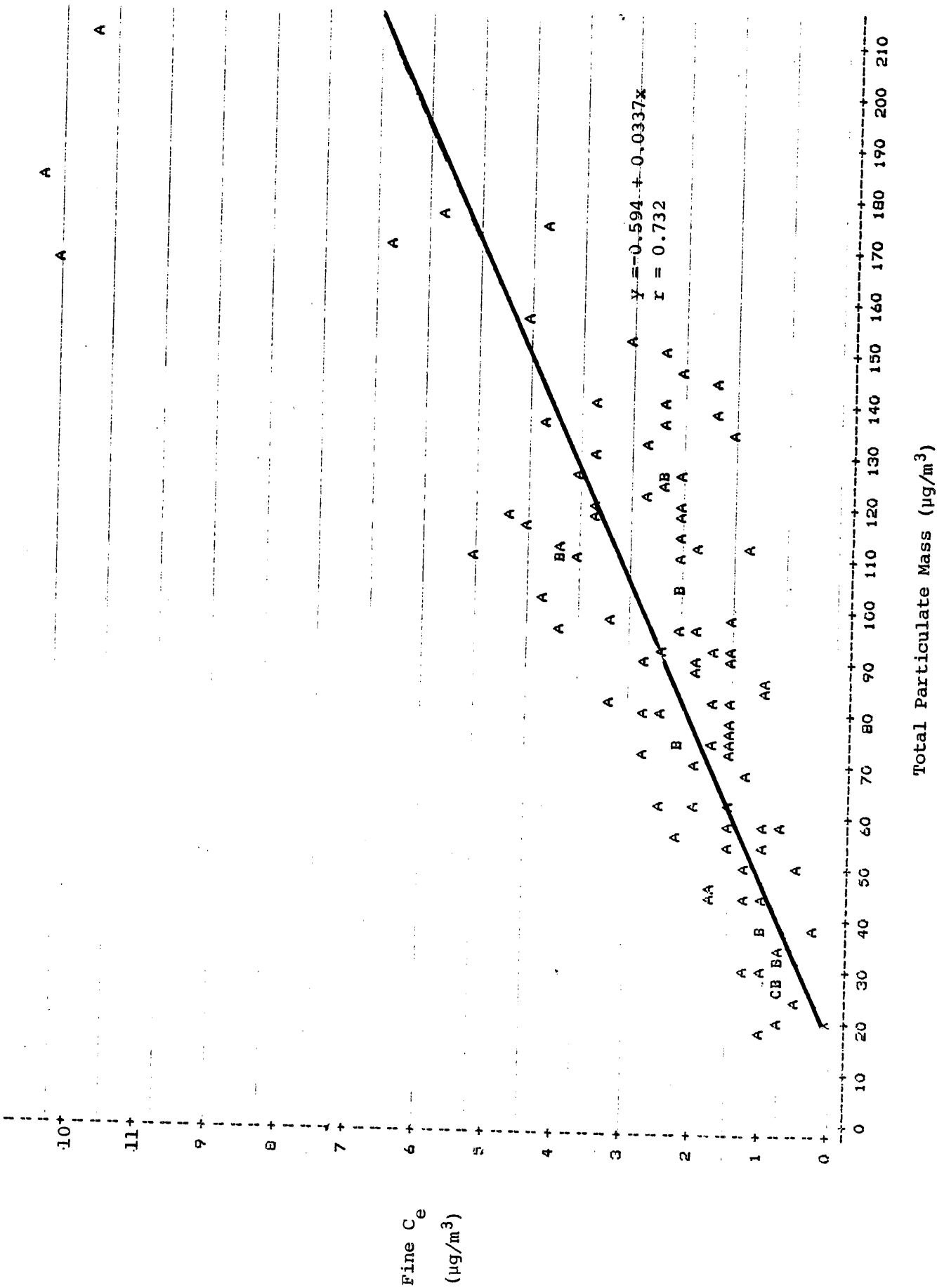


Figure 31 Total Particle Mass vs. Fine Particle Elemental Carbon



difference may be indicative of acidic aerosols although other cations besides  $\text{NH}_4^+$  and  $\text{H}^+$  may be significant.

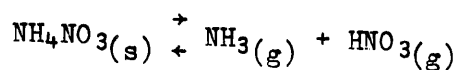
F. True Particle Carbon (PC) and Total Low Volatility Carbon (LVC)

Figure 32 compares total results for quartz filter samples collected with a preceding  $\text{Al}_2\text{O}_3$  -coated denuder (sampler 4) against total carbon results without the denuder. The results show about 17% less carbon on the filter with the denuder, which might infer that a corresponding amount of carbon was retained in the denuder of sampler 4. However, this assumes that the presence of the denuder does not influence the loss of carbon from the filter by volatilization. If the denuder does remove vapor-phase, material in equilibrium with material in particle phase, then volatilization could be enhanced, decreasing retention of carbon on the filter.

As discussed in Appendix F, water retained by the  $\text{Al}_2\text{O}_3$  and its subsequent elution with  $\text{CH}_2\text{Cl}_2$  - MeOH appeared to greatly decrease the precision of the subsequent carbon measurements. In contrast to prior work using  $\text{CH}_2\text{Cl}_2$  alone for elution (40) tests of the consistency of these results with those from other carbon measurements have caused us to reject these data from further analysis. Accordingly, no PC and LVC data can be considered.

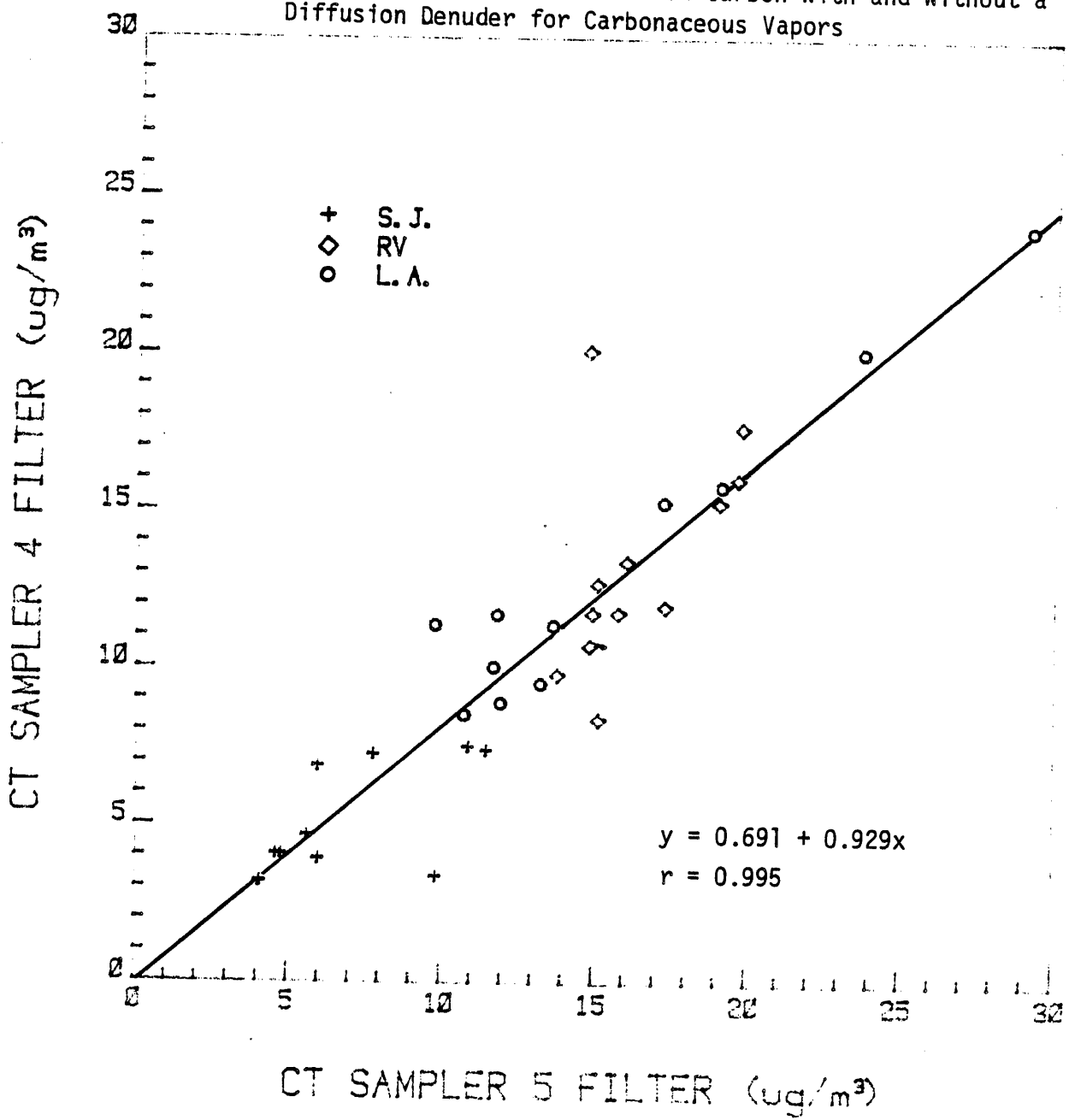
G. Atmospheric Nitric Acid

It has been proposed and demonstrated (53, 54) that the concentrations of atmospheric  $\text{HNO}_3$  and  $\text{NH}_3$  can be influenced by the equilibrium:



The dissociation constant is strongly dependent on temperature. At relative humidities below that needed to cause  $\text{NH}_4\text{NO}_3$  to deliquesce,

Figure 32 Comparison of Filter Collected Carbon With and Without a Diffusion Denuder for Carbonaceous Vapors



- 46a -

a knowledge of the temperature and corresponding dissociation constant, together with the  $\text{NH}_3$  level, should permit calculation of the corresponding equilibrium values for the  $\text{HNO}_3$ . Employing reported values for the temperature dependent dissociation constant (54), and 4-hour average measurements of  $\text{NH}_3$  and temperature, observed and calculated  $\text{HNO}_3$  were compared. Observed  $\text{HNO}_3$  values at San Jose, Riverside and Los Angeles, measured by the denuder difference technique (21), ranged from 0.25 to 8.5, 0.5 to 16.5 and 1 to 60  $\mu\text{g}/\text{m}^3$ , respectively. However, only at San Jose was a significant correlation observed ( $r = 0.73$ ) between calculated and observed values. The corresponding regression equation was:

$$\text{Calc. HNO}_3 = 3.21 + 12.3 (\text{obs. HNO}_3).$$